INORGANIC CARBON FIXATION AND TROPHIC INTERACTIONS IN HIGH-TEMPERATURE GEOTHERMAL SPRINGS OF YELLOWSTONE NATIONAL PARK, WY, USA

by

Ryan deMontmollin Jennings

A dissertation submitted in partial fulfillment
of the requirements for the degree

of

Doctor of Philosophy

in

Ecology and Environmental Science

MONTANA STATE UNIVERSITY
Bozeman, Montana

July 2015

©COPYRIGHT

by

Ryan deMontmollin Jennings

2015

All Rights Reserved

DEDICATION

This work represents nearly a decade of professional growth as a biologist and personal growth as but one biological entity, among many living organisms on our fascinating planet. Fortunate to have obtained the carbon, energy, and nutrients necessary to not only live but also to pursue knowledge, this thesis is dedicated to my own complex biological community – my source of carbon, energy, nutrients, support, and inspiration. Moreover, this thesis is dedicated to those who, with great ambition, seek to find the extent of their abilities and, through the process, discover self-realization while exceeding expectations. Finally, this thesis is dedicated to family and friends whose steadfast support and love, which both made my graduate career possible and continues to make life beautiful.

ACKNOWLEDGEMENTS

I gratefully and sincerely acknowledge the professional and personal support of my major advisor, Dr. Bill Inskeep, who through his role as a mentor and friend showed me that science is fun and incremental. I am further indebted to Dr. Ross Carlson for his professional guidance and kind manner, and members of my committee, Dr. Michael Franklin and Dr. Margie Romine, whose friendliness and appreciation for genetics was valued. Biology is inherently interactive and biological science requires interactive collaboration. I am grateful for and acknowledge the collaborations that enriched my development as a scientist and made this thesis possible. I sincerely appreciate the friendship and opportunity to work with Kristopher Hunt, Laura Whitmore, Jacob Beam, Zackary Jay, Jim Moran, Mark Kozubal, Roslyn Brown, Hans Bernstein, Helen Kruezer, and countless others.

TABLE OF CONTENTS

1. THESIS INTRODUCTION....1

Introduction....1

2. CARBON DIOXIDE FIXATION BY METALLOSPHAERA YELLOWSTONENSIS AND ACIDOTHERMOPHILIC IRON-OXIDIZING MICROBIAL COMMUNITIES FROM YELLOWSTONE NATIONAL PARK....13

Contribution of Authors and Co-Authors....13
Manuscript Information Page....14
Abstract....15
Introduction....16
Materials and Methods....19
Field Sites....19
Genome Analysis....19
Phylogenetic Tree Construction....20
Culture Media and Conditions....21
Pure-Culture CO_2 Uptake Experiments....21
Ex situ Incubations....22
Isotope Ratio Mass Spectrometry....22
Fractionation Factors/Mixing Models....24
Results....24
Genome and Metagenome Analysis....24
Pure-Culture Experiments....25
Ex situ Assays Using Fe(III)-Oxide Mats....27
Discussion....27
Acknowledgements....32
References....37

3. THE EXTENT AND MECHANISMS OF CARBON DIOXIDE FIXATION ACROSS GEOCHEMICALLY DIVERSE HIGH-TEMPERATURE MICROBIAL COMMUNITIES....41

Contribution of Authors and Co-Authors....41
Manuscript Information Page....43
Abstract....44
Introduction....45
Methods....50
Sample Locations....50
Solid Phase Carbon Stable Isotope Analysis....50

TABLE OF CONTENTS - CONTINUED

Function Analysis of *De Novo* Phylotype Genomes....54
Abundance of Different Inorganic C Fixing Micororganisms Across Sites....55
Mixing Model Construction....55
Results....56
^{13}C Content of DIC, DOC and Landscape Sources....56
^{13}C Content of Chemotrophic Iron Mats, Sulfur Sediments, and Streamer Communities....57
Abundance of Inorganic C Fixing Microorganisms across Sites....58
Extent of Autotrophy....60
Discussion....63
Acknowledgements....67
References....74

4. GENOME-ENABLED MULTI-SCALE ANALYSIS OF AUTOTROPH-HETEROTROPH INTERACTIONS IN A HIGH-TEMPERATURE MICROBIAL COMMUNITY....80

Contribution of Authors and Co-Authors....80
Manuscript Information Page....81
Abstract....82
Introduction....83
Materials and Methods....87
Genome Analysis and Model Construction....87
Computational Packages and Analyses....88
Relative Biomass Production and Substrate Consumption Rates....89
Results and Discussion....90
Production of Chemolihoautotrophic Biomass....90
Production of Organoheterotrophic Biomass....91
Oxygen Consumption, Iron Oxidation and Total Biomass Production....92
Comparison to *in situ* Observations....94
Autotroph-Heterotroph Abundance and Implications for Differential Turnover....97
References....108

5. CONCLUSIONS AND FUTURE DIRECTIONS....113

Final Statement....117

REFERENCES CITED....118

TABLE OF CONTENTS - CONTINUED

APPENDICES 129

APPENDIX A: Practical Application of Stable Carbon Isotope Analysis in Biological Systems 130
APPENDIX B: Supplemental Material to “Carbon Dioxide Fixation by Metallosphaeara Yellowstonensis and Acidothermophilic Iron-Oxidizing Microbial Communities from Yellowstone National Park” 133
APPENDIX C: Supplemental Material to “The Extent and Mechanisms of Carbon Dioxide Fixation across Geochemically Diverse High-Temperature Microbial Communities” 137
APPENDIX D: Supplemental Material to “Genome-Enabled Multi-Scale Analysis of Autotroph-Heterotroph Interactions in a High-Temperature Microbial Community” 145

LIST OF TABLES

Table Page

2.1. Carbon isotope values of *M. yellowstonensis* strain MK1 biomass in growth experiments using labeled versus unlabeled CO_2 and 1% yeast extract 33

2.2. Carbon isotope composition of microbial mat samples incubated after *ex situ* experiments to detect CO_2 uptake in Fe(III)-oxide microbial mat communities from Norris Geyser Basin, YNP, October 2011 33

2.3. Carbon isotope ratios of dissolved inorganic carbon, dissolved organic C, and total C present in Fe(III)-oxide microbial mats collected from Norris Geyser Basin, YNP, 2011 to 2013 34

3.1. Key geochemical parameters, and ^{13}C stable isotope content (δ, **‰)** of dissolved inorganic C, dissolved organic C (DIC, DOC) and microbial mat C determined across 15 different high-temperature springs in Yellowstone National Park (WY, USA) 65

3.2. Relative abundance (R.A.)[1], expected inorganic C fixation pathways, and predicted fractionation factors (ε)[2], of candidate autotrophs in different geothermal systems of Yellowstone National Park 66

4.1. Cost of electron donors, carbon sources, and oxygen (electron acceptor) of most efficient metabolisms identified through elementary flux mode (EFM) analysis for the lithoautotroph (*M. yellowstonensis*) and organoheterotroph ('Geoarchaeota') 95

LIST OF FIGURES

Figure Page

2.1. Phylogenetic trees of key proteins in the 3-HP/4-HB pathway for fixation of carbon dioxide 35

2.2. Predicted $\delta^{13}C$ content of Fe(III)-oxide microbial mats as a function of the fraction of microbial biomass originating from dissolved inorganic C (DIC) relative to total biomass C and the fraction of biomass C relative to total Fe mat C 36

3.1. Concentration and stable carbon isotope content of dissolved organic C (DOC) and dissolved inorganic C (DIC) in fifteen geochemically diverse high temperature environments of Yellowstone National Park, WY, USA 67

3.2. Isotope mixing models of sulfur sediment microbial communities 68

3.3. Isotope mixing models of acidic Fe(III)-oxide microbial communities 69

3.4. Isotope mixing models of thermophilic filamentous streamer communities 70

4.1. Conceptual representation of a metabolic interaction model between a primary autotroph (*M. yellowstonensis*) and heterotroph (*"Geoarchaeota sp."* strain OSP) present in high-temperature (70-80°C) acidic Fe-oxide mats 96

4.2. Primary mechanisms and stoichiometry of electron transport reactions in *M. yellowstonensis* for the oxidation of ferrous iron and reduced sulfur-species coupled to oxygen reduction 97

4.3. Oxygen consumption as a function of moles electron donor consumed or moles electrons consumed for all biomass producing elementary flux modes of *M. yellowstonensis* 98

4.4. Oxygen and substrate consumption (per Cmol biomass) for all biomass producing *Geoarchaeota* elementary flux modes 99

LIST OF FIGURES – CONTINUED

Figure Page

4.5. Oxygen consumption plotted as a function of biomass production for autotrophic *M. yellowstonensis* and for heterotrophic Geoarchaeota 100

4.6. Total community growth rate predicted as a function of oxygen flux, autotrophic and heterotrophic biomass production yields, and the relative abundances of *M. yellowstonensis* and Geoarchaeota 101

4.7. Relationship between Fe(II) oxidation and oxygen consumption rates predicted for production of total community biomass from dissolved inorganic C 102

ABSTRACT

Numerous chemotrophic microorganisms inhabit high-temperature (> 65 °C) systems of Yellowstone National Park (WY, USA). Prior geochemical and metagenome characterization has identified the primary electron donors and acceptors and phylotypes distributed across a range in pH and geochemical conditions. Although several chemolithoautotrophs are expected to play a direct role in the fixation of inorganic C in these communities, little work has directly identified the importance of this process *in situ*. Consequently, the primary goal of this thesis was to evaluate the role of CO_2 fixation across numerous types of geothermal habitats and to explore autotroph-heterotroph interactions that may control community composition. Genes encoding enzymes for inorganic C fixation pathways were identified in assembled genome sequence corresponding to the predominant autotrophs (Crenarchaeota and Aquificales) observed in Fe(III)-oxide mats, sulfur sediments, and filamentous streamer communities. Carbon isotope (^{13}C) mixing models were used to interpret the ^{13}C compositional values of microbial samples as a function of ^{13}C-dissolved inorganic C (DIC) and ^{13}C-organic C (DOC and/or landscape sources). The relative abundance of autotrophs versus heterotrophs identified in complementary metagenome analysis and respective CO_2-fixation fractionation factors were utilized in site-specific mixing models to calculate minimum contributions of DIC-derived microbial C across 15 different microbial communities. Genome sequence was also used to develop stoichiometric reaction networks for a primary autotroph (*Metallosphaera yellowstonensis*) and heterotroph ('Geoarchaeota') important in acidic Fe(III)-oxide mats. Possible modes of biomass production were evaluated for different C sources and/or electron donors as a function of oxygen cost. The total oxygen flux was also used to predict the rate of Fe(II)-oxidation, and these values were compared to Fe(III)-oxide deposition rates and oxygen fluxes measured *in situ*. Stoichiometric modeling and elementary flux mode analysis established an optimum autotroph to heterotroph ratio (2.4:1) for DIC-derived biomass dependent on Fe(II) as the electron donor. Comparison of predicted Fe(II)-oxidation rates with observed Fe(III)-oxide deposition rates and oxygen flux measurements using microelectrodes suggest the importance of other oxygen consuming processes. Results from this thesis demonstrated the importance of inorganic C fixation in numerous geochemically distinct high-temperature microbial habitats, and the potential for DIC-derived biomass to support other hyperthermophilic heterotrophic organisms.

CHAPTER 1

Introduction

The majority of food webs on the planet start with the fixation of inorganic carbon (e.g., carbon dioxide, CO_2), which requires significant energy inputs. Organisms capable of reducing inorganic C for anabolic processes have been described in all three domains of Life (*Archaea*, *Bacteria* and *Eukarya*). These primary producers harvest energy from either photons or reduced chemical species and reduce CO_2 through one of six known C 'fixation' pathways. Thus, organisms capable of inorganic C fixation and the pathways responsible for this metabolism are of significant importance to the global C cycle on Earth. Moreover, given anthropogenic influence on the global carbon cycle, it is essential to evaluate the ecology of primary producers and the mechanisms of C flux into and through specific ecosystems.

The fixation of inorganic C (i.e., C sequestration) is an important global biogeochemical process. Specifically, terrestrial systems fix significant amounts of CO_2 resulting in nearly 60 $PgC \cdot y^{-1}$ net primary production (NPP), while the NPP in ocean systems totals ~ 45 $PgC \cdot y^{-1}$ (1) (1 Petagram = $1x10^{15}$ g). Many organisms capable of inorganic C fixation are distributed throughout the three domains of life, and microorganisms constitute a significant fraction of reduced C on Earth. The total number of microorganisms on Earth is estimated at $4\text{-}6 \times 10^{30}$ cells, which corresponds to a carbon reservoir of 350-550 Pg (2). Yet, despite the widespread distribution and

significance of microorganisms, the contribution of microbial inorganic C fixation to the global C cycle is not well-resolved (3, 4).

Carbon dioxide fixation, which is important in numerous trophic webs, occurs via one of six currently known pathways in *Archaea*, *Bacteria* and/or *Eukarya*. Energy for the reduction of CO_2 to biomass C is obtained from either photons (i.e. phototrophy) or the oxidation of reduced chemical species (i.e. chemotrophy). The Calvin Benson Bassham (CBB) cycle and the 3-hydroxypropionate (3-HP) cycle use light energy harvested via different photosystems to reduce CO_2 (5, 6). Carbon dioxide (CO_2) reduction pathways common among chemotrophic organisms include the reductive tricarboxylic acid cycle, reductive acetyl-CoA pathway, 3-hydroxypropionate/4-hydroxybutyrate cycle and the dicarboxylate/4-hydroxybutyrate cycle (7). A plethora of inorganic electron donors, such as reduced forms of hydrogen, sulfur, nitrogen, arsenic, and numerous transition metals (e.g., iron and manganese) are available in Earth systems to drive chemoautotrophy. The reductive tricarboxylic acid (r-TCA) cycle fixes two CO_2 molecules by reversing the TCA cycle and has been described in numerous bacterial lineages, including the hyperthermophilic Aquificales, which are known inhabitants of marine hydrothermal vents and geothermal environments (8-11). The reductive acetyl-CoA (Wood-Ljungdahl) pathway reduces CO_2 to CO, which is directly converted to acetyl-CoA and has been identified in acetogenic bacteria and methanogenic archaea, as well as sulfate reducing bacteria and archaea (7). These organisms are often found in sub-oxic environments including sediments, soils, sludge, and intestinal tracts (12-14). The 3-hydroxypropionate/4-hydroxybutyrate (3-HP/4-HB) cycle reduces two bicarbonate

molecules to succinyl-CoA via 3-hydroxypropionate and has been identified in several major lineages of *Archaea*, including the Crenarchaeaota (order Sulfolobales) and marine Thaumarchaeota (15). The dicarboxylate/4-hydroxybutyrate (DC/4-HB) cycle reduces CO_2 and bicarbonate, is identical with the regenerative half of the 3-HP/ 4-HB cycle, and has been identified in the Thermoproteales and Desulfurococcales (phylum Crenarchaeota) (16, 17). The DC/4-HB and 3-HP/4-HB cycle are homologous in the regeneration of acetyl-CoA from succinyl-CoA, and the presence of a Type 1 4-hydroxybutyryl-CoA dehydratase is common to both pathways (7, 15, 18). The DC/4-HB and 3-HP/4-HB cycles differ in the CO_2 reductive steps: phosphonenolpyruvate carboxylase (PEPc) catalyzes the reduction of bicarbonate in the DC/4-HB cycle, while the bifunctional acetyl/propionyl-CoA carboxylase catalyzes the reduction of inorganic carbon in the 3-HP/4-HB cycle. Many cultured Sulfolobales are capable of inorganic C fixation via the 3-HP/4-HB pathway (19); however, the capacity for and extent of autotrophy within the Thermoproteales and Desulfurococcales is still unclear, as many isolated representatives from these orders will only grow on complex C (20, 21). Consequently, different chemotrophic microorganisms, which occupy varied geochemical niches, utilize a range of electron donors to drive the reduction of CO_2 via different inorganic C fixation pathways. Despite the importance of these microbial mechanisms, little is known of the contribution that chemoautotrophs make at local community scales, or even the global carbon cycle.

The contribution of inorganic C fixation to community biomass is a major question in understanding the assembly and succession of microbial communities. High-

temperature environments (e.g., deep sea hydrothermal systems and Yellowstone geothermal environments) are often energy-rich with respect to reduced inorganic constituents and these microbial communities are often dominated by fewer phylotypes. Thus, high-temperature (65 – 85 ^{o}C) environments are excellent habitats in which to study different microbial contributions to CO_2 fixation. Specifically, acidic Fe-oxide mats (pH 2.5 – 4), sub-oxic S sediments (pH ~ 2 – 6), and filamentous streamer communities (pH ~ 3 – 9) are ideal environments to examine specific microorganisms and microbial interactions in naturally occurring populations. Possible inorganic electrons donors and acceptors have been established in these natural systems and metagenome sequences of these microbial communities provides the foundation for examining the metabolism of specific populations as well as potential exchange of carbon and energy within the community.

Iron oxide microbial mats are found in numerous acidic (pH ~3) geothermal outflow channels of Yellowstone National Park (YNP) and are inhabited by a variety of *Archaea*, including several crenarchaeal populations (orders Sulfolobales, Desulfurococcales, and Thermoproteales) and representatives of the candidate phylum Geoarchaeota (22-25). Additionally, *Hydrogenobaculum* spp. of the acidophilic bacterial order Aquificales are the dominant bacterial population(s) present in high-temperature (i.e., > 65°C) acidic Fe mats and are important colonizers during the formation of Fe mats (26, 27). The aqueous and solid-phase geochemistry of these microbial environments has been thoroughly documented (e.g., (26, 28-32)) and provides a critical foundation for evaluating the microbial community. The primary electron donors available to drive

lithotrophy in Fe-oxide microbial mats include reduced sulfur species (dissolved sulfide < 5 - 10 µM), ferrous iron (~ 30 - 40 µM), arsenite (25 – 30 µM) and hydrogen (~ 30 nM.). Different Fe-oxide solid-phases have been observed in varied geothermal systems and include amorphous Fe-oxyhydroxide and ferrihydrite as well as crystalline iron-oxides such as goethite and hematite (32, 33), and evidence has been presented for the biotic Fe(II)-oxidation in these low pH environments (34). Oxygen (DO ~ 30 µM) is an important terminal electron acceptor in Fe-oxide communities and gradients exist within the mat, resulting in aerobic, microaerobic, and sub-oxic microenvironments (29). Nevertheless, aerobic chemolithotrophs gain sufficient energy for CO_2 fixation in Fe-oxide mats.

In contrast to Fe-oxide mats, sulfur sediments contain significant amounts of dissolved sulfide (2 – 160 µM), which results in the deposition of elemental S^0 and sub-oxic (DO < 3 µM) conditions (24, 35). Additionally, sulfur sediments are found in acidic (pH ~2) to circumneutral (pH ~6) geothermal systems and thiosulfate is present (~55 – 700 µM) in environments of intermediate pH (pH ~4 – 6) (24). Therefore, oxidation and/or reduction of sulfur species represents a potential energy source for microorganisms that may couple chemolithotrophic metabolism with inorganic C fixation. Sulfur sediments are inhabited predominantly by crenarchaea of the orders Sulfolobales, Thermoproteales, and Desulfurococcales (22, 24, 25, 35, 36). The distribution of microorganisms across studied sulfidic systems is a function of pH (24, 35, 36). *Sulfolobus* and *Stygiolobus* spp. (Sulfolobales) have been identified in low pH

(pH ~2) environments, while members of the Thermoproteales and Desulfurococcales inhabit sulfur sediments of intermediate pH (pH ~4 – 6) (24, 36, 37).

Filamentous streamer communities are found in high-velocity, turbulent outflow channels of geothermal springs that exhibit a wide pH range (pH ~3 – 9) (38-40). Rapid outgassing of dissolved CO_2 and H_2S coupled with in-gassing of oxygen is a characteristic feature of the turbulent environments inhabited by filamentous streamer communities (25, 38-40). Possible electron donors in these systems include sulfide (~10 – 100 µM), arsenite (~25 µM), ferrous iron (~40 µM in acidic habitats), and hydrogen (~10 – 65 nM). Consequently, microorganisms can obtain energy from the oxidation of these inorganic constituents and couple this with the reduction of CO_2 into biomass. Distinct lineages of the bacterial order Aquificales inhabit these environments and their distribution is a function of pH. *Hydrogenobaculum* spp. were observed in low pH (pH ~3) habitats and *Sulfurihydrogenibium* spp. were identified in circumneutral (pH ~6) environments; alkaline systems are inhabited by *Thermocrinis* and *Pyrobaculum* (crenarchaeal order Thermoproteales) spp. (37, 39).

The extent of inorganic C fixation in different nonphotosynthetic geothermal microbial communities was initiated on Fe(III)-oxide mat communities. This study (Chapter 2) demonstrated facultative inorganic C fixation by *Metallosphaera yellowstonensis*, an Fe-oxidizing O_2-reducing crenarchaeon isolated in prior work from the Beowulf iron mat (34). Pure cultures of *M. yellowstonensis* str. MK1 grown with $^{13}CO_2$ provided physical evidence of inorganic C fixation while genome analysis identified candidate genes for a complete 3-HP/4-HB pathway. Moreover, evaluation of

M. yellowstonensis-like genes from Fe-oxide metagenomes also identified a near complete 3-HP/4-HB pathway. The stable carbon isotope (^{13}C) content of microbial mat C was evaluated as a mixture of dissolved inorganic C (DIC), dissolved organic C (DOC), and exogenous landscape C, and fractionation factors for the fixation of DIC by the dominant autotrophs known to inhabit Fe-oxide mats (i.e., *M. yellowstonensis* or *Hydrogenobaculum*). This analysis demonstrated that no less than ~ 40% of the microbial biomass carbon in the mat was of DIC-origin.

Research focused on the source of C in chemotrophic Fe(III)-oxide mats led to a broader study of 15 different types of microbial communities across disparate geochemical environments that included Fe-oxide mats, sulfur sediments, and filamentous streamers (Chapter 3). Stable carbon isotope content ($\delta^{13}C$) of possible carbon sources and microbial biomass was evaluated in Chapters 2 and 3; an overview of stable carbon isotope ($\delta^{13}C$) analysis is provided in Appendix A. To identify candidate autotrophs in these 15 microbial communities, assembled metagenome sequence corresponding to different phylotypes was evaluated for genes encoding inorganic C fixation pathways. Relative abundance estimates were incorporated in isotope mixing models, which evaluated the fraction of DIC-derived microbial biomass and the possible extent of landscape C in the sample. This study identified candidate autotrophs in all geothermal microbial communities evaluated and showed that inorganic carbon fixation is an important metabolic process in numerous high-temperature (T ~ 70 - 85 ^{o}C) chemotrophic systems, including sulfur sediments, iron oxide microbial mats, and filamentous streamer communities, ranging in pH from 2.5 to 9. Significant heterotrophic

consumption of biomass generated from inorganic C was evident in numerous habitats as well as the possible heterotrophic consumption of DOC, and/or contributions from non-microbial biomass (i.e., landscape sources).

The extent to which autotroph-heterotroph interactions occur in other geothermal systems had not been studied extensively, despite significant interest in the phylotypes responsible for inorganic C fixation and the identification of numerous heterotophic populations. Establishment of DIC as an appreciable C source in Fe-oxide mats and identification of genome sequence for both *M. yellowstonensis* (autotroph) and Geoarchaeota (heterotroph) provided the foundation for examining autotroph-heterotroph interactions in this geothermal habitat (Chapter 4). This study focused on construction of elementally and electronically balanced stoichiometric metabolic models of these organisms based on genome analysis, identified all possible metabolisms for each organism, and evaluated possible trophic interactions between the two populations in the Fe-oxide mat community. Results from this work provided possible explanations for autotroph-heterotroph interactions occurring *in situ,* and revealed oxygen costs for the production of DIC-derived biomass by *M. yellowstonensis* using Fe(II) as an electron donor for energy generation. Comparisons between model output versus measurements of oxygen consumption and Fe(III)-oxide deposition *in situ* confirm the importance of Fe(II) oxidation as a major oxygen consuming process, and also suggested that other oxygen reducing processes are occuring. Moreover, differential turnover rates of the two interacting populations may contribute to the relatively low abundance of autotrophs necessary to support the amount of observed DIC-derived heterotrophy.

The major findings and impacts of this thesis are summarized along with suggestions for future research directions (Chapter 5). This thesis showed that many thermophilic microbial communities are comprised of carbon originating from both dissolved inorganic C (DIC) as well as DOC/OC. Thus, thus future work should resolve estimates of total microbial C compared to exogenous organic C originating from landscape sources, while determining the composition and bioavailability of DOC. Furthermore, the role of differential biomass turnover among community members participating in the microbial trophic web should be evaluated, as well as the possible role of viruses and frequency of viral predation. Finally, forthcoming meta-transcriptomes and meta-proteomes will refine genome-enable metabolic predictions, which are linked with observable processes *in situ* such as inorganic C fixation, oxygen reduction, and Fe(II) oxidation.

References

1. Prentice IC, G.D. Farquhar, M.J.R. Fasham, M.L. Goulden, M. Heimann, V.J. Jaramillo, et al. The Carbon Cycle and Atmospheric Carbon Dioxide. Climate Change 2001: The Scientific Basis Contribution of Working Group I to the Third Assessment Report of the Intergovernmental Panel on Climate Change. 2001.

2. Whitman WB, Coleman DC, Wiebe WJ. Prokaryotes: the unseen majority. Proc Natl Acad Sci U S A. 1998;95(12):6578-83.

3. Shively JM, English RS, Baker SH, Cannon GC. Carbon cycling: the prokaryotic contribution. Curr Opin Microbiol. 2001;4(3):301-6.

4. Reinthaler T, van Aken HM, Herndl GJ. Major contribution of autotrophy to microbial carbon cycling in the deep North Atlantic's interior. Deep-Sea Res Pt Ii. 2010;57(16):1572-80.

5. Blankenship RE. Early evolution of photosynthesis. Plant Physiol. 2010;154(2):434-8.

6. Bryant DA, Frigaard NU. Prokaryotic photosynthesis and phototrophy illuminated. Trends Microbiol. 2006;14(11):488-96.

7. Hugler M, Sievert SM. Beyond the Calvin cycle: autotrophic carbon fixation in the ocean. Ann Rev Mar Sci. 2011;3:261-89.

8. Reysenbach A-L, Banta AB, Boone DR, Cary SC, Luther GW. Biogeochemistry: microbial essentials at hydrothermal vents. Nature. 2000;404(6780):835-.

9. Reysenbach AL, Ehringer M, Hershberger K. Microbial diversity at 83 degrees C in Calcite Springs, Yellowstone National Park: another environment where the Aquificales and "Korarchaeota" coexist. Extremophiles. 2000;4(1):61-7.

10. Reysenbach A-L, Gotz D, Banta A, Jeanthon C, Fouquet Y. Expanding the distribution of the Aquificales to the deep-sea vents on Mid-Atlantic Ridge and Central Indian Ridge. CBM-Cahiers de Biologie Marine. 2002;43(3-4):425-8.

11. Huber R, Eder W. Aquificales. In: Dworkin M, Falkow S, Rosenberg E, Schleifer K-H, Stackebrandt E, editors. The Prokaryotes: Springer New York; 2006. p. 925-38.

12. Breznak JA, Kane MD. Microbial H2/CO2 acetogenesis in animal guts: nature and nutritional significance1990 1990-12-01 00:00:00. 309-13 p.

13. Whitman W, Bowen T, Boone D. The Methanogenic Bacteria. In: Dworkin M, Falkow S, Rosenberg E, Schleifer K-H, Stackebrandt E, editors. The Prokaryotes: Springer New York; 2006. p. 165-207.

14. Drake HL, Gossner AS, Daniel SL. Old acetogens, new light. Ann N Y Acad Sci. 2008;1125:100-28.

15. Berg IA, Kockelkorn D, Buckel W, Fuchs G. A 3-hydroxypropionate/4-hydroxybutyrate autotrophic carbon dioxide assimilation pathway in Archaea. Science. 2007;318(5857):1782-6.

16. Huber H, Gallenberger M, Jahn U, Eylert E, Berg IA, Kockelkorn D, et al. A dicarboxylate/4-hydroxybutyrate autotrophic carbon assimilation cycle in the hyperthermophilic Archaeum Ignicoccus hospitalis. Proc Natl Acad Sci U S A. 2008;105(22):7851-6.

17. Ramos-Vera WH, Berg IA, Fuchs G. Autotrophic carbon dioxide assimilation in Thermoproteales revisited. J Bacteriol. 2009;191(13):4286-97.

18. Berg IA, Kockelkorn D, Ramos-Vera WH, Say RF, Zarzycki J, Hugler M, et al. Autotrophic carbon fixation in archaea. Nat Rev Microbiol. 2010;8(6):447-60.
19. Huber H, Prangishvili D. Sulfolobales. In: Dworkin M, Falkow S, Rosenberg E, Schleifer K-H, Stackebrandt E, editors. The Prokaryotes: Springer New York; 2006. p. 23-51.

20. Huber H, Huber R, Stetter KO. Thermoproteales. Prokaryotes: A Handbook on the Biology of Bacteria, Vol 3, Third Edition. 2006:10-22.

21. Huber H, Stetter KO. Desulfurococcales. Prokaryotes: A Handbook on the Biology of Bacteria, Vol 3, Third Edition. 2006:52-68.

22. Jay ZJ, Rusch DB, Tringe SG, Bailey C, Jennings RM, Inskeep WP. Predominant Acidilobus-like populations from geothermal environments in yellowstone national park exhibit similar metabolic potential in different hypoxic microbial communities. Appl Environ Microbiol. 2014;80(1):294-305.

23. Kozubal MA, Romine M, Jennings R, Jay ZJ, Tringe SG, Rusch DB, et al. Geoarchaeota: a new candidate phylum in the Archaea from high-temperature acidic iron mats in Yellowstone National Park. ISME J. 2013;7(3):622-34.

24. Inskeep WP, Jay ZJ, Herrgard MJ, Kozubal MA, Rusch DB, Tringe SG, et al. Phylogenetic and Functional Analysis of Metagenome Sequence from High-Temperature Archaeal Habitats Demonstrate Linkages between Metabolic Potential and Geochemistry. Front Microbiol. 2013;4:95.

25. Inskeep WP, Rusch DB, Jay ZJ, Herrgard MJ, Kozubal MA, Richardson TH, et al. Metagenomes from high-temperature chemotrophic systems reveal geochemical controls on microbial community structure and function. PLoS One. 2010;5(3):e9773.

26. Beam JP, Bernstein HC, Jay ZJ, Kozubal MA, Jennings Rd, Tringe SG, et al. Assembly and Succession of Iron Oxide Microbial Mat Communities in Acidic Geothermal Springs. Geobiology. 2015.

27. Macur RE, Langner HW, Kocar BD, Inskeep WP. Linking geochemical processes with microbial community analysis: successional dynamics in an arsenic-rich, acid-sulphate-chloride geothermal spring. Geobiology. 2004;2(3):163-77.

28. Langner HW, Jackson CR, McDermott TR, Inskeep WP. Rapid oxidation of arsenite in a hot spring ecosystem, Yellowstone National Park. Environ Sci Technol. 2001;35(16):3302-9.

29. Bernstein HC, Beam JP, Kozubal MA, Carlson RP, Inskeep WP. In situ analysis of oxygen consumption and diffusive transport in high-temperature acidic iron-oxide microbial mats. Environ Microbiol. 2013;15(8):2360-70.

30. Inskeep W, Macur R, Ackerman G, Kozubal M, Taylor W, Korf S. Linking microbial and geochemical processes in geothermal habitats. Geochim Cosmochim Ac. 2005;69(10):A226-A.

31. Inskeep WP, Ackerman GG, Taylor WP, Kozubal M, Korf S, Macur RE. On the energetics of chemolithotrophy in nonequilibrium systems: case studies of geothermal springs in Yellowstone National Park. Geobiology. 2005;3(4):297-317.

32. Inskeep WP, Macur RE, Harrison G, Bostick BC, Fendorf S. Biomineralization of As(V)-hydrous ferric oxyhydroxide in microbial mats of an acid-sulfate-chloride geothermal spring, Yellowstone National Park. Geochim Cosmochim Ac. 2004;68(15):3141-55.

33. Kozubal MA, Macur RE, Jay ZJ, Beam JP, Malfatti SA, Tringe SG, et al. Microbial iron cycling in acidic geothermal springs of yellowstone national park: integrating molecular surveys, geochemical processes, and isolation of novel fe-active microorganisms. Front Microbiol. 2012;3:109.

34. Kozubal MA. Geomicrobiology of iron oxyhydroxide mats in acidic geothermal springs of Yellowstone National Park, Wyoming, United States of America. 2010.

35. Macur RE, Jay ZJ, Taylor WP, Kozubal MA, Kocar BD, Inskeep WP. Microbial community structure and sulfur biogeochemistry in mildly-acidic sulfidic geothermal springs in Yellowstone National Park. Geobiology. 2013;11(1):86-99.

36. Jay ZJ. Linking geochemistry with microbial community structure and function in sulfidic geothermal systems of Yellowstone National Park. 2015.

37. Inskeep WP, Jay ZJ, Tringe SG, Herrgard MJ, Rusch DB, Committee YNPMPS, et al. The YNP Metagenome Project: Environmental Parameters Responsible for Microbial Distribution in the Yellowstone Geothermal Ecosystem. Front Microbiol. 2013;4:67.

38. Fouke BW. Hot-spring Systems Geobiology: abiotic and biotic influences on travertine formation at Mammoth Hot Springs, Yellowstone National Park, USA. Sedimentology. 2011;58(1):170-219.

39. Takacs-Vesbach C, Inskeep WP, Jay ZJ, Herrgard MJ, Rusch DB, Tringe SG, et al. Metagenome sequence analysis of filamentous microbial communities obtained from geochemically distinct geothermal channels reveals specialization of three aquificales lineages. Front Microbiol. 2013;4:84.

40. Kandianis MT, Fouke BW, Johnson RW, Veysey J, Inskeep WP. Microbial biomass: A catalyst for CaCO3 precipitation in advection-dominated transport regimes. Geol Soc Am Bull. 2008;120(3-4):442-50.

CHAPTER 2

CARBON DIOXIDE FIXATION BY METALLOSPHAERA YELLOWSTONENSIS AND ACIDOTHERMOPHILIC IRON-OXIDIZING MICROBIAL COMMUNITIES FROM YELLOWSTONE NATIONAL PARK

Contribution of Authors and Co-Authors

Manuscript in Chapter 2

Author: Ryan deM. Jennings

Contributions: Conceived, designed, and performed experiments. Data collection and analysis. Manuscript drafting and editing at all stages.

Co-Author: Laura M. Whitmore

Contributions: Performed experiments, data collection and analysis.

Co-Author: James J. Moran

Contributions: Data collection and analysis.

Co-Author: Helen W. Kreuzer

Contributions: Data collection and analysis.

Co-Author: William P. Inskeep

Contributions: Conceived and designed experiments. Data collection and analysis. Manuscript drafting and editing at all stages.

Manuscript Information Page

Ryan M. Jennings[a,b], Laura M. Whitmore[a,b], James J. Moran[c], Helen W. Kreuzer[c] and William P. Inskeep[a,b]
Journal Name: The American Society for Microbiology Applied and Environmental Microbiology Journal
__Prepared for submission to a peer-reviewed journal
__Officially submitted to a peer-reviewed journal
__Accepted by a peer-reviewed journal
X Published in a peer-reviewed journal

The American Society for Microbiology Applied and Environmental Microbiology Journal
Published in the AEM Journal Volume 80(9) May 2014
[a]Department of Land Resources and Environmental Sciences, Montana State University, Bozeman, Montana, USA
[b]Thermal Biology Institute, Montana State University, Bozeman, Montana, USA
[c]Pacific Northwest National Laboratories, Richland, Washington, USA

Abstract

The fixation of inorganic carbon has been documented in all three domains of life and results in the biosynthesis of diverse organic compounds that support heterotrophic organisms. The primary aim of this study was to assess carbon dioxide fixation in high-temperature Fe(III)-oxide mat communities and in pure cultures of a dominant Fe(II)-oxidizing organism (*Metallosphaera yellowstonensis* strain MK1) originally isolated from these environments. Protein-encoding genes of the complete 3-hydroxypropionate/4-hydroxybutyrate (3-HP/4-HB) carbon dioxide fixation pathway were identified in *M. yellowstonensis* strain MK1. Highly similar *M. yellowstonensis* genes for this pathway were identified in metagenomes of replicate Fe(III)-oxide mats, as were genes for the reductive tricarboxylic acid cycle from *Hydrogenobaculum* spp. (Aquificales). Stable-isotope ($^{13}CO_2$) labeling demonstrated CO_2 fixation by *M. yellowstonensis* strain MK1 and in *ex situ* assays containing live Fe(III)-oxide microbial mats. The results showed that strain MK1 fixes CO_2 with a fractionation factor of ~2.5‰. Analysis of the ^{13}C composition of dissolved inorganic C (DIC), dissolved organic C (DOC), landscape C, and microbial mat C showed that mat C is from both DIC and non-DIC sources. An isotopic mixing model showed that biomass C contains a minimum of 42% C of DIC origin, depending on the fraction of landscape C that is present. The significance of DIC as a major carbon source for Fe(III)-oxide mat communities provides a foundation for examining microbial interactions that are dependent on the activity of autotrophic organisms (i.e., *Hydrogenobaculum* and *Metallosphaera* spp.) in simplified natural communities.

Introduction

The fixation of inorganic carbon (i.e., carbon dioxide [CO_2]) is an important metabolic process in all three domains of life and can initiate trophic cascades that support ecosystem food webs. Photoautotrophs incorporate CO_2 by using the Calvin-Benson-Bassham cycle and have long been recognized as significant contributors to the global carbon cycle. The role of archaeal carbon dioxide fixation in microbial communities, however, is not well studied. Until recently, the contribution of chemoautotrophs (specifically Archaea) to CO_2 fixation has been underappreciated on a global scale, yet the contribution of chemoautotrophic prokaryotes to system productivity is important in numerous habitats. For example, members of the Thaumarchaeota (previously referred to as "marine Crenarchaeota") represent up to 40% of deep-ocean "bacterioplankton" (1) and have now been implicated as major contributors to global carbon and nitrogen cycling (2–4). Consequently, the discovery of new CO_2 fixation pathways and the identification of specific populations that contribute to the fixation of CO_2 in natural habitats provide a foundation for understanding how microbial systems contribute to global carbon cycling.

Numerous archaea are capable of CO_2 fixation via different mechanisms (5–8). The 3-hydroxypropionate/4-hydroxybutyrate (3-HP/4-HB) and dicarboxylate/4-hydroxybutyrate (DC/4-HB) pathways for CO_2 fixation have been identified recently in different members of the Crenarchaeota (9, 10). Both cycles regenerate acetyl coenzyme A (CoA) from succinyl-CoA via seven enzyme-catalyzed reactions, including a dehydration reaction (4-hydroxybutyryl-CoA to crotonyl-CoA), which is catalyzed by 4-

hydroxybutyryl-CoA dehydratase (4HCD). Consequently, the 4HCD gene (encoding the type 1 4HCD protein) is a marker gene for both pathways. The 3-HP/4-HB pathway has been identified in members of marine and soil Thaumarchaeota (1, 11), and the 4HCD gene was found at abundances similar to those of RubisCO, the marker gene for the Calvin-Benson-Bassham cycle, in the Global Ocean Survey (GOS) (9, 12). Therefore, it was suggested that abundant mesophilic autotrophic Thaumarchaeota in the open ocean utilize the 3-HP/4-HB cycle (or a variant thereof) to fix substantial quantities of CO_2 (9, 10, 13).

Iron oxide microbial mats from acidic (pH ~3) geothermal outflow channels of Yellowstone National Park (YNP) contain chemolithotrophic microorganisms responsible for the oxidation of Fe(II) and the biomineralization of Fe(III)-oxides (14–17). These microbial communities represent a consortium of numerous archaea, including several crenarchaeal populations (orders Sulfolobales, Desulfurococcales, and Thermoproteales) and representatives of the candidate phylum Geoarchaeota (18–20), as well as acidophilic bacteria from the order Aquificales. *Hydrogenobaculum* spp. are the dominant bacterial population(s) present in high-temperature (i.e., >65°C) acidic Fe mats, and these organisms fix CO_2 through a modified version of the reductive tricarboxylic acid (r-TCA) cycle that cleaves citrate via citryl-CoA lyase and citryl-CoA synthetase (21, 22). Mature Fe(III)-oxide mats of a 0.5- to 1-cm thickness contain relatively low levels of *Hydrogenobaculum*-like organisms (2 to 10% of random shotgun sequences). However, these bacteria are important colonizers during the formation of Fe mats (23)

and are often found in communities that contain Fe(II)-oxidizing members of the order Sulfolobales, such as *Metallosphaera yellowstonensis* (17).

M. yellowstonensis-like populations (>98% nucleotide identity to *M. yellowstonensis* strain MK1) represent 10 to 20% of random metagenome sequences from amorphous Fe(III)-oxide mats in YNP, over a temperature range of 60°C to 75°C and a pH range of 2.9 to 3.5 (n = 8 metagenome samples) (19, 24, 25). Recent work has shown that *Metallosphaera sedula*, as well as other members of the Sulfolobales, fixes CO_2 via the 3-HP/4-HB pathway (9, 26), and initial culture experiments with *M. yellowstonensis* in the presence of CO_2 and yeast extract (YE) suggested facultative autotrophy (17). However, the fixation of CO_2 was neither conclusively demonstrated in pure culture nor shown in environmental samples. Consequently, the objectives of the current study were to (i) identify all 15 candidate genes of the 3-HP/4-HB carbon dioxide fixation pathway in *M. yellowstonensis* strain MK1 and in de novo genome assemblies from acidothermophilic Fe(III)-oxide microbial mat communities in YNP, (ii) utilize stable-isotope ($^{13}CO_2$) labeling to obtain direct evidence of CO_2 fixation by *M. yellowstonensis* strain MK1 and live Fe(III)-oxide microbial mats, and (iii) determine the extent of CO_2 fixation *in situ* by using stable-isotope analysis of different carbon pools within replicate Fe(II)-oxidizing geothermal channels. Results from this study establish that high-temperature Fe(III)-oxide microbial mats contain significant fractions of carbon derived from dissolved inorganic carbon (DIC) and that *M. yellowstonensis*-like organisms present in these systems fix CO_2 via the 3-HP/4-HB pathway.

Materials and Methods

Field Sites

Three different acid-sulfate-chloride geothermal springs in the One Hundred Springs Plain of Norris Geyser Basin, YNP, were sampled for this study, including One Hundred Springs Plain Spring ("OSP Spring") (44°43′58.953″N, 110°42′32.374″W), "Grendel Spring" (44°43′58.0074″N, 110°42′34.4016″W), and "Beowulf Spring" (44°43′53.4″N, 110°42′40.9″W) (these are not official YNP names; thus, coordinates are provided). The source water temperature of all springs ranged from ~80°C to 84°C. Microbial mat samples (3 to 5 g [wet weight]) for the *ex situ* CO_2 uptake experiments as well as for direct isotope ratio measurements were excised from the Fe-oxide mat, approximately 2 to 3 m from the source, where the mat temperatures range from 65°C to 72°C. The sampling sites were designated OSP site B (OSP_B), GRN_D, and BE_D. Replicate metagenomes of Fe(III)-oxide mats from OSP Spring and Beowulf Spring were obtained previously (25, 27) and analyzed in this study for all genes important for a complete 3-HP/4-HB cycle. Replicate water samples from 2010 to 2013 were collected and analyzed for both the carbon concentration and isotope content ($\delta^{13}C$) of dissolved (0.2-μm-filtered) and total organic and inorganic carbon (Colorado Plateau Stable Isotope Laboratory, Flagstaff, AZ).

Genome Analysis

All genes involved in the 3-HP/4-HB cycle, including the key marker 4HCD gene (type I) (9) and the biotin carboxylase subunit of the bifunctional acetyl/propionyl-CoA

carboxylase (*accC*) (28), were used as queries to search the genome of *M. yellowstonensis* strain MK1 (National Center for Biotechnology Information BioProject PRJNA64481; taxon identification number 671065) as well as metagenome assemblies from Fe(III)-oxide mats in YNP. Five of these metagenomes were obtained by using 454-Ti sequencing on samples taken on 15 July 2010: Beowulf site D (Genomes OnLine Database [GOLD] sample identification number Gs0000973), Beowulf site E (GOLD sample identification number Gs0000972), One Hundred Springs Plain site B (GOLD sample identification number Gs0000781), One Hundred Springs Plain site C (GOLD sample identification number Gs0000782), and One Hundred Springs Plain site D (GOLD sample identification number Gs0000783). Two of the metagenomes, One Hundred Springs Plain YNP_8 (GOLD sample identification number Gs0000369; sample date, 30 August 2007) and One Hundred Springs Plain YNP_14 (GOLD sample identification number Gs0000371; sample date, 7 November 2007), were sequenced by using Sanger sequencing and were reported in a larger metagenome study of 20 geothermal sites (27). Both *M. yellowstonensis* strain MK1 and *M. yellowstonensis*-like sequences from the One Hundred Springs Plain metagenomes were evaluated for pathway completeness.

Phylogenetic Tree Construction

The phylogenetic relationship of type I 4-hydroxybutyryl-CoA dehydratases and the biotin carboxylase subunit of bifunctional acetyl/propionyl-CoA carboxylases was examined by using MEGA5 (29). Deduced 4HCD proteins were aligned by using the PAM algorithm, and deduced AccC proteins were aligned by using the MUSCLE

algorithm. Phylogenetic trees were constructed by using the neighbor-joining method; bootstrap consensus trees and values were inferred from 1,000 replicates. The evolutionary distances were computed by using the Dayhoff matrix-based method.

Culture Media and Conditions

All pure culture experiments and field incubations were performed at 65°C to 70°C in glass medium bottles (total volume, ~710 ml) (part number 219439; Wheaton Science Products) with butyl rubber septum screw caps (part number 240680; Wheaton Science Products). Aqueous medium was synthesized to mimic Fe(III)-oxide spring geochemistry and to provide nutrients sufficient to support up to 10^9 cells ml^{-1} (see Table S2 in the supplemental material); 300 ml of medium was supplied to each growth vessel. Two and a half grams of ground pyrite was used as a solid-phase ferrous electron donor for each culture. Oxygen headspace was maintained at a partial pressure of >0.6 atm to serve as the electron acceptor. A total of 5 mM inorganic carbon was supplied in the form of $NaHCO_3$ or $NaH^{13}CO_3$ through the bottle septum, after which the pH of the medium was readjusted to ~2.5 with H_2SO_4. In some cases, the medium was supplemented with 1% yeast extract as a source of organic carbon.

Pure-Culture CO_2 Uptake Experiments

M. yellowstonensis strain MK1 (17) was grown, as described previously, with $NaH^{13}CO_3$, unlabeled $NaHCO_3$, $NaH^{13}CO_3$, and 1% YE; $NaHCO_3$ and 1% YE; or 1% YE alone for ~10 days to post-log phase (~10^8 cells ml^{-1}). Culture purity was assessed by using PCR amplification of 16S rRNA with primers for *M. yellowstonensis* and known

Sulfolobales contaminants (primarily *Sulfolobus islandicus*). Biomass samples were harvested from pure cultures, centrifuged, washed in HCl overnight to remove any potential residual HCO_3^-, rinsed three times with deionized H2O, and lyophilized into cell pellets in preparation for isotope ($\delta^{13}C$) analysis via isotope ratio mass spectroscopy.

Ex situ Incubations

Approximately 3- to 4-g (wet weight) portions of Fe(III)-oxide microbial mats were excised from the outflow channels of two different Fe(II)-oxidizing geothermal springs (OSP Spring and Grendel Spring), placed into glass medium bottles containing 300 ml synthetic medium with 2.5 g autoclaved ground pyrite mineral, and then sealed with septum-containing lids. The experiment included one sample from OSP Spring, two samples from Grendel Spring that were treated as duplicates, and one sample from each spring that was killed with 0.5 mmol sodium azide. The bottles were purged with pure oxygen for approximately 15 s and brought to a slight positive pressure. Two hundred milliliters of either $^{13}CO_2$ or unlabeled CO_2 gas was then added through the septum. Sodium azide-killed controls were injected with $^{13}CO_2$, and all samples were incubated at 65°C to 70°C for 10 days. Positive pressure was maintained in the bottles by injection of additional O_2 as needed. After 10 days, biomass was harvested by centrifugation and prepared for isotope analysis, with an HCl wash, deionized H_2O rinse, and lyophilization.

Isotope Ratio Mass Spectrometry

Stable carbon isotope ratios ($\delta^{13}C$) were measured by using a Thermo-Finnegan (Bremen, Germany) Delta V Plus isotope ratio mass spectrometer coupled to a Costech Analytical Technologies (Valencia, CA, USA) 4010 Elemental Analyzer and a Zero-

Blank autosampler. Approximately 8 to 15 mg of lyophilized iron mat biomass (which contained significant amounts of iron oxide material) or 15 to 20 mg of culture biomass (which contained significant amounts of pyrite) was placed into tin capsules (Costech Analytical Technologies) and analyzed in triplicate. Analytical sample sets included in-house Pacific Northwest National Laboratory (PNNL) glutamic acid standards, which had been calibrated to U.S. Geological Survey (USGS) standard 40 ($\delta^{13}C = -26.39‰$) and USGS standard 41 ($\delta^{13}C = +37.63‰$) glutamic acid isotopic standards. Data were corrected to these standards by using the point-slope method (30). Stable-isotope content is measured as a ratio, R (e.g., $^{13}C/^{12}C$), and reported as a delta (δ) value, where δ equals $(R_A/R_{Std} - 1) \times 1{,}000$ and R_A and R_{Std} are the isotope ratios of the sample and an internationally recognized standard, respectively. The standard for C isotope ratio analysis is Vienna PeeDee belemnite (VPDB). Special precaution was taken to minimize carryover between analyses. Enriched samples containing large amounts of ^{13}C required up to three standard runs to flush the system, as measured by a return to established isotope values. Although excellent precision was obtained for both enriched and natural-abundance (NA) ^{13}C samples, enriched samples exhibited poorer analytical precision than natural-abundance samples (standard deviations of sample measurements are reported in Table 2.1). This was due in part to the fact that enriched samples exceeded the optimum calibration range of the instrument. Also, relatively large sample sizes (up to 20 mg) were required, due to the low carbon contents and large amounts of iron oxide and/or pyrite; this may have influenced combustion efficiency and decreased measurement precision. Despite these caveats, the strong signal from ^{13}C-enriched cultures and field incubation

mixtures provided definitive evidence that inorganic carbon was incorporated into biomass.

Fractionation Factors/Mixing Models

The fractionation factor (ε) for *M. yellowstonensis* was determined by using the equation $\varepsilon = 1{,}000 \times \ln(R_{product}/R_{substrate})$, where R is the $^{13}C/^{12}C$ ratio. The isotopic composition of mat C was predicted by using an isotope mixing model formulated based on $\delta^{13}C$ values of DIC, dissolved organic C (DOC), and landscape C (LC) (measured in this study) and the fractionation factors of *M. yellowstonensis* strain MK1 (this study) and *Hydrogenobaculum*-like organisms (31), which utilize 3-HP/4-HB and r-TCA carbon dioxide fixation pathways, respectively. The measured C isotope content of actual Fe(III)-oxide mat samples may contain contributions from microbial biomass of DIC origin, microbial biomass of DOC (or landscape C) origin, and exogenous landscape C. Given the difficulty in knowing absolute values of all necessary parameters, predicted mat C isotope values were obtained as a function of the ratios of microbial biomass of DIC origin relative to total microbial biomass ($f_{Biomass\text{-}DIC}$, where $f_{Biomass\text{-}DIC} + f_{Biomass\text{-}DOC/LC} = 1$) and the amount of biomass C relative to total mat C ($f_{Biomass\text{-}C}$, where $f_{Biomass\text{-}C} + f_{Nonbiomass\text{-}C} = 1$). Fractionation factors used in the mixing model included a $\varepsilon_{M.\ yellowstonensis}$ value of 2.5‰ (this study) and a $\varepsilon_{Hydrogenobaculum}$ value of 5.5‰ (reported value for *Hydrogenobacter thermophilus* [31]). The assumed fractionation factor for heterotrophic incorporation of organic carbon (DOC or landscape C) was 0‰ (32).

Results

Genome and Metagenome Analysis

All genes for a complete 3-HP/4-HB cycle were identified in the genome of *M. yellowstonensis* strain MK1 (see Table S1 in the supplemental material), which were similar to those identified in *M. sedula* (9, 33). Moreover, the key marker genes for this pathway (4-hydroxybutyryl-CoA dehydratase [the 4HCD gene] and the biotin subunit of acetyl/propionyl-CoA carboxylase [*accC*]) were found in metagenome sequence assemblies from replicate Fe(III)-oxide mat samples (n = 6). The deduced protein sequences obtained from metagenome assemblies are highly similar to and group with the same sequences identified in *M. yellowstonensis* strain MK1 (Fig. 1). Other copies of these marker genes belonging to different Sulfolobales were also found in Fe(III)-oxide microbial mats (24), and these populations may also contribute to the fixation of CO_2 *in situ*. PCR amplification of the 4HCD gene, *accC*, *accB*, and *pccB*, using primers specific to *M. yellowstonensis* strain MK1, further demonstrated the presence of these genes in both the isolate and Fe(III)-oxide systems (see Fig. S1 in the supplemental material). The metagenome sequence of MK1-like populations present in Fe(III)-oxide mats (~98 to 99% average genome nucleotide identity) contained all genes for a complete 3-HP/4-HB pathway, which were similar to those identified in strain MK1 and *M. sedula* (see Table S1 in the supplemental material). The consistent presence of *M. yellowstonensis*-like 4HCD and *accC* genes in Fe(III)-oxide mat metagenomes suggests that the fixation of CO_2 via the 3-HP/4-HB pathway is an important metabolic process conducted by *M.*

yellowstonensis populations *in situ* and may result in significant transformation of CO_2 to microbial biomass.

Pure-Culture Experiments

Growth experiments using *M. yellowstonensis* strain MK1 in the presence of different C sources provided definitive evidence for the incorporation of CO_2 into microbial biomass. The C isotope ratio ($\delta^{13}C$) of *M. yellowstonensis* biomass was −24.3‰ ± 0.2‰ when grown on yeast extract (YE) and ∼−18‰ ± 0.5 ‰ when grown on natural-abundance (NA) CO_2 (Table 2.1). When $^{13}CO_2$ was the sole carbon source, $\delta^{13}C$ values of *M. yellowstonensis* biomass were >50,000‰ (Table 2.1), which demonstrated the incorporation of inorganic carbonate species (H_2CO_3 and aqueous CO_2 [CO_2(aq)] are the dominant species at pH values near 3).

We estimated the ε value for *M. yellowstonensis* cultures grown on NA CO_2, with a measured ^{13}C isotope composition of ∼−15.9‰ ($R_{substrate}$ = 0.0114159) (Table 2.1). The average value of strain MK1 biomass (−18.45‰; $R_{product}$ = 0.0114445) measured in two replicate experiments was used to estimate a value of ε for *M. yellowstonensis* of ∼2.5‰. Although not the primary focus of our study, this ε value is similar to that observed for *M. sedula* (3.1‰) (31).

When *M. yellowstonensis* was supplied with 1% YE and CO_2 simultaneously, $\delta^{13}C$ values showed that carbon constituents from YE were the dominant sources used to build microbial biomass (Table 2.1). The ^{13}C isotope content of *M. yellowstonensis* biomass grown on YE and NA CO_2 was slightly higher ($\delta^{13}C$ = −23.3‰) than that of biomass grown on YE alone ($\delta^{13}C$ = −24.3‰), which suggested some incorporation of

inorganic carbon. The same pattern was observed when strain MK1 was grown on YE plus $^{13}CO_2$. $\delta^{13}C$ values were higher (~1,600‰) than those of biomass grown on YE alone ($\delta^{13}C = -24.3$‰) but not nearly as high as ^{13}C values obtained by using $^{13}CO_2$ alone. Together, these data showed that *M. yellowstonensis* strain MK1 is capable of growth using either CO_2 or organic C and that these processes may operate simultaneously (34).

Ex situ Assays Using Fe(III)-Oxide Mats

Evidence of a complete 3-HP/4-HB pathway in *M. yellowstonensis* strain MK1 is consistent with the observed incorporation of CO_2 using $^{13}CO_2$. The presence of these same genes in metagenome assemblies obtained from Fe(III)-oxide microbial mats (Fig. 1) suggested that this population may fix carbon dioxide *in situ*. To measure the uptake of CO_2 in Fe(III)-oxide microbial mats, excised mat samples were incubated *ex situ* with natural-abundance CO_2 and $^{13}CO_2$. The uptake of $^{13}CO_2$ into live Fe(III)-oxide mats was observed in two different geothermal communities studied (Table 2.2). Small increases in the ^{13}C content of killed controls were also observed, but these values were considerably lower than those observed with live mats and may be due to abiotic exchange between $^{13}CO_2$ and solid phases and/or incomplete sterility achieved by using sodium azide.

Discussion

The incorporation of $^{13}CO_2$ into live microbial Fe(III)-oxide mats demonstrated that organisms within these communities are capable of CO_2 fixation and that this is an important process *in situ*. We also showed that pure cultures of *M. yellowstonensis* strain

MK1, a significant community member in these Fe(III)-oxide microbial mats, grew using CO_2 as the sole C source in the absence of yeast extract (fractionation factor [ε] = 2.5‰). High-temperature acidic Fe(III)-oxide mat communities are typically composed of 5 to 7 major phylotypes, including *M. yellowstonensis* and *Hydrogenobaculum*-like populations, which represent 10 to 20% and 2 to 10% of the community, respectively, based on random sequence reads of mature Fe mat metagenomes (19, 24, 25). Other archaea present in these communities include members of two novel archaeal groups, the Thaumarchaeota and the Euryarchaeota (Thermoplasmatales-like), as well as other crenarchaea within the orders Thermoproteales and Desulfurococcales (19, 24, 25). However, sequence assemblies corresponding to these populations do not contain evidence of marker genes for known CO_2 fixation pathways and appear to be primarily heterotrophic (18, 19, 24, 25, 37, 41). Despite the diversity of archaea in these Fe(II)-oxidizing communities, the only known CO_2 fixation pathways found in metagenome sequence analyses included the 3-HP/4-HB pathway (contributed by *M. yellowstonensis*-like and other Sulfolobales populations) and the r-TCA cycle (contributed by *Hydrogenobaculum*-like populations). Thus, our working hypothesis is that *M. yellowstonensis*- and *Hydrogenobaculum*-like populations are the primary members of mature Fe(III)-oxide mat communities that contribute to the fixation of CO_2 into mat biomass.

Isotopic analysis of the major carbon pools (DIC, DOC, landscape carbon, and Fe mat carbon) from three geothermal sites showed that mat carbon exhibits an isotopic composition of ~−16.1‰ (σ = 1.3‰) (Table 2.3), which is between the ^{13}C contents of

DIC and DOC (or landscape C) end members (Table 2.3). Therefore, the ^{13}C values of mat C can be explained as a mixture of biomass carbon originating from DIC (i.e., autotrophy), DOC, and/or landscape C (heterotrophy) and, simultaneously, as a possible mixture of biomass carbon and exogenous landscape C from foreign sources (e.g., plant material, insects, landscape detritus, and eukaryal biomass), although any visible macroscopic debris was avoided during sampling. An isotope mixing model (Fig. 2) was developed to predict the isotopic composition of C present in Fe(III)-oxide microbial mats as a function of (i) the fraction of biomass C of DIC origin (fDIC-Biomass) and (ii) the fraction of biomass C relative to total mat C (fBiomass-C) (Fig. 2). Given the similarity of $\delta^{13}C$ values for DOC and landscape C (−22 to −26‰), it is not possible to distinguish heterotrophic biomass generated from either of these carbon sources. Carbon isotope fractionation factors for heterotrophic metabolism are near 0‰ (32); consequently, the ^{13}C content of biomass C generated from either DOC or landscape C will also range from ∼−22 to −26‰.

Two different isotopic mixing models were evaluated based on autotrophic contributions from either the 3-HP/4-HB cycle (*M. yellowstonensis*) or the r-TCA cycle (*Hydrogenobaculum* spp.) (Fig. 2). Fractionation factors for the conversion of DIC to microbial biomass were obtained either in this study (*M. yellowstonensis*, $\varepsilon = 2.5‰$) or from literature sources (*Hydrogenobaculum*, $\varepsilon = 5.5‰$ [31]). Estimates of the autotrophic contribution to biomass C ($f_{DIC\text{-}Biomass}$) (x axis in Fig. 2) are relatively insensitive to the range of fractionation factors available for the conversion of CO_2 to microbial biomass, due to the large differences in $\delta^{13}C$-DIC versus $\delta^{13}C$-DOC values. Although the fixation

of CO_2 can also be weighted based on the relative ratio of the amount of *Metallosphaera* to the amount of *Hydrogenobaculum* observed in random metagenome sequencing (~4:1), the model solution falls between those shown for the two cases based on either organism alone (Fig. 2A and B).

The average observed Fe(III)-oxide mat $\delta^{13}C$ value of −16.1‰ (Fig. 2, dotted line) is constrained by a unique set of the fraction of DIC in microbial biomass ($f_{DIC\text{-}Biomass}$) versus the fraction of microbial biomass C relative to total Fe mat C ($f_{Biomass\text{-}C}$). The observed ^{13}C isotopic composition can be explained only when the $f_{DIC\text{-}Biomass}$ ranges from about 0.42 to >0.99, depending on the dilution of microbial biomass C with nonmicrobial C from landscape sources (Fig. 2). Greater contributions of nonmicrobial landscape C to Fe mat C result in correspondingly higher estimates of $f_{DIC\text{-}Biomass}$. In the simplest case, where the Fe mat contains no exogenous landscape C ($f_{Biomass\text{-}C} = 1$), the mat ^{13}C content is explained by $f_{DIC\text{-}Biomass}$ values of ~0.42 to 0.50, depending on whether CO_2 is fractionated via the 3-HP/4-HB or r-TCA pathway (Fig. 2A and B). Interestingly, this is greater than, but agrees favorably with, the absolute abundance of the two primary DIC-fixing populations identified previously by using metagenome sequencing (the combined abundance of *Metallosphaera* and *Hydrogenobaculum* populations has ranged from 20 to 35% of the community). Growth and turnover rates of all populations present in these communities may not be equal, and less abundant, faster-growing autotrophic populations (relative to heterotrophic populations) could also influence observed mat $\delta^{13}C$ values. It is possible that heterotrophic populations present in these communities utilize biomass or metabolites produced only from autotrophs (i.e., classical primary

production), which would correspond to $f_{DIC\text{-}Biomass}$ values close to 1. In this scenario, nearly 50 to 60% of the total mat C would have to be nonmicrobial C from landscape sources (Fig. 2).

The total C content of Fe-oxide microbial mats is ~1%, and only a fraction of this carbon (as much as 10%) can be accounted for in estimates of live-cell counts (~10^9 cells g^{-1}) (18, 24, 25, 38), although the filamentous nature of specific phylotypes makes accurate cell counting difficult. The remaining carbon present in Fe(III)-oxide mats is comprised of dead microbial biomass generated *in situ* and/or exogenous landscape C. The sorption of DOC by Fe(III)-oxides may also contribute to mat C (39); however, the available surface sites of the amorphous Fe(III)-oxide phases present in these systems are nearly saturated with arsenate as bidentate surface complexes (16). Consequently, future efforts should focus on evaluation of live versus dead biomass C, other solid phases of exogenous C, and a more detailed characterization of components comprising the DOC fraction.

Results from this study have important implications for possible microbial interactions occurring among community members in thermoacidic Fe(II)-oxidizing microbial communities. The isotopic composition of total mat C in all three springs showed that CO_2 fixation is an important process *in situ*, which provides a source of organic carbon and numerous possible substrates for heterotrophic community members. These data are consistent with the hypothesis that *M. yellowstonensis* and *Hydrogenobaculum* spp. serve founding roles in the development of Fe(III)-oxide mats and community succession (23, 40). Now that the incorporation of inorganic carbon by

members of these communities has been firmly established, more detailed trophic cascades and metabolite interactions may be resolvable by using stable-isotope probing coupled with metabolomic and/or proteomic analyses. Colonization by one or both of the predominant CO_2-fixing populations (*Metallosphaera* and *Hydrogenobaculum*) may be a necessary condition for establishing acidothermophilic Fe(III)-oxide mat communities, which also support significant heterotrophic diversity.

Acknowledgements

We acknowledge and appreciate funding from the National Science Foundation Integrative Graduate and Education Training (IGERT) Program (DGE 0654336) for support to R.M.J.; the Howard Hughes Undergraduate Fellowship Program for support to L.M.W.; the Department of Energy Genome Science Program, Microbial Interactions Foundational Science Focus Area (Pacific Northwest National Laboratory subcontract 112443 to Montana State University); and the Montana Agricultural Experiment Station (project 911300 to W.P.I.).

We appreciate research permits (permit no. YELL-5568, 2007-2010) managed by C. Hendrix and S. Gunther (Center for Resources, YNP) and discussion with J. Beam, Z. Jay, M. Kozubal, and M. Romine.

TABLE 2.1
Carbon isotope values of *M. yellowstonensis* strain MK1 biomass in growth experiments using labeled versus unlabeled CO_2 and 1% yeast extract

Growth condition	Mean $\delta^{13}C$ value (‰) (σ) (n = 3)		
	C source	MK1 biomass	
		Culture 1	Culture 2
1% YE	−25.1 (0.04)	−24.2 (0.2)	−24.4 (0.2)
NA CO_2	−15.9 (0.2)	−19.3 (1.1)	−17.6 (0.8)
NA CO_2 + 1% YE		−23.2 (0.1)	−23.2 (0.1)
$^{13}CO_2$		71,500 (14,373)	80,637 (4,166)
$^{13}CO_2$ + 1% YE		1,677 (37)	1,540 (153)

TABLE 2.2

Carbon isotope composition of microbial mat samples incubated after *ex situ* experiments to detect CO_2 uptake in Fe(III)-oxide microbial mat communities from Norris Geyser Basin, YNP, October 2011

Treatment	Sample[a]	$\delta^{13}C$ value (‰) (σ) (n = 3)
CO_2 NA, live mat	OSP_B	−16.1 (0.1)
CO_2 NA, live mat	GRN_D	−13.8 (0.2)
$^{13}CO_2$, live mat	OSP_B, assay 1	1,278 (61)
$^{13}CO_2$, live mat	GRN_D, assay 1	1,267 (95)
$^{13}CO_2$, live mat	GRN_D, assay 2	1,458 (54)
$^{13}CO_2$, killed	OSP_B	27.3 (2.0)
$^{13}CO_2$, killed	GRN_D	46.9 (3.7)

[a] OSP_B, One Hundred Springs Plain Spring site B; GRN_D, Grendel Spring site D.

TABLE 2.3

Carbon isotope ratios of dissolved inorganic carbon, dissolved organic C, and total C present in Fe(III)-oxide microbial mats collected from Norris Geyser Basin, YNP, 2011 to 2013

Carbon pool	Sample[a]	$\delta^{13}C$ value (‰) (σ) (no. of samples)	Concn (mg kg^{-1}) (σ) (no. of samples)[b]
DIC	OSP_B	−5.1 (0.8) (3)	1.5 (0.8) (3)
	BE_D	−3.2 (0.2) (4)	2.0 (1.9) (4)
	GRN_D	−0.5 (2.6) (3)	0.6 (0.1) (3)
DOC	OSP_B	−21.0 (1.6) (3)	0.8 (0.5) (3)
	BE_D	−22.3 (1.0) (5)	0.8 (0.7) (4)
	GRN_D	−23.0 (2.1) (4)	0.6 (0.2) (3)
Microbial mat[c]	OSP_B	−15.0 (1.8) (3)	10,200
	BE_D	−16.4 (1.1) (8)	11,500
	GRN_D	−16.5 (0.9) (3)	7,600

[a] OSP_B, One Hundred Springs Plain Spring site B; BE_D, Beowulf Spring site D; GRN_D, Grendel Spring site D.

[b] Expressed as mg per liter for DIC and DOC and mg per kg (dry weight) for microbial mat C.

[c] The total C level was determined on aggregate mat samples from each site during this time frame (n = 1). The range of 0.8 to 1.5% total C agrees favorably with values observed in previous studies (16).

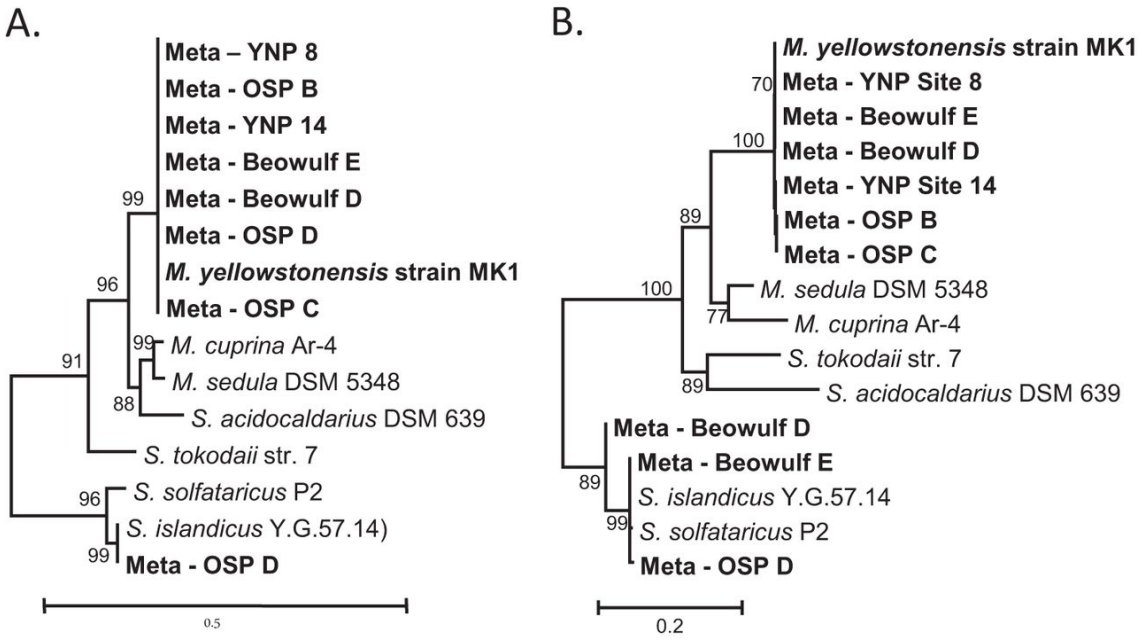


FIGURE 2.1

Phylogenetic trees of key proteins in the 3-HP/4-HB pathway for fixation of carbon dioxide (9). (A) Type I 4-hydroxybutyryl-CoA dehydratase (4HCD); (B) biotin carboxylase subunit of bifunctional acetyl/propionyl-CoA carboxylase (AccC). *Metallosphaera yellowstonensis*-like type I 4HCD and biotin carboxylase sequences were identified in numerous replicate metagenome samples from high-temperature Fe(III)-oxide microbial mats (Beowulf sites D and E, One Hundred Springs Plain sites B and C, YNP_8, and YNP_14).

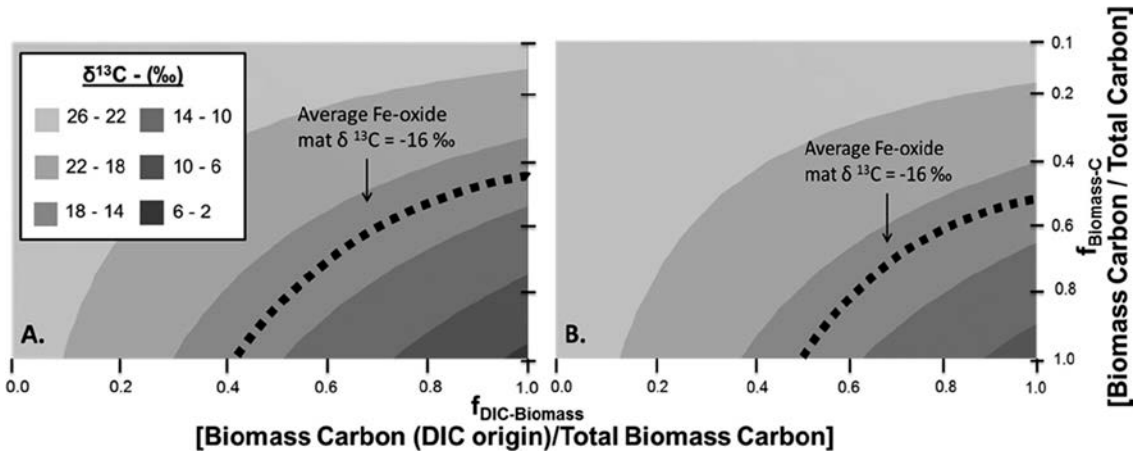


FIGURE 2.2
Predicted $\delta^{13}C$ content of Fe(III)-oxide microbial mats as a function of the fraction of microbial biomass originating from dissolved inorganic C (DIC) relative to total biomass C (x axis) and the fraction of biomass C relative to total Fe mat C (y axis). Fixation of CO_2 may occur via the 3-HP/4-HB pathway (i.e., *M. yellowstonensis*) (A) or the r-TCA pathway (i.e., *Hydrogenobaculum* sp.) (B). The isotope mixing model was based on the measured isotope composition of DIC, DOC, and landscape C sources and specific fractionation factors for the conversion of CO_2 to microbial biomass (see Materials and Methods). The average observed ^{13}C content ($\delta^{13}C$, ~−16‰) (dotted line) from replicate Fe(III)-oxide microbial mats shows that at least 42 to 50% of the biomass carbon has a DIC origin.

References

1. Karner MB, DeLong EF, Karl DM. 2001. Archaeal dominance in the mesopelagic zone of the Pacific Ocean. Nature 409:507–510. doi:10.1038/35054051.

2. Pearson A, McNichol AP, Benitez-Nelson BC, Hayes JM, Eglinton TI. 2001. Origins of lipid biomarkers in Santa Monica Basin surface sediment: a case study using compound-specific δ14C analysis. Geochim. Cosmochim. Acta 65:3123–3137. doi:10.1016/S0016-7037(01)00657-3.

3. Könneke M, Bernhard AE, De la Torre JR, Walker CB, Waterbury JB, Stahl DA. 2005. Isolation of an autotrophic ammonia-oxidizing marine archaeon. Nature 437:543–546. doi:10.1038/nature03911.

4. Tully BJ, Nelson WC, Heidelberg JF. 2012. Metagenomic analysis of a complex marine planktonic thaumarchaeal community from the Gulf of Maine. Environ. Microbiol. 14:254–267. doi:10.1111/j.1462-2920.2011.02628.x.

5. Huber H, Huber R, Stetter KO. 2006. Thermoproteales, p 10–22. In Dworkin M, Falkow S, Rosenberg E, Schleifer K-H, Stackebrandt E (ed), The prokaryotes. Springer, New York, NY.

6. Huber H, Prangishvili D. 2006. Sulfolobales, p 23–51. In Dworkin M, Falkow S, Rosenberg E, Schleifer K-H, Stackebrandt E (ed), The prokaryotes. Springer, New York, NY.

7. Huber H, Stetter KO. 2006. Desulfurococcales, p 52–68. In Dworkin M, Falkow S, Rosenberg E, Schleifer K-H, Stackebrandt E (ed), The prokaryotes. Springer, New York, NY.

8. Hügler M, Huber H, Stetter KO, Fuchs G. 2003. Autotrophic CO2 fixation pathways in archaea (Crenarchaeota). Arch. Microbiol. 179:160–173. doi:10.1007/s00203-002-0512-5.

9. Berg IA, Kockelkorn D, Buckel W, Fuchs G. 2007. A 3-hydroxypropionate/4-hydroxybutyrate autotrophic carbon dioxide assimilation pathway in archaea. Science 318:1782–1786. doi:10.1126/science.1149976.

10. Huber H, Gallenberger M, Jahn U, Eylert E, Berg IA, Kockelkorn D, Eisenreich W, Fuchs G. 2008. A dicarboxylate/4-hydroxybutyrate autotrophic carbon assimilation cycle in the hyperthermophilic archaeum Ignicoccus hospitalis. Proc. Natl. Acad. Sci. U. S. A. 105:7851–7856. doi:10.1073/pnas.0801043105.

11. Zhang L-M, Offre PR, He J-Z, Verhamme DT, Nicol GW, Prosser JI. 2010. Autotrophic ammonia oxidation by soil Thaumarchaea. Proc. Natl. Acad. Sci. U. S. A. 107:17240–17245. doi:10.1073/pnas.1004947107.

12. Rusch DB, Halpern AL, Sutton G, Heidelberg KB, Williamson S, Yooseph S, Wu D, Eisen JA, Hoffman JM, Remington K, Beeson K, Tran B, Smith H, Baden-Tillson H, Stewart C, Thorpe J, Freeman J, Andrews-Pfannkoch C, Venter JE, Li K, Kravitz S, Heidelberg JF, Utterback T, Rogers Y-H, Falcón LI, Souza V, Bonilla-Rosso G, Eguiarte LE, Karl DM, Sathyendranath S, Platt T, Bermingham E, Gallardo V, Tamayo-Castillo G, Ferrari MR, Strausberg RL, Nealson K, Friedman R, Frazier M, Venter JC. 2007. The Sorcerer II global ocean sampling expedition: northwest Atlantic through eastern tropical Pacific. PLoS Biol. 5:e77. doi:10.1371/journal.pbio.0050077.

13. Ramos-Vera WH, Berg IA, Fuchs G. 2009. Autotrophic carbon dioxide assimilation in Thermoproteales revisited. J. Bacteriol. 191:4286–4297. doi:10.1128/JB.00145-09.

14. Konhauser KO. 1998. Diversity of bacterial iron mineralization. Earth Sci. Rev. 43:91–121. doi:10.1016/S0012-8252(97)00036-6.

15. Nordstrom DK, Southam G. 1997. Geomicrobiology of sulfide mineral oxidation. Rev. Miner. Geochem. 35:361–390.

16. Inskeep WP, Macur RE, Harrison G, Bostick BC, Fendorf S. 2004. Biomineralization of As(V)-hydrous ferric oxyhydroxide in microbial mats of an acid-sulfate-chloride geothermal spring, Yellowstone National Park. Geochim. Cosmochim. Acta 68:3141–3155. doi:10.1016/j.gca.2003.09.020.

17. Kozubal MA, Macur RE, Korf S, Taylor WP, Ackerman GG, Nagy A, Inskeep WP. 2008. Isolation and distribution of a novel iron-oxidizing crenarchaeon from acidic geothermal springs in Yellowstone National Park. Appl. Environ. Microbiol. 74:942–949. doi:10.1128/AEM.01200-07.

18. Kozubal MA, Romine M, Jennings RM, Jay ZJ, Tringe SG, Rusch DB, Beam JP, McCue LA, Inskeep WP. 2013. Geoarchaeota: a new candidate phylum in the Archaea from high-temperature acidic iron mats in Yellowstone National Park. ISME J. 7:622–634. doi:10.1038/ismej.2012.132.

19. Inskeep WP, Jay ZJ, Herrgard MJ, Kozubal MA, Rusch DB, Tringe SG, Macur RE, Jennings RM, Boyd ES, Spear JR, Roberto FF. 2013. Phylogenetic and functional analysis of metagenome sequence from high-temperature archaeal habitats demonstrate linkages between metabolic potential and geochemistry. Front. Microbiol. 4:95. doi:10.3389/fmicb.2013.00095.

20. Takacs-Vesbach C, Inskeep WP, Jay ZJ, Herrgard MJ, Rusch DB, Tringe SG, Kozubal MA, Hamamura N, Macur RE, Fouke BW, Reysenbach A-L, McDermott TR, Jennings RM, Hengartner NW, Xie G. 2013. Metagenome sequence analysis of filamentous microbial communities obtained from geochemically distinct geothermal channels reveals specialization of three Aquificales lineages. Front. Microbiol. 4:84. doi:10.3389/fmicb.2013.00084.

21. Boyd ES, Leavitt WD, Geesey GG. 2009. CO2 uptake and fixation by a thermoacidophilic microbial community attached to precipitated sulfur in a geothermal spring. Appl. Environ. Microbiol. 75:4289–4296. doi:10.1128/AEM.02751-08.

22. Hügler M, Huber H, Molyneaux SJ, Vertriani C, Sievert SM. 2007. Autotrophic CO2 fixation via the reductive tricarboxylic acid cycle in different lineages within the phylum Aquificae: evidence for two ways of citrate cleavage. Environ. Microbiol. 9:81–92. doi:10.1111/j.1462-2920.2006.01118.x.

23. Macur RE, Langner HW, Kocar BD, Inskeep WP. 2004. Linking geochemical processes with microbial community analysis: successional dynamics in an arsenic-rich, acid-sulphate-chloride geothermal spring. Geobiology 2:163–177. doi:10.1111/j.1472-4677.2004.00032.x.

24. Kozubal MA, Macur RE, Jay ZJ, Beam JP, Malfatti SA, Tringe SG, Kocar BD, Borch T, Inskeep WP. 2012. Microbial iron cycling in acidic geothermal springs of Yellowstone National Park: integrating molecular surveys, geochemical processes, and isolation of novel Fe-active microorganisms. Front. Microbiol. 3:109. doi:10.3389/fmicb.2012.00109.

25. Inskeep WP, Rusch DB, Jay ZJ, Herrgard MJ, Kozubal MA, Richardson TH, Macur RE, Hamamura N, Jennings RM, Fouke BW, Reysenbach A-L, Roberto F, Young M, Schwartz A, Boyd ES, Badger JH, Mathur EJ, Ortmann AC, Bateson M, Geesey G, Frazier M. 2010. Metagenomes from high-temperature chemotrophic systems reveal geochemical controls on microbial community structure and function. PLoS One 5:e9773. doi:10.1371/journal.pone.0009773.

26. Berg IA, Kockelkorn D, Ramos-Vera WH, Say RF, Zarzycki J, Hügler M, Birgit E, Alber BE, Fuchs G. 2010. Autotrophic carbon fixation in archaea. Nat. Rev. Microbiol. 8:447–460. doi:10.1038/nrmicro2365.

27. Inskeep WP, Jay ZJ, Tringe SG, Herrgård MJ, Rusch DB, YNP Metagenome Project Steering Committee and Working Group Members. 2013. The YNP metagenome project: environmental parameters responsible for microbial distribution in the Yellowstone geothermal ecosystem. Front. Microbiol. 4:67. doi:10.3389/fmicb.2013.00067.

28. Hügler M, Krieger RS, Jahn M, Fuchs G. 2003. Characterization of acetyl-CoA/propionyl-CoA carboxylase in Metallosphaera sedula: carboxylating enzyme in the 3-hydroxypropionate cycle for autotrophic carbon fixation. Eur. J. Biochem. 270:736–744. doi:10.1046/j.1432-1033.2003.03434.x.

29. Tamura K, Peterson D, Peterson N, Stecher G, Nei M, Kumar S. 2011. MEGA5: molecular evolutionary genetics analysis using maximum likelihood, evolutionary distance, and maximum parsimony methods. Mol. Biol. Evol. 28:2731–2739. doi:10.1093/molbev/msr121.

30. Coplen TB, Brand WA, Gehre M, Gröning M, Meijer HAJ, Toman B, Verkouteren RM. 2006. New guidelines for δ13C measurements. Anal. Chem. 78:2439–2441. doi:10.1021/ac052027c.

31. House CH, Schopf JW, Stetter KO. 2003. Carbon isotopic fractionation by archaeans and other thermophilic prokaryotes. Org. Geochem. 34:345–356. doi:10.1016/S0146-6380(02)00237-1.

32. Boschker HTS, Middelburg JJ. 2002. Stable isotopes and biomarkers in microbial ecology. FEMS Microbiol. Ecol. 40:85–95. doi:10.1111/j.1574-6941.2002.tb00940.x.

33. Hawkins AS, Han Y, Bennett RK, Adams MWW, Kelly RM. 2013. Role of 4-hydroxybutyrate-CoA synthetase in the CO2 fixation cycle in thermoacidophilic archaea. J. Biol. Chem. 228:4012–4022. doi:10.1074/jbc.M112.413195.

34. Auernik KS, Kelly RM. 2010. Physiological versatility of the extremely thermoacidophilic archaeon Metallosphaera sedula supported by transcriptomic analysis of heterotrophic, autotrophic, and mixotrophic growth. Appl. Environ. Microbiol. 76:931–935. doi:10.1128/AEM.01336-09.

35. Ehleringer JR, Monson RK. 1993. Evolutionary and ecological aspects of photosynthetic pathway variation. Annu. Rev. Ecol. Syst. 24:411–439. doi:10.1146/annurev.es.24.110193.002211.

36. Stowe LG, Teeri JA. 1978. The geographic distribution of C4 species of the Dicotyledonae in relation to climate. Am. Nat. 112:609–623. doi:10.1086/283301.

37. Beam JP, Jay ZJ, Kozubal MA, Inskeep WP. 2013. Niche specialization of novel Thaumarchaeota to oxic and hypoxic acidic geothermal springs of Yellowstone National Park. ISME J. doi:10.1038/ismej.2013.193.

38. Bernstein HC, Beam JP, Kozubal MA, Carlson RP, Inskeep WP. 2013. In situ analysis of oxygen consumption and diffusive transport in high-temperature acidic iron-oxide microbial mats. Environ. Microbiol. 15:2360–2370. doi:10.1111/1462-2920.12109.

39. Ali MA, Dzombak DA. 1996. Competitive sorption of simple organic acids and sulfate on goethite. Environ. Sci. Technol. 30:1061–1071. doi:10.1021/es940723g.

40. Beam JP, Jay ZJ, Kozubal MA, Inskeep WP. 2011. Distribution and ecology of thaumarchaea in geothermal environments, abstr PA-009. Abstr. 11th Int. Conf. Thermophiles Res., Big Sky, MT.

41. Jay ZJ, Rusch DB, Tringe SG, Bailey C, Jennings RM, Inskeep WP. 2014. Predominant Acidilobus-like populations from geothermal environments in Yellowstone National Park exhibit similar metabolic potential in different hypoxic microbial communities. Appl. Environ. Microbiol. 80:294–305. doi:10.1128/AEM.02860-13.

CHAPTER 3

THE EXTENT AND MECHANISMS OF CARBON DIOXIDE FIXATION ACROSS GEOCHEMICALLY DIVERSE HIGH-TEMPERATURE MICROBIAL COMMUNITIES

Contribution of Authors and Co-Authors

Manuscript in Chapter 3

Author: Ryan deM. Jennings

Contributions: Conceived and co-designed experiments. Performed gas analysis for all sites and conducted bioinformatic analysis of CO_2 fixation pathways. Analyzed carbon concentration and isotope data. Drafted and edited manuscript at all stages.

Co-Author: James J. Moran

Contributions: Data collection and analysis.

Co-Author: Zackary J. Jay

Contributions: Data collection and analysis.

Co-Author: Jacob P. Beam

Contributions: Data collection and analysis.

Co-Author: Laura M. Whitmore

Contributions: Data collection and analysis.

Co-Author: Mark A. Kozubal

Contributions: Data collection and analysis.

Co-Author: Helen W. Kreuzer

Contributions: Data collection and analysis.

Co-Author: William P. Inskeep

Contribution of Authors and Co-Authors Continued

Contributions: Conceived and designed experiments. Data collection and analysis. Manuscript drafting and editing at all stages.

Manuscript Information Page

Ryan deM. Jennings[a,b], James J. Moran[c]*, Zackary J. Jay[a,b], Jacob P. Beam[a,b], Laura M. Whitmore[c], Mark A. Kozubal[a,b], Helen W. Kreuzer[c], and William P. Inskeep[a,b]*
Journal Name: Nature Publishing Group Nature Geosciences Journal
_X Prepared for submission to a peer-reviewed journal
__Officially submitted to a peer-reviewed journal
__Accepted by a peer-reviewed journal
__Published in a peer-reviewed journal

Nature Publishing Group Nature Geosciences Journal
[a]Department of Land Resources and Environmental Sciences, Montana State University, Bozeman, Montana, USA
[b]Thermal Biology Institute, Montana State University, Bozeman, Montana, USA
[c]Pacific Northwest National Laboratories, Richland, Washington, USA

Abstract

The fixation of inorganic C is an important biogeochemical process at local and global scales, has been documented in all three domains of life, and results in the biosynthesis of a diverse suite of reduced organic compounds, which are utilized by numerous chemoorganoheterotrophs on the planet. The possibility that early life forms were thermophiles suggests that high-temperature environments are important sites for investigating broader trends in autotroph-heterotroph associations. Consequently, the primary aim of this study was to assess carbon dioxide fixation in high-temperature Fe(III)-oxide mats, elemental sulfur sediments, and filamentous streamer communities across a wide range in pH and geochemical conditions. Protein-encoding genes of the 3-hydroxypropionate/4-hydroxybutyrate (3-HP/4-HB), dicarboxylate/4-hydroxybutyrate (DC/4-HB), and reverse tricarboxylic acid (r-TCA) carbon dioxide fixation pathways were identified in assembled genome sequence corresponding to the predominant Crenarchaeota and Aquificales phylotypes observed across this diverse habitat range. Stable isotope (^{13}C) analysis of dissolved inorganic carbon (DIC), organic C (DOC) and landscape C were used to interpret ^{13}C compositional values obtained from replicate samples of microbial communities in environments ranging from pH 2.5 to 9.4. Isotope mixing models were developed based on average ^{13}C-DIC and ^{13}C-OC values (‰) measured in specific springs, and were informed by the relative abundances of different autotrophic organisms and respective fractionation factors for incorporation of CO_2. These calculations showed that microbial C of DIC-origin is a significant fraction of the total microbial C in Fe-oxide mats, sulfur sediments and filamentous streamer

communities. The significance of DIC as a carbon source in these energetically-rich environments provides a foundation for examining microbial interactions that are dependent on the activity of autotrophic organisms in simplified natural communities.

Introduction

The ability of an organism to synthesize its own biomass as well as vitamins and cofactors from inorganic carbon (autotrophy) is recognized as a major evolutionary advance (1). Inorganic C fixation is an important biogeochemical process at local and global scales. Annually, inorganic C fixation in terrestrial systems results in ~60 Pg C net primary production (NPP), while NPP in ocean systems totals ~45 Pg C y^{-1} (1 Pg = 10^{15} g) (2). Numerous organisms distributed throughout all three domains of life are capable of inorganic C fixation, and microorganisms constitute a significant fraction of the reduced C on Earth. The total number of microbes on the planet is estimated at 4-6 × 10^{30} cells, which corresponds to a carbon reservoir of 350-550 Pg (3). Yet, despite the widespread distribution and significance of microorganisms, the contribution of microbial inorganic C fixation to the global C cycle is not well-resolved (4, 5).

The fixation of carbon dioxide is important in numerous trophic webs globally and occurs via one of six currently known pathways in *Archaea*, *Bacteria* and/or *Eukarya*. On an energetic basis, the reduction of CO_2 to biomass C is extremely costly and organisms obtain this energy either from photons (i.e., phototrophy) or the oxidation of reduced chemical species (i.e., chemotrophy). The Calvin-Benson-Bassham (CBB) cycle and the 3-hydroxyproprionate (3-HP) cycle reduce CO_2 using light-energy harvested via different photosystems (6, 7). Pathways responsible for the fixation of CO_2

in chemotrophic organisms include the reductive tricarboxylic acid cycle, reductive acetyl-CoA pathway, 3-hydroxypropionate/4-hydroxybutyrate cycle, and the dicarboxylate/4-hydroxybutyrate cycle (8, 9). The plethora of inorganic electron donors in Earth systems that are available to drive chemolithoautotrophy include reduced forms of hydrogen, sulfur, nitrogen, arsenic, and numerous transition metals, such as iron and manganese.

The reductive tricarboxylic acid (r-TCA) cycle has been described in numerous lineages of *Bacteria*, including the hyperthermophilic Aquificales, which are known to inhabit marine hydrothermal vents and geothermal environments (10-13). The reductive acetyl-CoA (Wood-Ljungdahl) pathway has been described in acetogenic bacteria and methanogenic archaea, as well as sulfate-reducing bacteria and archaea (9), which are found in hypoxic environments including sediments, soils, sludge, and intestinal tracts (14-16). The 3-hydroxypropionate/4-hydroxybutyrate (3-HP/4-HB) cycle has been identified in several major lineages of *Archaea*, including the Crenarchaeaota (order Sulfolobales) and marine Thaumarchaeota (17, 18). The dicarboxylate/4-hydroxybutyrate (DC/4-HB) cycle is identical to the regenerative half of the 3-HP/4-HB cycle and has been identified in the Thermoproteales and Desulfurococcales (phylum Crenarchaeota) (19, 20). The DC/4-HB and 3-HP/4-HB cycles are homologous in the regeneration of acetyl-CoA from succinyl-CoA, and this branch of both pathways is marked by the presence of 4-hydroxybutyryl-CoA dehydratase (8, 9, 17). The DC/4-HB and 3-HP/4-HB cycles differ in the reductive portion of the pathway: phosphonenolpyruvate carboxylase (PEPc) catalyzes the reduction of CO_2 in the DC/4-HB cycle, while the bi-functional

acetyl/propionyl-CoA carboxylase catalyzes the reduction of inorganic carbon in the 3-HP/4-HB cycle.

Many cultured Sulfolobales are capable of inorganic C fixation via the 3-HP/4-HB pathway (21); however, the capacity for and extent of autotrophy within the Thermoproteales and Desulfurococcales is still unclear, as many isolated representatives from these orders will only grow on complex C (22-26). Consequently, different chemotrophic microorganisms, which occupy varied geochemical niches, utilize a wide range of electron donors to drive the reduction of CO_2 via different inorganic C fixation pathways. Despite the importance of these microbial mechanisms, little is known regarding the contribution of chemoautotrophic microorganisms to the fixation of CO_2 in local communities, which also makes scaling to global C cycles extremely difficult (4).

The contribution of inorganic C fixation to community biomass is a major question in the assembly and succession of microbial communities. High-temperature environments (e.g., deep sea hydrothermal systems and Yellowstone geothermal environments) are excellent habitats in which to study different microbial contributions to CO_2 fixation, in part due to the fact that these systems are energy-rich with respect to reduced inorganic constituents, and that these microbial communities are often dominated by only several phylotypes. Prior efforts to determine the importance of inorganic C fixation in high-temperature microbial communities have included stable isotope measurements (27-29), $^{14}CO_2$ incorporation assays (30), and genome-enabled analysis of microbial communities and important isolates (31-34). Stable isotope studies have been employed to dissect the trophic structure of numerous different ecosystems, and can provide direct evidence of primary mechanisms of C cycling in biological systems (35).

Although several prior efforts have reported on the ^{13}C content of dissolved inorganic and organic C (DIC and DOC, respectively) from different geothermal springs in YNP (36-38), little work has reported on the ^{13}C content of microbial community biomass present in these thermal environments. Consistent $\delta^{13}C$ (‰) values of DIC and DOC (averaging approximately -2.8‰ and -23‰, respectively) have been observed in selected springs from prior studies (38, 39). The large difference in ^{13}C content between inorganic and organic C pools has been used to evaluate the extent of CO_2 fixation in acidic Fe(III)-oxide microbial mats (39). Results from this prior study established a ^{13}C isotope fractionation factor ($\varepsilon = 2.5$) for the autotrophic iron-oxidizing population *Metallosphaera yellowstonensis*, and determined that inorganic C fixation contributes no less than ~ 40% of the microbial C in these biomineralized mat communities. *M. yellowstonensis* and *Hydrogenobaculum* are the dominant early-colonizing autotrophic populations, whereas heterotrophic organisms do not increase in abundance until ~ 15-30 d after initial colonization by autotrophs (40). It is hypothesized that the succession of heterotrophs is dependent on primary colonization by autotrophic organisms and that CO_2 incorporated into biomass and/or excreted as metabolites or exopolymeric substances represents an important source of C for subsequent colonizers (40). The extent to which autotroph-heterotroph interactions occur in other geothermal systems has not been studied extensively, despite significant interest in both the phylotypes responsible for autotrophy in microbial systems as well as the distribution of specific CO_2 fixation pathways as a function of geochemical conditions.

Assembled genome sequence of numerous different microbial populations (and several relevant YNP isolates) observed in different high-temperature systems across

YNP has revealed details of the CO_2 fixation pathways distributed as a function of geochemical conditions (e.g., pH, O_2, sulfide) (32-34). However, direct evidence of CO_2 fixation (and its extent) across disparate geochemical environments has not been obtained. Consequently, the primary objectives of this study were to i) determine the stable ^{13}C isotope contents of dissolved inorganic and organic C, exogenous landscape C, and microbial mat and/or sediment samples from YNP geothermal systems, ii) identify the abundance of different chemotrophic microbial populations capable of inorganic C fixation across sites, as well as the respective pathways responsible for this metabolism, and iii) evaluate the extent of microbial inorganic C fixation in chemotrophic communities using isotope mixing models informed from assembled metagenome sequence from these same sites. Results showed that inorganic carbon fixation is an important metabolic process in nearly all high-temperature (T ~ 70-85 ^oC) chemotrophic systems, including sulfur sediments, iron oxide microbial mats, and filamentous streamer communities ranging in pH from 2.5 to 9. The fixation of inorganic C by several deeply-branching thermophiles using different biochemical pathways reveals the importance of this fundamental process in establishing trophic food webs in extreme environments thought to be representative of habitats common in early Earth (41). Significant heterotrophic consumption of microbial C generated from DIC was evident in several habitats, as well as the possible heterotrophic consumption of DOC, and/or contributions from non-microbial biomass (i.e., landscape sources). Carbon isotope mixing models were used to establish minimum amounts of DIC-incorporation into microbial community biomass.

Methods

Sample Locations

The geothermal samples (Table 3.1) obtained in the current study encompassed a wide range of chemotrophic environments designed to capture major phylogenetic groups known to inhabit YNP geothermal systems (33, 34). These sites have been the subject of extensive prior characterization and represent three distinct habitat types: hypoxic sulfur sediments, iron oxide microbial mats, and filamentous streamer communities. The site names are not official, thus the coordinates are provided (Table S1). The pH of these geothermal systems ranged from 2.2 to 9.4, and the temperature ranged from 68° to 87°C (Table 3.1). Water samples were collected and analyzed for isotope content (^{13}C) and total concentration of dissolved (0.2 µm filtered) organic and inorganic carbon. Molecular samples were collected in sterile 50 mL tubes, transported on dry ice, and stored at -80 °C prior to metagenome sequencing and/or 16S rRNA amplicon sequencing (described in more detail in prior studies, (33, 34)).

Solid Phase Carbon Stable Isotope Analysis

Solid phase sediment, mat, and streamer stable carbon isotope ratios ($\delta^{13}C$) were measured using a Thermo-Finnegan (Bremen, Germany) Delta V Plus isotope ratio mass spectrometer coupled to a Costech Analytical Technologies (Valencia, CA, USA) 4010 Elemental Analyzer and a Zero-Blank autosampler. Approximately 8 to 15 mg of lyophilized sediment, mat, or streamer was placed into tin capsules (Costech Analytical Technologies) and analyzed. Samples from calcium carbonate systems (i.e. – Conch and Narrow Gauge) were pre-treated overnight in a 1 N HCl solution to remove the carbonate

mineral. Data were corrected using the point-slope method (42) to in-house Pacific Northwest National Laboratory (PNNL) glutamic acid standards, which were calibrated to U.S. Geological Survey (USGS) standard 40 ($\delta^{13}C$ = -26.39‰) and USGS standard 41 ($\delta^{13}C$ = +37.63‰) glutamic acid isotopic standards. Carbon stable isotope content is measured as a ratio, R ($^{13}C/^{12}C$), then reported as a delta (δ) value, where δ equals $(R_A/R_{Std} - 1) \times 1{,}000$ and R_A and R_{Std} are the isotope ratios of the sample and the internationally recognized standard, PeeDee belemnite (PDB).

Functional Analysis of *De Novo* Phylotype Genomes

Assembled genome sequence of numerous thermophilic microorganisms (33, 34) from YNP geothermal environments were evaluated for protein encoding genes responsible for inorganic C fixation. Genomes analyzed included *Hydrogenobaculum* spp. (Taxon ID 2522125046), *Sulfurihydrogenebium* spp. (Taxon ID 2551306708), *Thermocrinis* spp. (Taxon ID 2547132474), *Metallosphaera* spp. (Taxon ID 2508501049), Sulfolobales T1 (Taxon ID 2522125034), Sulfolobales T2 (Taxon ID 2522125035), *Sulfolobus* spp. (Taxon ID 2522125035), Thermoproteales T1 (Taxon ID 2522125038), Thermoproteales T2 (Taxon ID 2522125042), and Acidilobus T1 (Taxon ID 2522125037). Sequences were annotated by the Joint Genome Institute's Integrated Microbial Genome Expert Review (JGI – IMG/ER) pipeline (43). Genomes were evaluated for all genes in the rTCA, 3HP/4HB and/or DC/4HB cycles, and results tabulated in Supplemental Table 2.

Abundance of Different Inorganic
C Fixing Microorganisms across Sites

Random metagenome sequencing of sulfur sediments, Fe(III)-oxide mats, and filamentous streamer communities was performed using Sanger, 454, and/or Illumina technology. Raw metagenome reads were binned to previously compiled *de novo* genome assemblies (33, 34) at 90% nucleotide identity. The relative abundance of individual populations (i.e., genus-species level) was estimated as the percentage of individual sequence reads binned to each phylotype genome. Illumina sequenced 16S rRNA amplicons (iTags) were generated for microbial communities for which metagenomes were not available. The relative abundance was estimated as the percentage of amplicons for each operational taxonomic unit (OTU); sequences belonging to an OTU were grouped at the 99% nucleotide identity, and OTU sequences were then identified with high confidence to a reference set of long-fragment 16S rRNA gene sequences from geothermal features in YNP.

Mixing Model Construction

The ^{13}C stable-isotope composition of microbial mat samples was predicted using a mixing model, formulated on $\delta^{13}C$ values of dissolved inorganic C (DIC), dissolved organic C (DOC), and landscape organic C (OC), as well as the weighted fractionation factor based on the relative abundance of inorganic C fixing microorganisms in the community. The measured $\delta^{13}C$ of sulfur sediments, Fe(III)-oxide mats, and filamentous streamer communities may contain carbon from microbial biomass of inorganic C origin, microbial biomass of organic C origin, and exogenous non-biomass organic C. Given the range of observed $\delta^{13}C$-DIC values (-4.4 to 3.7 ‰) and the statistically similar $\delta^{13}C$

content of DOC and exogenous organic C (mean = -22.8 ‰, σ = 3.0), an isotope mixing model was developed for each system based the measured δ^{13}C-DIC and the mean δ^{13}C of dissolved organic carbon (DOC) and exogenous landscape C for all systems. Mat isotope values were predicted as a function of the ratios of microbial biomass of inorganic C origin relative to total microbial biomass ($f_{Microbial\text{-}DIC}$, where $f_{Microbial\text{-}DIC} + f_{Microbial\text{-}DOC/OC} = 1$) and the amount of biomass C relative to total mat C ($f_{Microbial\text{-}C}$, where $f_{Microbial\text{-}C} + f_{Non\text{-}microbial\text{-}C} = 1$). Weighted fractionation factors used in the mixing model were based on ε values reported for cultured relatives (28, 39, 44), and the relative abundance of each inorganic C fixing microorganism in the system (Table 3.2). A fractionation factor of 0‰ was assumed for the incorporation of organic carbon (45).

Results

^{13}C Content of DIC, DOC and Landscape Sources

The ^{13}C contents of dissolved inorganic and organic C pools measured across 15 geothermal systems (with significant replication) averaged -2.8 ‰ and -21.9 ‰, respectively (Figure 3.1). The δ^{13}C signature of either carbon pool is well-constrained; however, the ^{13}C-DIC values of spring waters containing > 0.7 mM DIC are most representative of geothermal sources of CO_2(g). The high DIC values (up to 20 mM) at Mammoth Hot Springs (MHS) reflect the dissolution of Madison limestone during ascent of hydrothermal fluids (46). The large majority of geothermal source pools and outflow channels sampled in this study exhibited DOC concentrations that were approximately 10-fold lower than DIC (Figure 3.1, Table 3.1). Moreover, many of these sites contained DOC levels near the analytical detection limit (~ 20-40 µM), which has also made it

difficult to obtain direct information regarding the composition of DOC in these systems. Nevertheless, the high concentrations of DIC relative to DOC in many geothermal springs suggest that microorganisms capable of CO_2 incorporation will be important members of many communities, and may provide reduced C (i.e., biomass and EPS) necessary for supporting heterotrophic populations.

The ^{13}C isotope content of potential landscape C sources was determined for animal dung (bison, wolf), needles, leaf, algal and cyanobacterial communities, and soils, which were collected from areas near and/or upslope of nearly all geothermal springs sampled. The average $\delta^{13}C$ values of landscape samples was -23.7 ‰ (n = 29) and ranged from -10.7 to -28.6 ‰ (Table S1). The less negative values (i.e., -10.7 ‰) were observed only in algae mats and are consistent with *Zygogonium* spp. (47). The average C isotope content of leaf, soil, and dung samples ($\delta^{13}C$ ~ -26 ‰) is consistent with the importance of C_3 photosynthesis as the primary C source in these samples (48). Landscape organic C may contribute to the total C present in geothermal samples either as C that was utilized to produce microbial biomass and/or as direct landscape sources.

^{13}C Content of Chemotrophic Iron Mats, Sulfur Sediments, and Streamer Communities

The ^{13}C content of microbial community samples were between the average $\delta^{13}C$ values for DIC and DOC (or landscape C) (Table 3.1). Mat and/or sediment samples exhibiting ^{13}C values closer to the ^{13}DIC value for that specific spring contain a greater amount of DIC-derived microbial C. Conversely, mat and/or sediment samples with ^{13}C values closer to ^{13}C-DOC or ^{13}C-landscape C (hereafter referred to as organic C, OC) may either reflect significant heterotrophic consumption of OC and/or the presence of

exogenous landscape C. Nearly all microbial samples exhibited ^{13}C values significantly higher (less negative) than ^{13}C-OC, which provides direct evidence for the presence of DIC-derived microbial biomass. Several S sediment communities (i.e., Monarch Geyser, Joseph's Coat Hot Springs [JC3_A, JC2_E]) exhibited ^{13}C values ranging from ~ -6 to -16 ‰, and all Fe(III)-oxide sites exhibited ^{13}C values ranging from ~ -8 to -16 ‰, which is indicative of significant DIC-derived biomass. Moreover, the ^{13}C content of filamentous streamer samples (containing different members of the Aquificales) showed that these communities exhibit significant, although variable amounts of autotrophic C fixation (Table 3.1). A more accurate determination of the amount of DIC-derived microbial C present in these communities is possible after considering the appropriate fractionation factors (below) for incorporation of ^{13}C-DIC and/or ^{13}C-OC into microbial biomass, which is dependent on the primary microorganisms present and their respective pathways for CO_2 fixation.

Abundance of Inorganic C
Fixing Microorganisms across Sites

Bacteria and/or archaea containing known pathways for the fixation of inorganic C were present at varying abundances in all microbial communities studied (Table 3.2). Microbial community members that did not contain known pathways for CO_2 fixation were lumped into heterotrophic populations for purposes of interpreting ^{13}C stable isotope data; the phylogeny and metabolic attributes of many of these populations are elucidated in more detail in other studies (25, 32, 40, 49, 50). The relative amount(s) of autotrophic populations varied considerably across the sample and habitat types evaluated (Table 3.2), and ranged from as high as 94.3% at MHS (e.g., *Sulfurihydrogenibium*-

dominated) to as low as 3.8% in Washburn Spring (sediment community), where the sample is heavily dominated by heterotrophic populations (33).

The most common phylotypes that contained CO_2 fixation pathways across these habitats included different members of the Sulfolobales (pH < 4), the Thermoproteales (pH 3-9), and the Aquificales (pH 3-9). *Metallosphaera yellowstonensis* and several other *Sulfolobus*-like organisms present in low pH Fe(III)-oxide microbial mats and sulfur sediments contained key marker genes of the 3HP/4HB pathway, and prior work has shown that *M. yellowstonensis* is a facultative autotroph in these habitats (39). *Caldivirga, Thermoproteus* and *Pyrobaculum* spp. were the predominant phylotypes capable of CO_2 fixation in higher pH (pH~ 5-9) sulfur sediment systems (Table 3.2) via the DC/4HB pathway (20, 25). However, pathway completeness of the DC/4HB cycle in several of the Thermoproteales phylotypes was more difficult to assess due to lower sequence coverage of *de novo* sequence assemblies (26). Nevertheless, pathway analysis indicated a high potential for CO_2 fixation in the Thermoproteales T1 (*Caldivirga*/*Vulcanisaeta*) and T2 (*Pyrobaculum*/*Thermoproteus*) phylotypes, and cultured isolates in these groups have been shown to grow autotrophically on CO_2 (20, 51). Members of the Aquificales were identified in acidic sulfur streamers and Fe(III)-oxide mats (i.e., *Hydrogenobaculum* spp.), circumneutral sulfur streamers (*Sulfurihydrogenibium* spp.), and higher-pH (> 7) filamentous ‘streamer’ communities (*Thermocrinis* spp.) (Table 3.2). All of the Aquificales phylotypes contained key marker genes and nearly complete pathways necessary for the fixation of CO_2 via the reductive TCA cycle, although slight variations exist regarding the mechanism of citrate cleavage among the three major lineages found in YNP (34) (Supplemental Table 2).

Fractionation factors (ε) for the incorporation of CO_2 into *Metallosphaera* biomass and other close Sulfolobales relatives via the 3HP/4HB pathway have been found to range from 0.2 to 3.6 ‰ (39, 44). For the DC/4HB pathway, ε values range from 2.0 to 2.9 ‰ in several Thermoproteales isolates (44), although initial estimates in a Thermoproteales isolate were greater (ε = 8.7 ‰) (52). Fractionation factors for Aquificales isolates range from 3.3 to 5.5 ‰, based on studies of representatives from the *Hydrogenobaculum*-like and *Thermocrinis*-like lineages (28, 44). Consequently, fractionation factors for the primary CO_2 fixation pathways identified in the dominant autotrophic populations present in these communities range from ~ 0.2 to 5.5 ‰. The fractionation of ^{13}C-OC (i.e., DOC or landscape C with an average ^{13}C composition of -23.1 ‰) into microbial biomass is assumed to be 0 ‰ (45).

Extent of Autotrophy

The extent of autotrophy cannot be ascertained directly from the abundance of populations with autotrophic potential, in part because most of these organisms are not obligate CO_2 fixers and may also obtain a fraction of their C from non-DIC sources. Moreover, the presence of exogenous OC in a microbial community sample will result in less ^{13}C, and must be factored in as a possible contribution to microbial community ^{13}C values. Consequently, the ^{13}C values of mat, streamer or sediment samples reflect contributions from DIC-derived and OC-derived microbial C as well as landscape sources, and must be interpreted using a mixing model with appropriate fractionation factors for either CO_2 fixation and/or incorporation of organic C (i.e., ε = 0‰). Weighted average fractionation factors based on predicted ε values and relative abundance

estimates were used to develop ^{13}C mixing models, which predicted the ^{13}C content of a community sample as a function of DIC-derived microbial C relative to total microbial C, and the ratio of microbial C to total mat C. Due to the small range of fractionation factors for conversion of ^{13}C-DIC into microbial biomass, and the large differences in $\delta^{13}C$-DIC and $\delta^{13}C$-OC, the isotope mixing models are relatively insensitive to the weighted average fractionation factor used in the calculations. The amount of microbial carbon relative to total carbon is difficult to determine accurately; however, the measured ^{13}C content can be used to constrain estimates of this parameter as a function of the ratio of DIC-derived microbial C to total microbial C (Figures 3.2–3.4).

With the exception of high-OC sediments in Crater Hills and Washburn Spring (Figure 3.2), sulfur sediment communities exhibited significant incorporation of DIC across a wide pH range from 2.0 - 6.2 (Figure 3.2). For example, the minimum fractions of DIC-microbial C in sulfur sediments from Joseph's Coat (JC2_E and JC3_A) and Monarch Geyser were > 50%. The primary autotrophs in low pH (pH < 3.0) sulfur systems include members of the Sulfolobales and Aquificales (*Hydrogenobaculum* spp.), while members of the Thermoproteales inhabit high S environments across a pH range from ~ 4 to 7 (Table 3.2). The lower fraction of DIC-microbial C relative to total microbial C (x-axis, Figure 3.2) observed in Crater Hills and Washburn Springs suggests contributions from heterotrophy (OC incorporation) and/or landscape C in the sample. Crater Hills is inhabited primarily by Sulfolobales populations (Table 3.2), which are capable of inorganic C fixation via the 3-HP/4-HB pathway, yet the minimum fraction of DIC-microbial C to total microbial C is quite low (< ~20%). Thus, the Crater Hills Sulfolobales populations (2 types) may utilize OC and/or the sample contains a high

amount of OC from landscape sources. The extent of autotrophy could exceed 50% of the microbial C if landscape C were to have contributed > 80% of the total sample C. Heterotrophic microorganisms constitute a significant fraction of the community (Table 3.2) present in Washburn Spring sediments (pH 6.4); this site is also in a depression (concave) and accumulates significant amounts of debris and landscape runoff. Both factors may contribute to the large fraction of ^{13}C-OC in these sediments.

The minimum fraction of DIC-microbial C in acidic Fe(III)-oxide mats ranged from 40 to 85% (Figure 3.3), and was consistent across several different types of Fe(III)-oxide systems (53). Moderately acidic (pH ~ 3.0-3.5) amorphous Fe(III)-oxide mats in Norris Geyser Basin (OSP_B, BE_D, and GRN_D) contain a relatively high abundance of heterotrophs, but at a minimum are comprised of 40 - 75% DIC-microbial C. An additional Fe(III)-oxide mat containing less arsenic also showed significant fractions of DIC-microbial C (ECH_B). Moreover, an extremely mineralized Fe(III)-oxide mat containing hematite (JC2_B, pH 2.5) showed a high relative abundance of organisms capable of inorganic C fixation (primarily Sulfolobales), and a minimum of 85% of the microbial C was predicted to be of DIC-origin (Figure 3.3). Consequently, definitive evidence was obtained showing significant autotrophy in numerous Fe(III)-oxide communities, and in all cases, metagenome sequence analysis confirmed the importance of different Sulfolobales genera and *Hydrogenobaculum* spp. as the primary autotrophic organisms in these systems, despite differences in pH (~ 2-4) and Fe(III)-oxide mineralogy (53, 54).

Filamentous streamer communities were sampled across a wide range of geochemical conditions (pH 3.0 - 9.4; high H_2S *vs.* high O_2), and in all cases, a

significant fraction of DIC-microbial C was observed (Figure 3.4). Different streamer communities included the low-pH Dragon Spring dominated by *Hydrogenobaculum*, the circumneutral (pH 6.4) Mammoth Hot Springs inhabited by *Sulfurihydrogenibium*, and the high-pH (pH 8 - 9) systems (Octopus and Conch Springs) with significant amounts of *Thermocrinis* spp. (Table 3.2). The direct evidence of inorganic C fixation, which occurs despite the different types of heterotrophic organisms distributed across this habitat range (34, 50), demonstrates the importance of the Aquificales and the r-TCA cycle in establishing high-temperature filamentous streamer communities.

Discussion

The primary thermophilic bacteria and archaea with known pathways for inorganic C fixation, and which were present in sites with significant fractions of DIC-derived microbial C included representatives of the Aquificales (3 different genera), as well as the Sulfolobales and Thermoproteales (phylum Crenarchaeota). The distribution of specific autotrophic populations as a function of geochemical parameters has shown that pH, sulfide, arsenic, and oxygen are among the most important variables that determine the presence or absence of specific genera (31, 32, 55-58). These chemotrophic organisms obtain energy for CO_2 fixation via the oxidation of electron donors including H_2, H_2S, S^0, As(III), and Fe(II). These chemolithoautotrophs are distributed based on metabolic (physiological) capabilities to utilize various electron donor-acceptor combinations, and provide reduced C to a wide range of heterotrophic assemblages that comprise the total microbial community. Reduced species of sulfur, H_2, ferrous Fe and arsenite appear to be the most important electron donors across the systems studied (e.g.,

Table 3.2), and in most cases, the respiration of autotrophic populations is coupled to the reduction of O_2 (e.g., Sulfolobales, Aquificales). Several sub-oxic autotrophic members of the Thermoproteales may also reduce elemental S, and/or arsenate (26). Consequently, our results show that inorganic C fixation occurs across extremely diverse geochemical conditions, and is responsible for significant amounts of microbial biomass important for supporting heterotrophic populations. The autotroph-heterotroph associations implicated from these ^{13}C stable-isotope measurements, combined with molecular data on community composition and function reveal that two to three major CO_2 fixation pathways are responsible for supporting a diverse array of different heterotrophic populations that are adapted to different geochemical circumstances (e.g., pH, oxygen, sulfur). The importance of autotrophy in thermal systems thought to be analogs of environments supporting early life on Earth (41) also suggest that trophic structure and heterotrophy are important themes in the evolution of co-adapted microbial populations among both the *Bacteria* and *Archaea*.

Stable ^{13}C isotope mixing models were used to constrain possible solutions to the observed ^{13}C content of Fe(III)-oxide, sulfur sediment and/or streamer microbial communities. Results demonstrated a minimum fraction of DIC-derived microbial C, which was greater than 40 - 50 % of total microbial C in many systems analyzed (x-axis, Figures 3.2–3.4). In some cases, further resolution of the fraction of non-microbial (i.e., landscape) C (y-axis, Figures 3.2–3.4) would assist in clarifying the extent of autotrophy, and this would be most beneficial in several sediment environments found in landscape depressions, which contain significant amounts of OC-derived microbial biomass and/or OC from landscape sources. Geothermal sites in concave topography (e.g., CH, WS)

receive significant inputs of landscape C through erosion, litter-fall and/or storm-water relative to convex systems (e.g., MHS, Conch Spring). Consequently, as it relates to the input of OC, landscape topography is a selective force in the establishment, assembly, and succession of geothermal microbial communities.

Chemoorganoheterotrophs in these high-temperature communities may obtain C sources from either DOC, landscape C and/or microbial biomass components produced by autotrophic community members. The similar ^{13}C contents of landscape C and geothermal DOC preclude the separation of these possible C sources to microbial community members using ^{13}C stable isotope analysis. Although little is known regarding the composition and availability of DOC in geothermal habitats (and should be addressed in future studies), the observed concentrations of DOC are considerably lower than DIC in the majority of systems examined (Figure 3.1). Recent succession studies in Fe(III)-oxide microbial mats (40) show that autotrophic organisms are early colonizers followed by increases in heterotrophs at later successional stages. These observations are consistent with the high amounts of DIC-derived microbial C observed in numerous Fe(III)-oxide mat systems (Figure 3.3), and which suggest that autotrophic C plays an important role in the succession of these communities. Higher concentrations of DOC were observed in Washburn Spring (1.0 mM, Table 3.1), and may explain the lower abundance of candidate autotrophs (3.8%, Table 3.2) in sediments present at this site. Moreover, a significant fraction of the total microbial C in these sediments is not of DIC-origin (Figure 3.2). The low-pH sulfur sediment site (Crater Hills) also contains a significant amount of DOC (~ 0. 2 mM), and this may contribute to the lower apparent autotrophic contribution to microbial C at this site.

The majority of high-temperature communities investigated exhibited significant fractions of DIC-derived microbial C across a wide range of geochemical conditions (e.g., S sediments, Fe(III)-oxide mats, filamentous streamers). Although autotrophic organisms were abundant in all sites that exhibited large fractions of DIC-derived microbial C, the absolute abundance of candidate autotrophs in these systems does not correlate with the minimum amounts of DIC-derived C established using ^{13}C mixing models. For example, the abundance of autotrophs in sites exhibiting > 90% DIC-derived C ranged from ~ 17 to 93% (Table 3.2). Consequently, other processes should be considered when interpreting the extent of DIC-derived microbial C versus the relative abundance of candidate autotrophs. Specifically, it cannot be assumed necessarily that the growth and turnover rates of autotrophic and heterotrophic microorganisms are equal. Viral predation likely impacts community members differentially, and could be one of the more important factors explaining lower autotroph abundances in communities with > 90 % DIC-derived microbial C. Future work on the composition and microbial utilization of thermogenic DOC, the relative turnover rates of autotrophs versus heterotrophs, and the activity of other metabolic processes (i.e., transcriptomics) will assist in defining the causal factors responsible for microbial community function and C cycling across these geochemically diverse systems.

Acknowledgements

The authors acknowledge support from the DOE-Pacific Northwest National Laboratory (subcontract no. 112443), the Department of Energy (DOE)-Joint Genome Institute Community Sequencing Program (CSP 787081), and the National Science Foundation IGERT (R. deM. J., J. P. B, and Z. J. J; DGE 0654336). Work conducted by the Pacific Northwest National Laboratory (Foundational Scientific Focus Area) and the Joint Genome Institute (DOE-AC02-05CH11231) is supported by the Genomic Science Program, Office of Biological and Environmental Research, U.S. DOE. The authors appreciate C. Carey and A. Mazurie (MSU) for Illumina metagenome and Tag data processing and thank C. Hendrix, S. Gunther, and D. Hallac (Center for Resources, YNP) for permitting this work in YNP (permits YELL-SCI-5068 and -5686).

Table 1. Key geochemical parameters, and ^{13}C stable isotope content (δ, **‰)** of dissolved inorganic C, dissolved organic C (DIC, DOC) and microbial mat C determined across 15 different high-temperature springs in Yellowstone National Park (WY, USA).

Site Type Location	pH	T °C	DIC mM	DOC mM	$\delta^{13}C$ DIC (‰) (σ, n)	$\delta^{13}C$ DOC (‰) (σ, n)	$\delta^{13}C$ Microbial Mat[1] (‰) (σ, n)[2]
Sulfur Sediments							
Crater Hills	2.0	76	0.13	.21	3.7 (3.1, 3)	-23.8 (0.2, 3)	-20.3 (0.7, 17)
Joseph's Coat 2 E	2.2	79	3.36	.06	-5.4	-24.9	-16.1 (0.5, 7)
Monarch Geyser	3.8	83	1.15	.05	-3.9 (0.8, 4)	-17.6 (1.8, 4)	-5.9 (1.1, 39)
Cistern Spring	4.5	79	0.67	.04	-4.3 (0.6, 4)	-18.3 (1.5, 4)	-18.6 (3.6, 47)
Josephs Coat 3 A	6.1	87	0.38	.05	-2.4	-16.9	-13.8 (1.0, 9)
Washburn Spring	6.2	72	3.85	1.01	0.9	-22.8	-23.4 (0.4, 9)
Acidic Fe-Oxide Mats							
Joseph's Coat 2 B	2.2	75	0.05	.05	-3.4 (1.4, 4)	-23.7 (1.05, 5)	-8.3 (0.5, 7)
Beowulf Spring D	2.9	68	1.02	.05	-3.2 (3.1, 8)	-22.7 (1.4, 8)	-15.4 (1.5, 41)
Grendel Spring D	3.4	70	0.20	.06	-3.9 (8.3, 2)	-22.8 (3.2, 2)	-16.3 (0.7, 15)
Echinus Geyser B	3.5	68	0.26	.03	-4.4 (0.4, 5)	-22.4 (0.95, 5)	-11.5 (0.8, 32)
100 Springs Plain B	3.5	74	0.23	.06	-3.7 (2.9, 8)	-22.9 (2.3, 8)	-14.5 (1.6, 22)
Streamer Communities							
Dragon Spring B	3.0	75	1.62	.05	-3.4	-23.9 (0.9, 2)	-9.1 (0.8, 7)
Narrow Gauge	6.3	72	13.16	.07	1.2 (1.2, 4)	-20.8 (3.5, 4)	-11.9 (0.6, 22)
Octopus Spring B	8.1	84	5.19	.02	-1.9 (0.15, 7)	-23.0 (1.7, 7)	-16.3 (0.6, 13)
Conch Spring B	9.4	85	3.43	.02	-2.5 (0.2, 9)	-21.8 (3.4, 9)	-4.5 (2.6, 9)

[1] $\delta^{13}C$ Microbial Mat = sulfur sediment, iron oxide mat, or filamentous streamer samples.
[2] Standard deviation and n are based on total number of replicates, including subsamples obtained at different sampling dates

Table 2. Relative abundance (R.A.)[1], expected inorganic C fixation pathways, and predicted fractionation factors (ε)[2], of candidate autotrophs in different geothermal systems of Yellowstone National Park.

Candidate Autotrophs	R.A. (%)[1]	C Fixation Pathway	ε (‰)[2]
Sulfur Sediments[5]			
Crater Hills			
Sulfolobales - T1	68.9	3-HP/4-HB	3.1
Sulfolobales - T2	7.9	3-HP/4-HB	3.6
Joseph's Coat 2 E			
Hydrogenobaculum	15.9	r-TCA	5.5
Sulfolobus spp.	2.5	3-HP/4-HB	0.2
Monarch			
Thermoproteales T1	14.5	DC/4-HB	2.0
Thermoproteales T2	2.9	DC/4-HB	2.9
Cistern			
Sulfolobales - T1	9.4	3-HP/4-HB	3.1
Sulfolobales - T2	0.8	3-HP/4-HB	3.6
Thermoproteales T1	26.2	DC/4-HB	2.0
Thermoproteales T2	23.6	DC/4-HB	2.9
Joseph's Coat 3 A			
Thermoproteales T1	14.4	DC/4-HB	2.0
Thermoproteales T2	25.5	DC/4-HB	2.9
Sulfolobales - T1	2.4	3-HP/4-HB	3.1
Thermocrinis spp.	0.4	r-TCA	3.3
Washburn			
Pyrobaculum T1	3.7	DC/4-HB	2.9
Thermoproteales T1	0.1	DC/4-HB	2.0
Filamentous Streamer Communities[5]			
Dragon B[6]			
Hydrogenobaculum	67.0	r-TCA	5.5
Narrow Gauge			
Sulfurihydrogenibium	94.3	r-TCA	5.5
Octopus B			
Pyrobaculum T1	8.7	DC/4-HB	2.9
Thermocrinis spp.	28.4	r-TCA	3.3
Conch B			
Pyrobaculum T1	15.0	DC/4-HB	2.9
Thermocrinis spp.	45.2	r-TCA	3.3

Candidate Autotrophs	R.A. (%)[1]	C Fixation Pathway	ε (‰)[2]
Iron Oxide Mats[5]			
Joseph's Coat 2 B[3]			
Stygiolobus spp.	53.1	3-HP/4-HB	3.6
Metallosphaera	29.3	3-HP/4-HB	2.5
Acidianus spp.	10.8	3-HP/4-HB	0.2
Beowulf East D			
Metallosphaera	7.2	3-HP/4-HB	2.5
Sulfolobus spp.	2.3	3-HP/4-HB	0.2
Hydrogenobaculum	2.5	r-TCA	5.5
Grendel D[4]			
Metallosphaera	7.2	3-HP/4-HB	2.5
Sulfolobus spp.	2.3	3-HP/4-HB	0.2
Hydrogenobaculum	2.5	rTCA	5.5
Echinus B			
Metallosphaera	9.7	3-HP/4-HB	2.5
Sulfolobus spp.	2.4	3-HP/4-HB	0.2
Sulfolobales - T2	0.6	3-HP/4-HB	3.6
Hydrogenobaculum	2.6	r-TCA	5.5
100 Springs Plain B			
Metallosphaera	13.2	3-HP/4-HB	2.5
Sulfolobus spp.	2.5	3-HP/4-HB	0.2
Hydrogenobaculum	3.1	r-TCA	5.5

[1] Relative abundance values are based on metagenome read recruitment to known *de novo* phylotype genomes, unless otherwise noted.
[2] Fractionation factor estimates are based on phylogenetic relationship of phylotypes to ε values reported for cultured isolates.
[3] Relative abundance estimates based on iTag data.
[4] Relative abundance estimates based on Beowulf East D.
[5] Other detailed descriptions of organisms present in these sites include: (25, 26, 33, 34, 40, 50, 54, 60, 61)

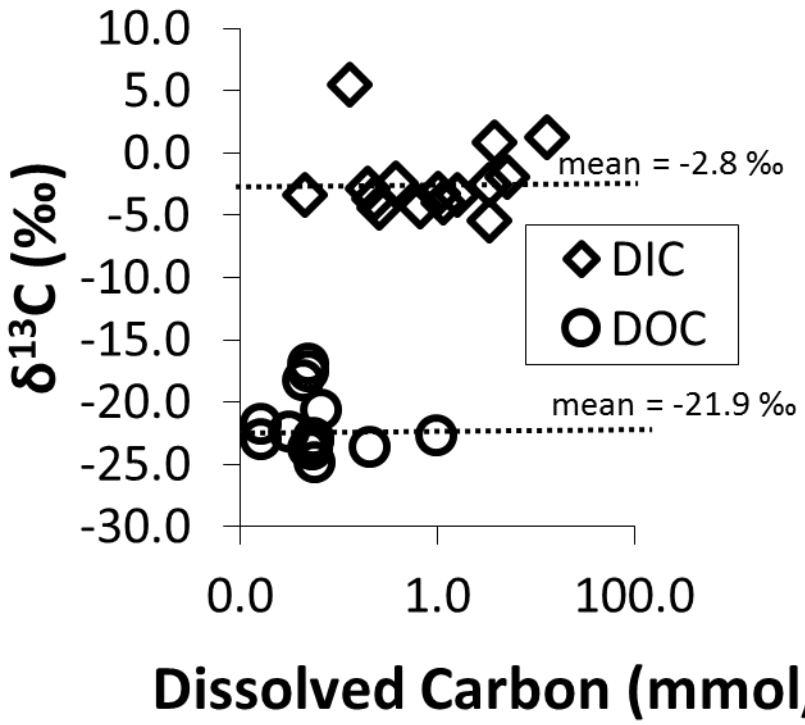


Figure 3.1. Concentration and stable carbon isotope content of dissolved organic C (DOC) and dissolved inorganic C (DIC) in fifteen geochemically diverse high temperature environments of Yellowstone National Park, WY, USA.

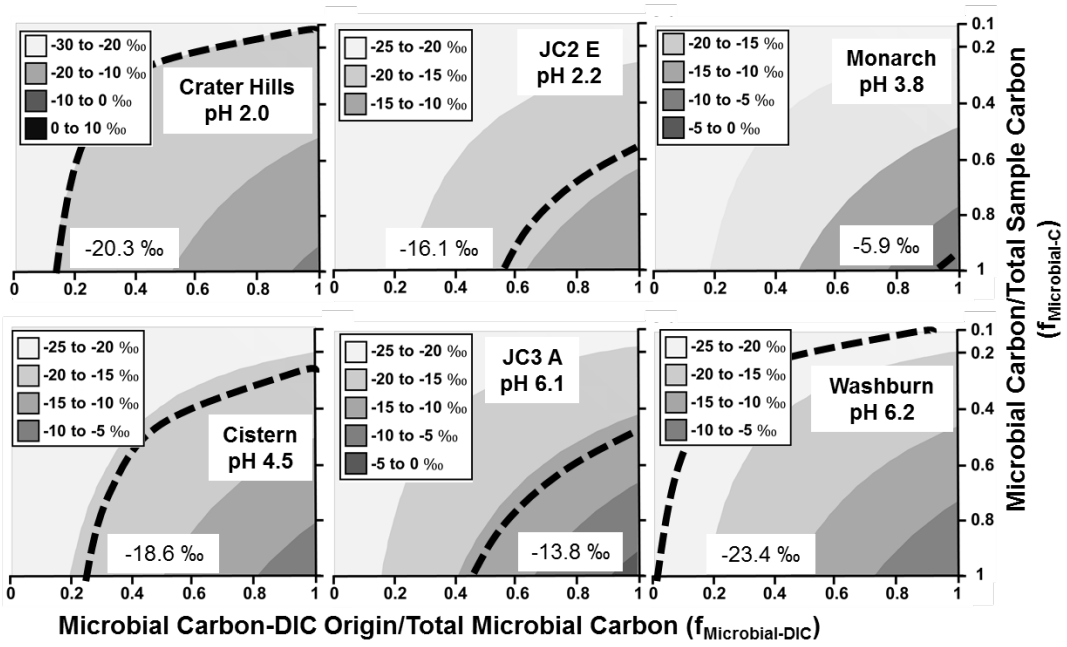


Figure 3.2. Isotope mixing models of sulfur sediment microbial communities. The fraction of microbial C of DIC origin relative to total microbial C ($f_{Microbial\text{-}DIC}$) is plotted as a function of the fraction of microbial C to total sample C ($f_{Microbial\text{-}C}$) where gray scale depicts the range of possible sample ^{13}C content. Dotted lines indicate possible combinations of $f_{Microbial\text{-}DIC}$ and $f_{Microbial\text{-}C}$ that are consistent with observed ^{13}C values (‰) of microbial samples (boxed).

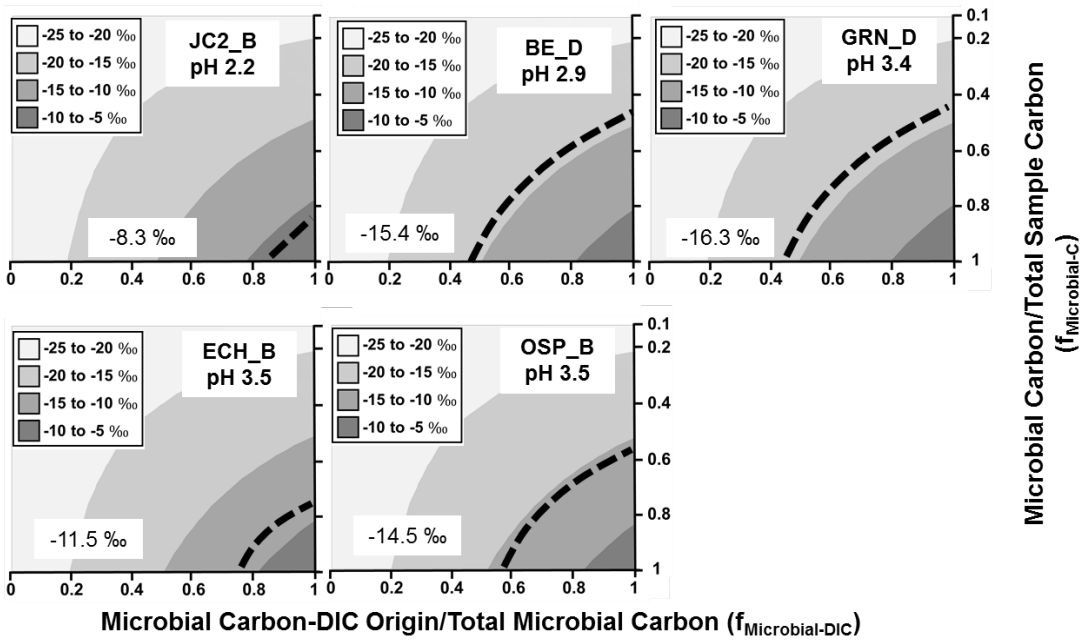


Figure 3.3. Isotope mixing models of acidic Fe(III)-oxide microbial communities. The fraction of microbial C of DIC origin relative to total microbial C ($f_{Microbial\text{-}DIC}$) is plotted as a function of the fraction of microbial C to total sample C ($f_{Microbial\text{-}C}$) where gray scale depicts the range of possible sample ^{13}C content. Dotted lines indicate possible combinations of $f_{Microbial\text{-}DIC}$ and $f_{Microbial\text{-}C}$ that are consistent with observed ^{13}C values (‰) of microbial samples (boxed).

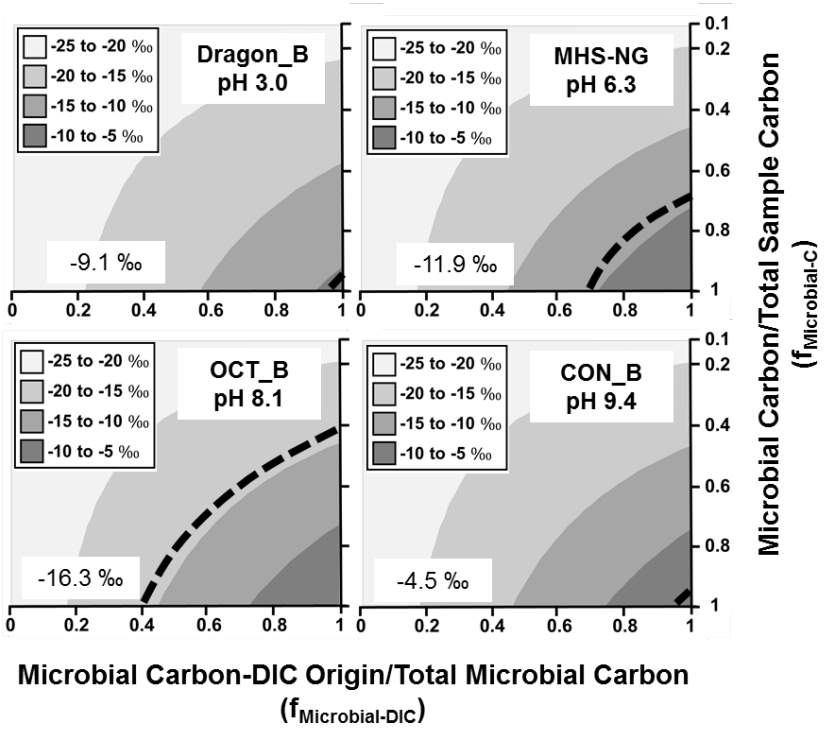


Figure 3.4. Isotope mixing models of thermophilic filamentous streamer communities. The fraction of microbial C of DIC origin relative to total microbial C ($f_{Microbial\text{-}DIC}$) is plotted as a function of the fraction of microbial C to total sample C ($f_{Microbial\text{-}C}$) where gray scale depicts the range of possible sample ^{13}C content. Dotted lines indicate possible combinations of $f_{Microbial\text{-}DIC}$ and $f_{Microbial\text{-}C}$ that are consistent with observed ^{13}C values (‰) of microbial samples (boxed).

References

1. Quayle JR, Ferenci T. Evolutionary aspects of autotrophy. Microbiol Rev. 1978;42(2):251-73.

2. Prentice IC, G.D. Farquhar, M.J.R. Fasham, M.L. Goulden, M. Heimann, V.J. Jaramillo, et al. The Carbon Cycle and Atmospheric Carbon Dioxide. Climate Change 2001: The Scientific Basis Contribution of Working Group I to the Third Assessment Report of the Intergovernmental Panel on Climate Change. 2001.

3. Whitman WB, Coleman DC, Wiebe WJ. Prokaryotes: the unseen majority. Proc Natl Acad Sci U S A. 1998;95(12):6578-83.

4. Shively JM, English RS, Baker SH, Cannon GC. Carbon cycling: the prokaryotic contribution. Curr Opin Microbiol. 2001;4(3):301-6.

5. Reinthaler T, van Aken HM, Herndl GJ. Major contribution of autotrophy to microbial carbon cycling in the deep North Atlantic's interior. Deep-Sea Res Pt Ii. 2010;57(16):1572-80.

6. Bryant DA, Frigaard NU. Prokaryotic photosynthesis and phototrophy illuminated. Trends Microbiol. 2006;14(11):488-96.

7. Blankenship RE. Early evolution of photosynthesis. Plant Physiol. 2010;154(2):434-8.

8. Berg IA, Kockelkorn D, Ramos-Vera WH, Say RF, Zarzycki J, Hugler M, et al. Autotrophic carbon fixation in archaea. Nat Rev Microbiol. 2010;8(6):447-60.

9. Hugler M, Sievert SM. Beyond the Calvin cycle: autotrophic carbon fixation in the ocean. Ann Rev Mar Sci. 2011;3:261-89.

10. Reysenbach A-L, Banta AB, Boone DR, Cary SC, Luther GW. Biogeochemistry: microbial essentials at hydrothermal vents. Nature. 2000;404(6780):835-.

11. Reysenbach AL, Ehringer M, Hershberger K. Microbial diversity at 83 degrees C in Calcite Springs, Yellowstone National Park: another environment where the Aquificales and "Korarchaeota" coexist. Extremophiles. 2000;4(1):61-7.

12. Reysenbach A-L, Gotz D, Banta A, Jeanthon C, Fouquet Y. Expanding the distribution of the Aquificales to the deep-sea vents on Mid-Atlantic Ridge and Central Indian Ridge. CBM-Cahiers de Biologie Marine. 2002;43(3-4):425-8.

13. Huber R, Eder W. Aquificales. In: Dworkin M, Falkow S, Rosenberg E, Schleifer K-H, Stackebrandt E, editors. The Prokaryotes: Springer New York; 2006. p. 925-38.

14. Breznak JA, Kane MD. Microbial H2/CO2 acetogenesis in animal guts: nature and nutritional significance1990 1990-12-01 00:00:00. 309-13 p.

15. Whitman W, Bowen T, Boone D. The Methanogenic Bacteria. In: Dworkin M, Falkow S, Rosenberg E, Schleifer K-H, Stackebrandt E, editors. The Prokaryotes: Springer New York; 2006. p. 165-207.

16. Drake HL, Gossner AS, Daniel SL. Old acetogens, new light. Ann N Y Acad Sci. 2008;1125:100-28.

17. Berg IA, Kockelkorn D, Buckel W, Fuchs G. A 3-hydroxypropionate/4-hydroxybutyrate autotrophic carbon dioxide assimilation pathway in Archaea. Science. 2007;318(5857):1782-6.

18. Walker CB, de la Torre JR, Klotz MG, Urakawa H, Pinel N, Arp DJ, et al. Nitrosopumilus maritimus genome reveals unique mechanisms for nitrification and autotrophy in globally distributed marine crenarchaea. Proc Natl Acad Sci U S A. 2010;107(19):8818-23.

19. Huber H, Gallenberger M, Jahn U, Eylert E, Berg IA, Kockelkorn D, et al. A dicarboxylate/4-hydroxybutyrate autotrophic carbon assimilation cycle in the hyperthermophilic Archaeum Ignicoccus hospitalis. Proc Natl Acad Sci U S A. 2008;105(22):7851-6.

20. Ramos-Vera WH, Berg IA, Fuchs G. Autotrophic carbon dioxide assimilation in Thermoproteales revisited. J Bacteriol. 2009;191(13):4286-97.

21. Huber H, Prangishvili D. Sulfolobales. In: Dworkin M, Falkow S, Rosenberg E, Schleifer K-H, Stackebrandt E, editors. The Prokaryotes: Springer New York; 2006. p. 23-51.

22. Huber H, Huber R, Stetter KO. Thermoproteales. Prokaryotes: A Handbook on the Biology of Bacteria, Vol 3, Third Edition. 2006:10-22.

23. Huber H, Stetter KO. Desulfurococcales. Prokaryotes: A Handbook on the Biology of Bacteria, Vol 3, Third Edition. 2006:52-68.

24. Boyd ES, Jackson RA, Encarnacion G, Zahn JA, Beard T, Leavitt WD, et al. Isolation, characterization, and ecology of sulfur-respiring crenarchaea inhabiting acid-sulfate-chloride-containing geothermal springs in Yellowstone National Park. Appl Environ Microbiol. 2007;73(20):6669-77.

25. Jay ZJ, Rusch DB, Tringe SG, Bailey C, Jennings RM, Inskeep WP. Predominant Acidilobus-like populations from geothermal environments in yellowstone national park exhibit similar metabolic potential in different hypoxic microbial communities. Appl Environ Microbiol. 2014;80(1):294-305.

26. Jay ZJ. Linking geochemistry with microbial community structure and function in sulfidic geothermal systems of Yellowstone National Park. 2015.

27. Estep MLF. Carbon and Hydrogen Isotopic Compositions of Algae and Bacteria from Hydrothermal Environments, Yellowstone-National-Park. Geochim Cosmochim Ac. 1984;48(3):591-9.

28. Jahnke LL, Eder W, Huber R, Hope JM, Hinrichs KU, Hayes JM, et al. Signature lipids and stable carbon isotope analyses of Octopus Spring hyperthermophilic communities compared with those of Aquificales representatives. Appl Environ Microbiol. 2001;67(11):5179-89.

29. Havig JR, Raymond J, Meyer-Dombard DAR, Zolotova N, Shock EL. Merging isotopes and community genomics in a siliceous sinter-depositing hot spring. Journal of Geophysical Research. 2011;116(G1).

30. Boyd ES, Leavitt WD, Geesey GG. CO2 Uptake and Fixation by a Thermoacidophilic Microbial Community Attached to Precipitated Sulfur in a Geothermal Spring. Applied and Environmental Microbiology. 2009;75(13):4289-96.

31. Inskeep WP, Rusch DB, Jay ZJ, Herrgard MJ, Kozubal MA, Richardson TH, et al. Metagenomes from high-temperature chemotrophic systems reveal geochemical controls on microbial community structure and function. PLoS One. 2010;5(3):e9773.

32. Inskeep WP, Jay ZJ, Tringe SG, Herrgard MJ, Rusch DB, Committee YNPMPS, et al. The YNP Metagenome Project: Environmental Parameters Responsible for Microbial Distribution in the Yellowstone Geothermal Ecosystem. Front Microbiol. 2013;4:67.

33. Inskeep WP, Jay ZJ, Herrgard MJ, Kozubal MA, Rusch DB, Tringe SG, et al. Phylogenetic and Functional Analysis of Metagenome Sequence from High-Temperature Archaeal Habitats Demonstrate Linkages between Metabolic Potential and Geochemistry. Front Microbiol. 2013;4:95.

34. Takacs-Vesbach C, Inskeep WP, Jay ZJ, Herrgard MJ, Rusch DB, Tringe SG, et al. Metagenome sequence analysis of filamentous microbial communities obtained from geochemically distinct geothermal channels reveals specialization of three aquificales lineages. Front Microbiol. 2013;4:84.

35. Peterson BJ, Fry B. Stable Isotopes in Ecosystem Studies. Annu Rev Ecol Syst. 1987;18:293-320.

36. Craig H. The Geochemistry of the Stable Carbon Isotopes. Geochim Cosmochim Ac. 1953;3(2-3):53-92.

37. Craig H. Isotopic Geochemistry of Hot Springs. Geol Soc Am Bull. 1953;64(12):1410-.

38. Bergfeld D, Lowenstern, J.B., Hunt, A.G., Shanks, W.C.P., III, and Evans, W.C. Gas and isotope chemistry of thermal features in Yellowstone National Park, Wyoming (ver. 1.1, September 2014): U.S. Geological Survey Scientific Investigations Report 2011–5012. 2014.

39. Jennings RM, Whitmore LM, Moran JJ, Kreuzer HW, Inskeep WP. Carbon dioxide fixation by Metallosphaera yellowstonensis and acidothermophilic iron-oxidizing microbial communities from Yellowstone National Park. Appl Environ Microbiol. 2014;80(9):2665-71.

40. Beam JP, Bernstein HC, Jay ZJ, Kozubal MA, Jennings Rd, Tringe SG, et al. Assembly and Succession of Iron Oxide Microbial Mat Communities in Acidic Geothermal Springs. Geobiology. 2015.

41. Nisbet EG, Sleep NH. The habitat and nature of early life. Nature. 2001;409(6823):1083-91.

42. Coplen TB, Brand WA, Gehre M, Groning M, Meijer HA, Toman B, et al. New guidelines for delta13C measurements. Anal Chem. 2006;78(7):2439-41.

43. Markowitz VM, Chen IM, Palaniappan K, Chu K, Szeto E, Grechkin Y, et al. IMG: the Integrated Microbial Genomes database and comparative analysis system. Nucleic Acids Res. 2012;40(Database issue):D115-22.

44. House CH, Schopf JW, Stetter KO. Carbon isotopic fractionation by Archaeans and other thermophilic prokaryotes. Organic Geochemistry. 2003;34(3):345-56.

45. Boschker HT, Middelburg JJ. Stable isotopes and biomarkers in microbial ecology. FEMS Microbiol Ecol. 2002;40(2):85-95.

46. Fouke BW. Hot-spring Systems Geobiology: abiotic and biotic influences on travertine formation at Mammoth Hot Springs, Yellowstone National Park, USA. Sedimentology. 2011;58(1):170-219.

47. Rothschild L, DesMarais D, Tharpe A. Ultraviolet Radiation Effects on Carbon Isotope Fractionation. 1998.

48. Ehleringer JR, Monson RK. Evolutionary and ecological aspects of photosynthetic pathway variation. Annu Rev Ecol Syst. 1993:411-39.

49. Beam JP, Jay ZJ, Kozubal MA, Inskeep WP. Niche specialization of novel Thaumarchaeota to oxic and hypoxic acidic geothermal springs of Yellowstone National Park. ISME J. 2014;8(4):938-51.

50. Colman DR, Jay ZJ, Inskeep WP, Jennings Rd, Maas KR, Rusch DB, et al. Characterization of Novel, Deep-branching Heterotrophic Bacterial Populations Recovered from Thermal Spring Metagenomes ISME J. 2015.

51. Schäfer S, Barkowski C, Fuchs G. Carbon assimilation by the autotrophic thermophilic archaebacterium Thermoproteus neutrophilus. Arch Microbiol. 1986;146(3):301-8.

52. Preuß A, Schauder R, Fuchs G, Stichler W. Carbon Isotope Fractionation by Autotrophic Bacteria with Three Different CO2 Fixation Pathways. Zeitschrift für Naturforschung C. 1989;44(5-6):397-402.

53. Kozubal MA, Macur RE, Jay ZJ, Beam JP, Malfatti SA, Tringe SG, et al. Microbial iron cycling in acidic geothermal springs of yellowstone national park: integrating molecular surveys, geochemical processes, and isolation of novel fe-active microorganisms. Front Microbiol. 2012;3:109.

54. Inskeep WP, Macur RE, Harrison G, Bostick BC, Fendorf S. Biomineralization of As(V)-hydrous ferric oxyhydroxide in microbial mats of an acid-sulfate-chloride geothermal spring, Yellowstone National Park. Geochim Cosmochim Ac. 2004;68(15):3141-55.

55. Macur RE, Langner HW, Kocar BD, Inskeep WP. Linking geochemical processes with microbial community analysis: successional dynamics in an arsenic-rich, acid-sulphate-chloride geothermal spring. Geobiology. 2004;2(3):163-77.

56. Inskeep W, Macur R, Ackerman G, Kozubal M, Taylor W, Korf S. Linking microbial and geochemical processes in geothermal habitats. Geochim Cosmochim Ac. 2005;69(10):A226-A.

57. Inskeep WP, Ackerman GG, Taylor WP, Kozubal M, Korf S, Macur RE. On the energetics of chemolithotrophy in nonequilibrium systems: case studies of geothermal springs in Yellowstone National Park. Geobiology. 2005;3(4):297-317.

58. Pearson A, Pi Y, Zhao W, Li W, Li Y, Inskeep W, et al. Factors controlling the distribution of archaeal tetraethers in terrestrial hot springs. Appl Environ Microbiol. 2008;74(11):3523-32.

59. Kozubal MA, Romine M, Jennings R, Jay ZJ, Tringe SG, Rusch DB, et al. Geoarchaeota: a new candidate phylum in the Archaea from high-temperature acidic iron mats in Yellowstone National Park. ISME J. 2013;7(3):622-34.

60. Beam JP, Jay ZJ, Schmid MC, Rusch DB, Romine MF, R MJ, et al. Ecophysiology of an uncultivated lineage of Aigarchaeota from an oxic, hot spring filamentous 'streamer' community. ISME J. 2015.

CHAPTER 4

GENOME-ENABLED MULTI-SCALE ANALYSIS OF AUTOTROPH-HETEROTROPH INTERACTIONS IN A HIGH-TEMPERATURE MICROBIAL COMMUNITY

Contribution of Authors and Co-Authors

Manuscript in Chapter 4

Author: Ryan deM. Jennings

Contributions: Conceived, designed, and performed experiments. Data collection and analysis. Manuscript drafting and editing at all stages.

Co-Author: Kristopher A. Hunt

Contributions: Performed experiments. Data collection and analysis.

Co-Author: Ross P. Carlson

Contributions: Conceived and designed experiments. Data collection and analysis.

Co-Author: William P. Inskeep

Contributions: Conceived and designed experiments. Data collection and analysis. Manuscript drafting and editing at all stages.

Manuscript Information Page

Ryan deM. Jennings[1, 2], Kristopher A. Hunt[3, 4], Ross P. Carlson[1, 3, 4], William P. Inskeep[1, 2, 3]

Journal Name: The International Society for Microbial Ecology Journal
X_Prepared for submission to a peer-reviewed journal
__Officially submitted to a peer-reviewed journal
__Accepted by a peer-reviewed journal
__Published in a peer-reviewed journal
The International Society for Microbial Ecology Journal

[1]Thermal Biology Institute, Montana State University, Bozeman, MT
[2]Department of Land Resources and Environmental Sciences, Montana State University, Bozeman, MT
[3]Center for Biofilm Engineering, Montana State University, Bozeman, MT
[4]Department of Chemical and Biological Engineering, Montana State University, Bozeman, MT

Abstract

Microorganisms constitute a major portion of the biosphere and make significant contributions to biogeochemical cycles via metabolic activity and community interactions. Iron-oxide mat communities in acidic high temperature environments (Yellowstone National Park, YNP) have been studied intensively and are excellent model communities for identifying trophic interactions between distinct microbial populations and associated geochemical processes (e.g., Fe(II)-oxidation). Consequently, the major goal of the current study was to examine the trophic interaction between a primary autotroph and heterotroph in the context of environmental variables such as electron donors and the terminal electron acceptor, oxygen. Elementary flux mode analysis of genome-enabled stoichiometric metabolic models for *Metallsophaera yellowstonensis* and a Geoarchaeota str. OSP was used to evaluate biomass production as a function of C sources, and/or specific electron donors or acceptor. Biomass production was evaluated as a function of oxygen cost, to assess the potential for competition for this limiting substrate. Moreover, the rate of Fe(II)-oxidation was predicted as a function of total oxygen flux, allowing comparison to Fe(III)-oxide deposition rates and oxygen flux measurements performed *in situ*. Thus, this study utilized genome content to model phenomena also observable at the macroscopic level to understand the realized Fe(II)-oxidizing niche of *M. yellowstonensis*. Results from this study also provided possible explanations for autotroph-heterotroph interactions as well as an understanding of carbon and energy flux within high-temperature Fe(III)-oxide microbial mats.

Introduction

Microorganisms are estimated to be the largest component of the biosphere and make a significant contribution to biogeochemical cycles through metabolic activity (1). Microorganisms commonly exist in biofilm communities, which contain numerous micro-environments based on various hydrodynamic and diffusional conditions, and specific microorganisms establish different niches within this matrix (2). Microbial communities are complex and temporally dynamic systems, where numerous populations, carbon sources, electron trafficking, and microbial physiologies intersect with the physical world. Microbial interactions, such as predation, competition, and symbiosis are explicitly linked to key metabolic processes within a community. However, the complexity of many natural microbial communities, such as soil and marine systems, is difficult to represent due to the phylogenetic diversity as well as the array of carbon and energy sources present. Conversely, microbial communities with fewer members make an excellent test case to examine microbial metabolism and interaction in an established environmental context.

The phylogenetic diversity of microbial communities present in acidic ferric oxyhydroxide mats of Yellowstone National Park (YNP) is limited due to high temperature (65 - 75°C) and low pH (~ 3) (3-7). These biomineralizing communities are formed and inhabited by 5 - 7 distinct phylotypes including crenarchaea from the Sulfolobales (e.g., *M. yellowstonensis*), Desulfurococcales and Thermoproteales, as well as novel archaeal groups (Candidate phylum Geoarchaeota) and acidophilic members of the deeply-rooted bacterial order Aquificales (*Hydrogenobaculum* sp.) (6-12). The

aqueous and solid-phase geochemistry of these environments has been studied in detail (3, 5, 12-15) and provides a critical link for modeling microbial community interactions. The primary electron donors that drive chemolithoautotrophy in Fe-oxide microbial mats include ferrous iron (~ 30 - 40 µM), reduced forms of S (dissolved sulfide < 5 - 10 µM), and potentially arsenite and hydrogen (*Hydrogenobaculum* spp.). Thiosulfate concentrations are below detection (< 3 µM) in these acidic systems (13, 16). The oxidation of ferrous iron coupled with the reduction of oxygen provides energy necessary for the fixation of inorganic carbon by populations of *M. yellowstonensis*, a key autotrophic member of these acidic systems (6, 8, 14, 17, 18). The presence of heme Cu oxidases in *Metallosphaera yellowstonensis*, Geoarchaeota, and *Hydrogenobaculum spp.*, as well as recent observations using mRNA, show that these populations utilize oxygen as an electron acceptor (7, 17, 19). Oxygen consumption is diffusion-limited in Fe-oxide microbial mats, which results in a steep oxygen gradient from ~ 60 to < 1 µM over a distance of approximately 0.5 to 1 mm (14), and establishes a conceptual basis on which to consider competition for this substrate. The measured oxygen gradient also corresponds to different habitat preferences as revealed from analysis of microbial community composition as a function of mat depth (12). Several Desulfurococcales and Thermoproteales populations that do not appear to require oxygen (20, 21) are found in higher abundances at lower mat depths and function primarily as organoheterotrophs (10, 20, 22).

Inorganic C fixation has been demonstrated in both *M. yellowstonensis* cultures and *ex situ* Fe-oxide mat incubations (18). Carbon dioxide fixation by *M. yellowstonensis* and/or *Hydrogenobaculum* contributes a minimum of ~ 40% of the total microbial carbon

in acidic Fe-oxide mats of YNP (18), and metagenome analysis and molecular studies have established that Geoarchaeota is one of the primary aerobic heterotrophs, often comprising > 20-50 % of the total microbial community at pH values near 3.5 (7, 12). The presence of Sulfolobales viruses in metagenome sequences (10) also suggests that viral predation of *M. yellowstonensis* may make microbial biomass available for heterotrophic metabolism by other community members such as Geoarchaeota. Chemolithoautotrophy by *M. yellowstonensis* and subsequent transfer of carbon, energy, and nutrients to Geoarchaeota represents an excellent example of potential autotroph-heterotroph interactions occurring in high-temperature environments.

Genome-enabled stoichiometric modeling, such as elementary flux mode analysis (EFMA), is a powerful approach for examining different metabolic processes and potential interactions among community members (23-25). Briefly, metabolic networks are reconstructed *in silico* by compiling stoichiometrically balanced reactions inferred from genome sequence analysis, which represents the metabolic potential of the organism (26). These metabolic networks define possible routes of energy conservation and central carbon metabolism, including details of electron transport, the acquisition of C, and anabolic processes necessary to synthesize biomass. EFMA identifies all biochemically distinct and indecomposable routes (modes) through the metabolic network (27). These distinct modes (and non-negative combinations thereof) describe all possible physiological states of an organism, which makes EFMA well suited for evaluating energetic costs of different electron donors, acceptors, and C sources required to form microbial biomass. Stoichiometric modeling has been used to predict optimal genotypes in engineered systems (23, 28), interpret physiological behavior (24, 29), and evaluate the

transfer of mass and energy between distinct populations in a natural phototrophic microbial community (25).

One of the broader goals in environmental microbiology is to understand and predict microbial behavior in natural (or engineered) communities, where key interactions among different populations lead to emergent properties such as total biomass production per unit of energy (30). Consequently, the objectives of this study were to 1) construct genome-enabled metabolic models of *M. yellowstonensis* and Geoarchaeota, two of the dominant autotrophic and heterotrophic populations, respectively, of acidic Fe(III)-oxide mat communities, 2) identify ecologically-relevant and competitive metabolisms for each population as a function of electron donor, electron acceptor and/or carbon source, and 3) perform cost-benefit scenarios of total biomass production and Fe-oxidation as a function of autotroph-heterotroph composition and oxygen consumption. The multi-scale microbial interaction model predicts the production of microbial biomass as a function of electron donor-acceptor and C source assumptions, and these results were compared to measurements conducted *in situ* at different scales (e.g., microelectrode studies of oxygen gradients; Fe(III)-oxide deposition). To our knowledge, this is the first stoichiometric interaction model between two archaea, and provides a foundation for interpreting mass and energy transfer in microbial communities where the fixation of inorganic C by chemolithotrophs supports the production of heterotrophic biomass.

Materials and Methods

Genome Analysis and Model Construction

In silico stoichiometric models were constructed for *M. yellowstonensis* (NCBI Taxon ID 671065, GOLD ID Gi04920) and *Geoarchaeota* archaeon OSPB-1 (NCBI Taxon ID 1448933, GOLD ID Gi0000638). Elementally and electronically balanced reactions, representing carbon and energy metabolism were compiled based on genome sequence (Joint Genome Institute - Integrated Microbial Genomes (JGI-IMG) (31). Prior genome analysis (6-8, 10, 17, 18), literature surveys, MetaCyc (32, 33), and KEGG (34) were crossed-referenced during metabolic reconstruction and reactions were assumed to close pathway gaps that would have resulted in auxotrophy. The modeled macromolecular compositions of biomass for each organism were based on previous reports (35). The publically available genomes were mined for monomer distributions of DNA, RNA, and protein, based on the GC content, the ribosomal subunits, and the average amino acid distribution of all protein encoding genes, respectively. Maintenance energy requirements were adjusted to calibrate individual models to relevant observed yields. A maintenance energy of 172 mmol ATP · g biomass^{-1} was used for the *M. yellowstonensis* model to match published yields for *Acidothiobacillus ferroxidans*, a representative thermoacidophilic autotrophic iron-oxidizing bacterium(36). A maintenance energy of 150 mmol ATP · g biomass^{-1} was used for the Geoarchaeota str. OSP model to match published yields for *Alicyclobacillus acidocaldarius*, a representative thermoacidophilc heterotrophic bacteria (37). While additional electron donors and carbon sources were modeled for *M. yellowstonensis* and Geoarchaeota, only

Fe oxidation and glucose consumption, respectively, were used to set the maintenance energy. Predicted yields for other substrates based on the maintenance energies used were within experimental error.

Computational Packages and Analyses

In silico stoichiometric models were constructed using CellNetAnalyzer version 2014.1 (38, 39), and exported to RegEFMTool version 2.0 (40, 41) to enumerate EFMs for each metabolic model. The RegEFMTool software package employs user-defined gene regulatory rules governing the co-occurrence of reactions within an EFM to simplify the model, thus decreasing the computational burden. The incorporation of gene regulatory rules removed futile cycles that both synthesized and degraded potential carbon or energy sources (Geoarchaeota) or used multiple electron donors (*M. yellowstonensis*). Moreover, independent simulations for each carbon source were performed for the Geoarchaeota model, while the *M. yellowstonensis* model included a single carbon source (CO_2) and EFMs were enumerated in full through a single simulation. The macronutrients available to both organisms were modeled as illustrated in Figure 4.1. Metabolic reconstructions for both organisms, including reactions, genomic evidence, specific literature references, metabolites, stoichiometric balance, and gene regulatory rules can be found in the supplemental material. All computations were processed on a machine with at most two Intel Xeon X5690 and 120 GB RAM.

Relative biomass production
and substrate consumption rates

Competitive utilization of oxygen to produce community biomass was examined with respect to population relative abundance and growth rates of the community members dependent on oxygen. The volume of interest was constrained by the depth of oxygen penetration, 800 ± 88 µm (14) and a homogenous steady state system was assumed. Mass balances described the relative total growth rates, R_G/R_M, as a function of the relative abundance, X_G/X_M, and the yield of 'Geoarchaeota strain OSP' grown on *M. yellostonensis*, $Y_{M/G}$ (2.4 Cmol Myell · Cmol Geo^{-1}, Table 4.1), Equation 1.

Equation 1: $R_M/R_G = (X_M/X_G) + Y_{M/G}$

Applying the cost of oxygen to produce biomass ($Y_{O_2/M}$ and $Y_{O_2/G}$, Table 4.1) described the relationship between oxygen flux into the mat and the biomass production rate of the community as a function of population relative abundance and relative growth rate, Equation 2, shown in Figure 4.6.

Equation 2: $O_{2_{flux}} = R_M [Y_{O_2/M} + Y_{O_2/G}(R_M/R_G)]$

Incorporating the cost of iron in the production of *M. yellowstonensis* biomass ($Y_{Fe/M}$, Table 4.1) described a relationship between iron oxidation and oxygen flux, Equation 3, shown in Figure 4.7.

Equation 3: $Fe_{ox} = R_M Y_{Fe/M}$

The system volume, estimated by the depth of oxygen penetration into mature Fe mats, was held constant, assuming constant substrate feed rates and growth conditions. To examine the relationship between autotroph and heterotroph, carbon dioxide was included in the mathematical model as the sole carbon source for the aerobic microbial

community. These assumptions bound potential carbon and electron sources relative to substrate uptake rates and therefore the potential activity of the aerobic Fe mat community.

Results and Discussion

Production of Chemolithoautotrophic Biomass

Metallosphaera yellowstonensis (str. MK1) is one of the primary autotrophs in acidic Fe-oxide mats of YNP (8, 18) and the metabolism of this organism was limited in the current interaction model to the acquisition of inorganic carbon through the 3-hydroxypropionate/4-hydroxybutyrate (3-HP/4-HB) pathway. The electrons required to drive anabolic processes in *M. yellowstonensis* metabolism were obtained from the oxidation of either ferrous iron, sulfide, sulfur, sulfite, or thiosulfate, using oxygen as the terminal electron acceptor (17). Fixed inorganic carbon via the 3-HP/4-HB pathway (18) was used to derive *M. yellowstonensis* biomass (Cmol) via many possible elementary flux modes (EFMs) for each electron donor (e.g., Fe, S) as a function of the oxygen requirement (Figure 4.3B). The moles of electron donor required to form biomass was lowest for sulfide and highest for ferrous iron, which follows the thermodynamic favorability expected for the oxidation of these electron donors (42). The EFMs that result in *M. yellowstonensis* biomass production also consume variable amounts of oxygen. The oxidation of Fe(II) requires the highest O_2 consumption per Cmol of biomass, compared to other primary inorganic electron donors that could be utilized by *M. yellowstonensis.* Additionally, when evaluated on an electron-basis (Figure 4.3B),

Fe(II) oxidation requires more oxygen (per Cmol biomass) than the oxidation of reduced sulfur species.

The biomass producing modes for *M. yellowstonensis* are based on the fixation of CO_2 followed by anabolic pathways that produce polysaccharides, amino acids, nucleic acids and isoprenoids, and which together constitute 'Myell' biomass. These pathways included the tricarboxylic acid cycle with gluconeogenesis, the pentose phosphate pathway via ribulose monophosphate (43), as well as the mevalonate and isoprenoid pathways (44). A total of 6,337 possible flux modes to produce *M. yellowstonensis* biomass were assessed based on different inorganic electron donors (Figure 4.3).

Production of Organoheterotrophic Biomass

Metabolic pathway analysis of 'Geoarchaeota strain OSP' shows that this population has the potential to function as a generalist and utilize one or more classes of biomass components, including peptides, lipids, polysaccharides, and RNA. Numerous EFMs were observed for the production of 'Geoarchaeota str. OSP' biomass from reduced C constituents synthesized by *M. yellowstonensis* (Figure 4.4). The possible EFMs for each carbon (and energy) source, shown as response surfaces, reveal trade-offs between the amounts of C substrate and O_2 required to produce Geoarchaeota biomass, and the thermodynamic favorability of more reduced organic electron donors. Differences in oxygen cost (y-axis, Figure 4.4) are a function of the average C oxidation state(s) in the different substrates as well as specific degradation pathways that include substrate-level phosphorylation. For example, the lowest average C oxidation state for lipids translates to a greater oxygen cost for catabolism per Cmol of Geoarchaeota

biomass than either the degradation of peptides or polysaccharides. The carbon cost of metabolism can also be evaluated (x-axis, Figure 4.4), which provides insight on the efficiency of biomass synthesis from individual carbon sources. For example, the catabolism of lipids, polysaccharides, and amino acids leads to common central carbon metabolites (e.g. - acetyl-CoA, succinyl-CoA, 2-oxoglutarate) that can be easily transformed to biomass. In contrast, rRNA is not energetically rich and transformation into other biomass components (i.e., amino acids, polysaccharides, and isoprenoids) requires extensive molecular rearrangement. Thus, catabolism of rRNA requires greater amounts of substrate compared to proteins, lipids and polysaccharides.

The most efficient EFMs for producing Geoarchaeota biomass from *M. yellowstonensis* substrates range from 2.1 - 3.1 Cmol substrate · Cmol biomass^{-1}, which consumes roughly 1.0 – 1.5 mol O_2 (Table 4.1; Figure 4.4). Utilization of all *M. yellowstonensis* biomass (genome-enabled weighted average of macromolecule distribution) by Geoarchaeota shows the most efficient EFMs at ~ 2.4 Cmol substrate · Cmol biomass^{-1}, which consume ~ 1.6 mol O_2. Results from stoichiometric reaction network analysis show that production of biomass from CO_2 (*M. yellowstonensis*) can support a heterotrophic partnership (Geoarchaeota) where 2.4 Cmol of autotrophic biomass is required to form 1 Cmol of heterotrophic biomass (Table 4.1, Figure 4.4).

Oxygen Consumption, Iron Oxidation and Total Biomass Production

The oxygen cost to form microbial biomass is significantly higher for *M. yellowstonensis* compared to Geoarchaeota and shows that the production of cellular components via the oxidation of Fe(II) consumes nearly 25 times more oxygen than the

oxidation of reduced C (Table 4.1, Figure 4.5). Less oxygen per Cmol biomass is required when more energetically favored electron donors are used to support the growth of *M. yellowstonensis* (e.g., sulfide, elemental S). Organoheterotrophs have the advantage of utilizing reduced C substrates as both electron donors and anabolic precursors, which results in less oxygen consumed per Cmol biomass produced compared to autotrophs and the extra energetic costs of reducing inorganic C. If Geoarchaeota populations grow exclusively on DIC-derived *M. yellowstonensis* biomass, the large majority of the total oxygen required is necessary to support the Fe(II)-oxidizing lithoautotroph (Figure 5).

Significant amounts of oxygen are required to form both *M. yellowstonensis* and Geoarchaeota biomass, which introduces the possibility that oxygen may be a limiting substrate and that partitioning of available O_2 to each population will vary with population abundance. Moreover, the amount of oxygen consumed to form *M. yellowstonensis* biomass varies with the electron donor used to drive CO_2 fixation (i.e., Figure 3A). Total community biomass production rate is a function of the total oxygen flux, costs of autotrophic and heterotrophic biomass production, and the relative population abundances. Details of this relationship were examined for conditions where *M. yellowstonensis* biomass is produced using Fe(II) as the sole electron donor and Geoarchaeota biomass production is constrained by the yield term 2.4 Cmol Myell · Cmol Geo^{-1} (Figure 6). The total community biomass production rate (sum of *M. yellowstonensis* and Geoarchaeota) is highest when the community is dominated by *Metallosphaera* (i.e., $X_M >> X_G$). Any utilization of DIC-derived biomass (*M. yellowstonensis*) for heterotrophic consumption reduces the total community biomass production rate due to the fact that 2.4 Cmol *M. yellowstonensis* is required to support a

Cmol of Geoarchaeota biomass ($Y_{M/G}$). Repeated measurements in high-temperature mats of One Hundred Spring Plain show that the relative abundance *in situ* of Geoarchaeota is generally twice that of *M. yellowstonensis* (i.e., $X_M/X_G = 0.5$). The predicted community biomass production rates at these autotroph:heterotroph ratios are less than an optimum abundance ratio (X_M/X_G) of ~ 3.4, which would provide enough *M. yellowstonensis* to sustain itself and Geoarchaeota. The observed abundance ratios reflect the reality that *Hydrogenobaculum* spp. also provide autotrophic biomass in these communities, which reduces heterotrophic dependence on *M. yellowstonensis* alone. Moreover, ^{13}C stable isotope analysis shows that as much as 50% of the microbial biomass may be supported by non-DIC sources (Chapter 3), which would also reduce the potential dependence of Geoarchaeota on *M. yellowstonensis* biomass.

Comparison to *In Situ* Observations

It was understood at the outset that a model construct between only two of the major populations present in Fe(III)-oxide mats of One Hundred Springs Plain (OSP) may not represent *in situ* conditions, especially given that these microbial communities contain several additional populations that have been characterized (11, 12, 20), and are important in establishing actual ratios of total oxygen consumption to the amount of Fe(II)-oxidized. Nevertheless, one of our major goals was to compare insights gained from modeling results with detailed *in situ* measurements that have been made by other members of our group studying Fe(III)-oxide mats in Norris Geyser Basin (YNP). Iron(III)-oxide accretion rates measured in a long-term temporal study (12) at the OSP Fe-deposition site (OSP_B) are shown along with oxygen flux rates measured *in situ*

using microelectrodes (12, 14) (Figure 7). These two sets of measurements are compared to EFM analysis of the Fe(II) oxidized (expressed as a flux) as a function of oxygen flux, which includes the oxygen required for Fe(II) oxidation (i.e., $Fe:O_2 = 4:1$) as well as that required for heterotrophic consumption by Geoarchaeota (Figure 7). Heterotrophic metabolism exerts no appreciable effect on predicted Fe(II) oxidation rates as a function of oxygen consumed, in part due to the interdependence assumed in the model that Geoarchaeota requires *M. yellowstonensis* biomass (2.4 Cmol *M. yellowstonensis* · Cmol Geoarchaetoa^{-1}), which is generated using an electron donor (i.e., Fe) that consumes a large amount of oxygen. These analyses suggest that the majority of oxygen flux *in situ* would be partitioned to *M. yellowstonensis* populations. Consequently the model results can be used as a framework for comparison to major processes measured *in situ*.

The measured flux of oxygen into Fe(III)-oxide mats represents the total biological demand for this substrate (i.e., BOD) and results have shown a steep oxygen gradient from the aqueous-mat interface to ~ 0.5 to 1 mm depth (14). Other oxygen consuming processes in the Fe(III)-oxide mats explain the higher amounts of measured oxygen flux relative to the measured Fe(III)-oxide deposition rates (Figure 7). For example, at least three major oxygen consuming processes (i.e., additional electron donors) are known that account for the higher amounts of measured oxygen flux than predicted based on Fe(II) as the sole electron donor. Firstly, the biotic oxidation of arsenite (present at 25 – 30 µM in ASC springs of NGB) by specific members of the Fe(III)-mat communities (*Hydrogenobaculum* spp.) results in nearly complete conversion to arsenate in Fe-mat systems (45, 46), and the subsequent formation of arsenate-rich iron oxides ($As^V:Fe^{III}$ ratios of ~ 0.6 – 0.7) (3). Secondly, the oxidation of reduced C by other

aerobic populations in these communities is occurring based on detailed metagenome analysis of different population types present in Fe(III)-oxide microbial mats (7, 12) as well as stable ^{13}C isotope analysis. The amount of microbial biomass originating from non-DIC sources may be as high as 60% in the Fe(III)-oxide mats under consideration (Chapters 2 and 3), and this represents additional oxygen consumption not accounted for based on obligate dependence of Geoarchaeota on DIC-derived *M. yellowstonensis* biomass.

Finally, small amounts of sulfide (< 5 μM) and occasional flocs of elemental sulfur are present in Fe(III)-oxide depositing zones of acid-sulfate-chloride springs, which if oxidized, will consume additional oxygen. It has already been shown that reduced S species are important to *Hydrogenobaculum* spp. up-gradient of Fe(III) deposition zones (47), and that *de novo* sequence assemblies of these populations contain necessary S oxidation pathways that utilize O_2 as an electron acceptor (19). In summary, although the measured *in situ* oxygen flux includes several significant oxygen-consuming reactions besides the oxidation of Fe(II) by *M. yellowstonensis*, evaluation of the most efficient flux modes provide a basis on which to understand chemolithoautotrophic metabolism (Fe(II) oxidation and CO_2 fixation) as a significant oxygen-consuming process relative to the oxidation of reduced C in these systems. The differential oxygen cost necessary for metabolism of two of the most abundant microorganisms in Fe(III)-oxide mats supports the hypothesis that these populations would likely be distributed differently across the measured oxygen gradient.

Autotroph-Heterotroph Abundance and Implications for Differential Turnover

The most efficient elementary flux modes describing the formation of Geoarchaeota biomass require 2.4 Cmol *M. yellowstonensis* substrate · Cmol Geoarchaeota^{-1} (Table 4.1). However, mature (0.5 – 1 cm) Fe(III)-oxide mats from the Fe-depositional zones of OSP Spring exhibit relative abundances of *M. yellowstonensis* and Geoarchaeota approximately 15 and 45 % of the community, respectively, based on several replicate metagenomes (7, 9, 10). Consequently, the actual ratios of *M. yellowstonensis*:Geoarchaeota range from ~ 0.2 – 0.5 and show a lower biomass ratio of *Metallosphaera* relative to Geoarchaeota than is necessary for an obligate autotroph-heterotroph partnership. Other elementary flux modes possible for Geoarchaeota only result in greater amounts of *M. yellowstonensis* biomass required (Figure 4).

The lower *M. yellowstonensis* abundances relative to Geoarchaeota measured *in situ* can be understood by comparing the assumptions of model predictions for an obligate autotroph-heterotroph interaction between only two populations versus other processes that occur in these communities. For example, the other predominant autotroph in these environments includes *Hydrogenobaculum* spp., which may also supply DIC-derived reduced C to Geoarchaeota populations *in situ*, and this would, in part, explain the observed ratios of *M. yellowstonensis* to Geoarchaeota. In fact, *Hydrogenobaculum* organisms have been shown to be the dominant population (along with *M. yellowstonensis*) in early stages (0 – 14 d) of Fe(III)-oxide mat assembly (4, 12); in mature (0.5 – 1 cm) iron mats, *Hydrogenobaculum* spp. account for only 5 - 10% of the total community (6, 10, 18). The metabolism of *in situ* Geoarchaeota populations may not

require *Metallosphaera* biomass specifically, but may also rely on proteins and/or other biomass components produced by *Hydrogenobaculum*. Although this would not change any major conclusions from the modeling aspects of this study, the autotrophic biomass would include two primary organisms and would shift the system dependence from Fe(II) as the predominant electron donor driving inorganic C fixation to include other energy sources such as reduced forms of S (e.g., sulfide, elemental S). This would also lower the overall oxygen costs of producing Geoarchaeota biomass.

A requirement of 2.4 Cmol *M. yellowstonensis* biomass to form one unit of heterotrophic biomass could also be met by assuming faster growth and turnover rates for the autotrophic versus the heterotrophic organism (Equation 1). For example, using the current set of model assumptions, a *M. yellowstonensis*:Geoarchaeota growth (turnover) rate ratio would have to range from ~ 6 – 8 at an observed abundance ratio (X_M/X_G) of only 0.3 to 0.5 in order to generate optimum *Metallosphaera* biomass to support Geoarchaeota (i.e., $Y_{M/G} = 2.4$). The differences in growth and/or turnover rates of these organisms *in situ* is not known at the current time; however, it is clear that viruses play a role in these microbial communities and may impact the two archaeal populations used in the current modeling efforts differentially. Numerous Sulfolobales viruses have been identified (48, 49), and more specifically, the genome of *M. yellowstonensis* contains an extremely high abundance of transposases and integrases (50), which suggests that viruses are likely highly important in the life cycle of this organism. Assembled sequence of Sulfolobales viruses has been obtained from Fe(III)-oxide microbial mats (10), and viruses have been detected *in situ* using scanning electron microscopy (Inskeep, unpl). Although little is known regarding possible viruses specific to Geoarchaeota, it is highly

likely that *M. yellowstonensis* is subject to significant viral predation. Higher cell turnover rates of *M. yellowstonensis* relative to Geoarchaeota could supply greater amounts of DIC-derived biomass while maintaining a lower than optimum abundance ratio for an obligate autotroph-heterotroph relationship. It has been hypothesized that the high frequency of viral predation and subsequent cell-lysis represents a major contribution to the rate of C cycling in microbial communities (51, 52).

Finally, populations of *M. yellowstonensis* have not been found in sulfidic systems of acid-sulfate-chloride geothermal springs of NGB, despite the fact that these Sulfolobales contain the genetic potential for the oxidation of elemental sulfur and have been shown to do so in culture in the absence of significant sulfide (8). Iron oxidation terminal oxidase genes (*fox* complex) are more highly expressed under field conditions than S or OC-associated terminal oxidases (17), which is consistent with the realized niche for *M. yellowstonensis* in zones with higher O_2 concentrations (e.g., DO > 20 μM). Elemental S generally co-occurs with high sulfide concentrations (e.g., DS > 10 μM) in acid-sulfate and/or acid-sulfate-chloride geothermal springs of YNP, which precludes the necessary oxygen flux to support the generation of *M. yellowstonensis* biomass. Consequently, elementary flux mode analysis has assisted in understanding why *M. yellowstonensis* occupies an Fe(II)-oxidizing niche *in situ*, and has provided possible explanations for autotroph-heterotroph interactions occurring in high-temperature Fe-mat communities.

Table 4.1. Cost of electron donors, carbon sources, and oxygen (electron acceptor) of most efficient metabolisms identified through elementary flux mode (EFM) analysis for the lithoautotroph (*M. yellowstonensis*) and organoheterotroph ('Geoarchaeota').

	Cost per unit Biomass	
Organism/Donor	**e^- donor**	**O_2 (e^- acceptor)**
M. yellowstonensis	mol·Cmol Biomass^{-1}	
Ferrous Iron	156.2	38.0
Sulfide	2.6	4.2
Sulfur	3.0	3.5
Sulfite	4.2	1.0
Thiosulfate	42.5	9.5

	e- donor/ C source	**O_2 (e- acceptor)**	**Degree of Reduction (γ)**
'Geoarchaeota'	mol·Cmol Biomass^{-1}		
Myell Biomass	2.4	1.6	4.3
Peptide	2.6	1.7	4.2
RNA	3.1	1.5	2.9
Lipid	2.1	1.9	5.9
Polysaccharide	2.6	1.5	4.0

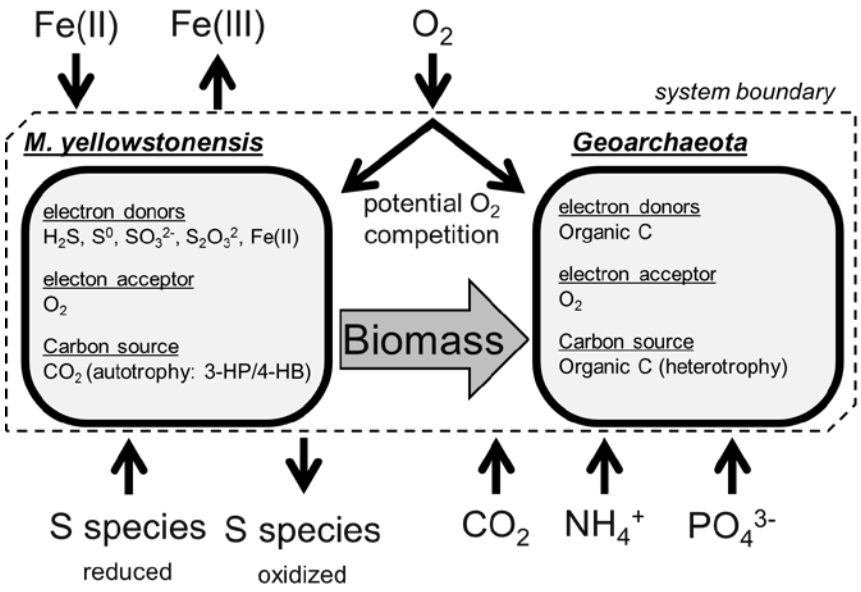
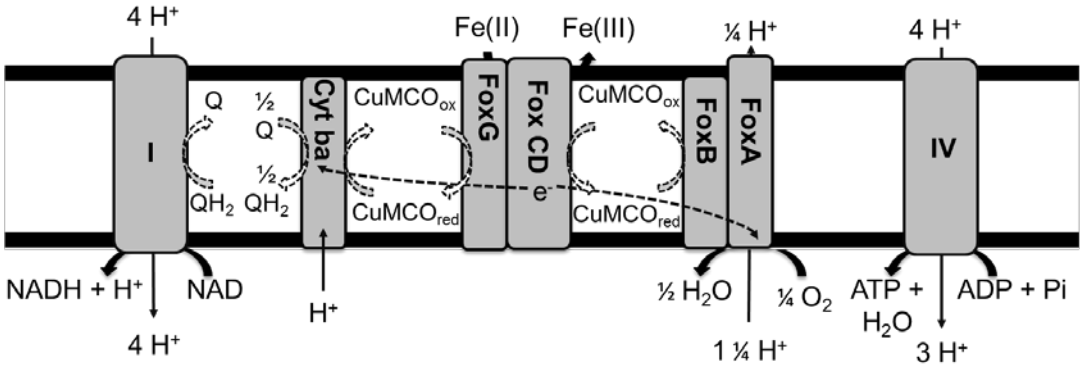


Figure 4.1. Conceptual representation of a metabolic interaction model between a primary autotroph (*M. yellowstonensis*) and heterotroph ("*Geoarchaeota sp.*" strain OSP) present in high-temperature (70-80°C) acidic Fe-oxide mats. The metabolic potential of each organism is depicted based on detailed genome and pathway analysis, and all biochemical reactions were formalized as a stoichiometric reaction network for each organism. Key inferences and assumptions of the model include: *M. yellowstonensis* – oxidation of iron and/or reduced sulfur species coupled to oxygen reduction and carbon dioxide fixation; *Geoarchaeota* – oxidation of organic carbon coupled to oxygen reduction.

A.



B.

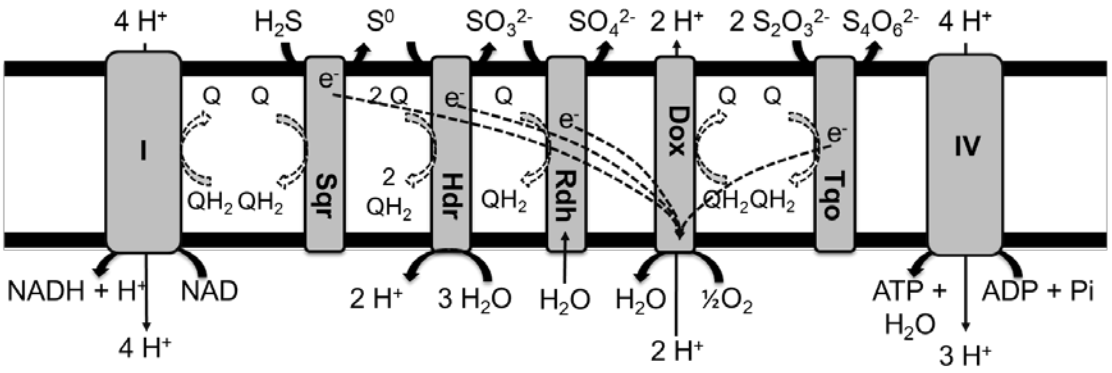


Figure 4.2. Primary mechanisms and stoichiometry of electron transport reactions in *M. yellowstonensis* for the oxidation of (A) ferrous iron and (B) reduced sulfur-species coupled to oxygen reduction. Electron flow is indicated by dashed lines.

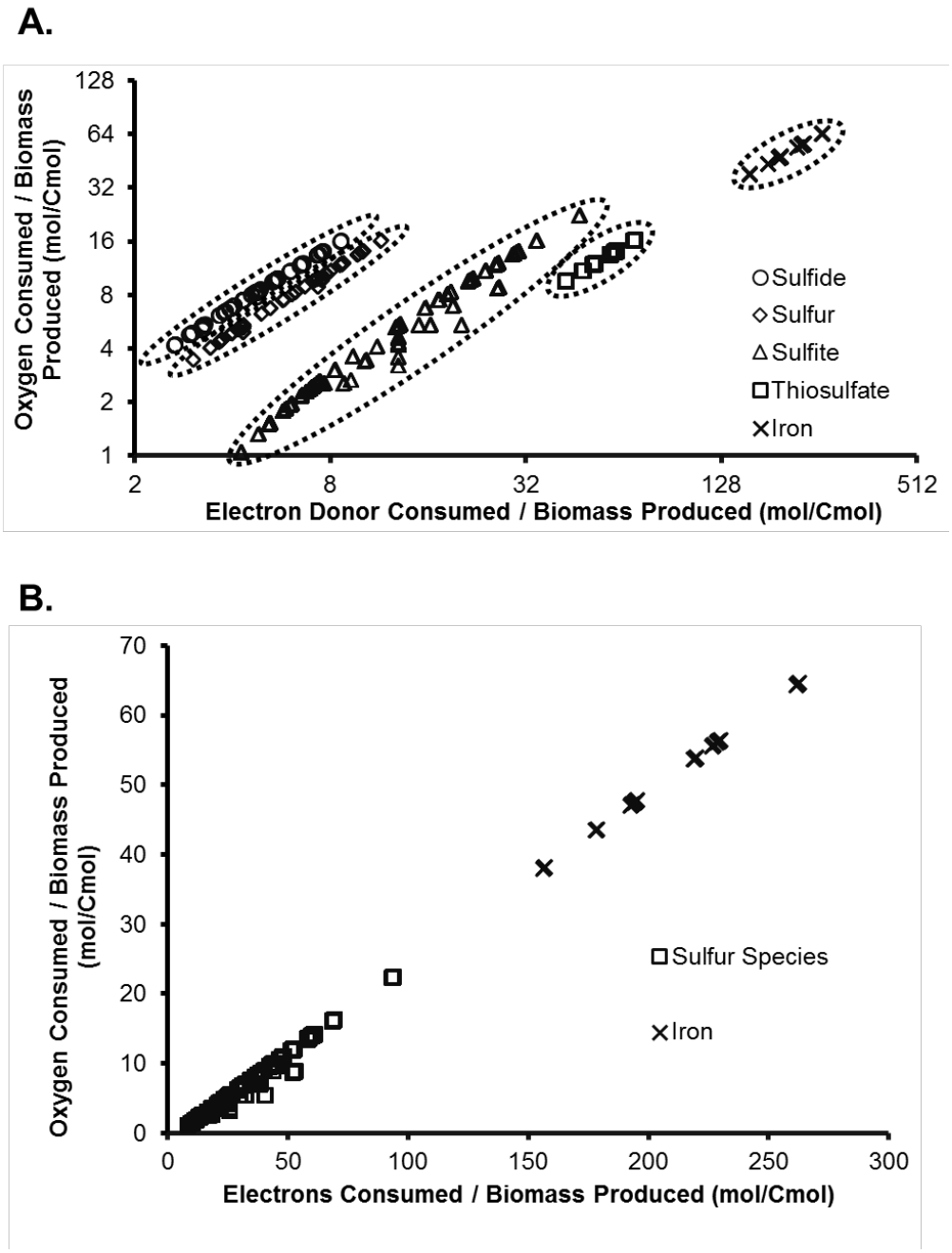


Figure 4.3. The oxygen consumption (per Cmol biomass) for all biomass producing elementary flux modes of *M. yellowstonensis* plotted as a function of moles electron donor consumed (A) or moles electrons consumed (B). Specific electron donors include sulfide, sulfur, sulfite, thiosulfate, and ferrous iron.

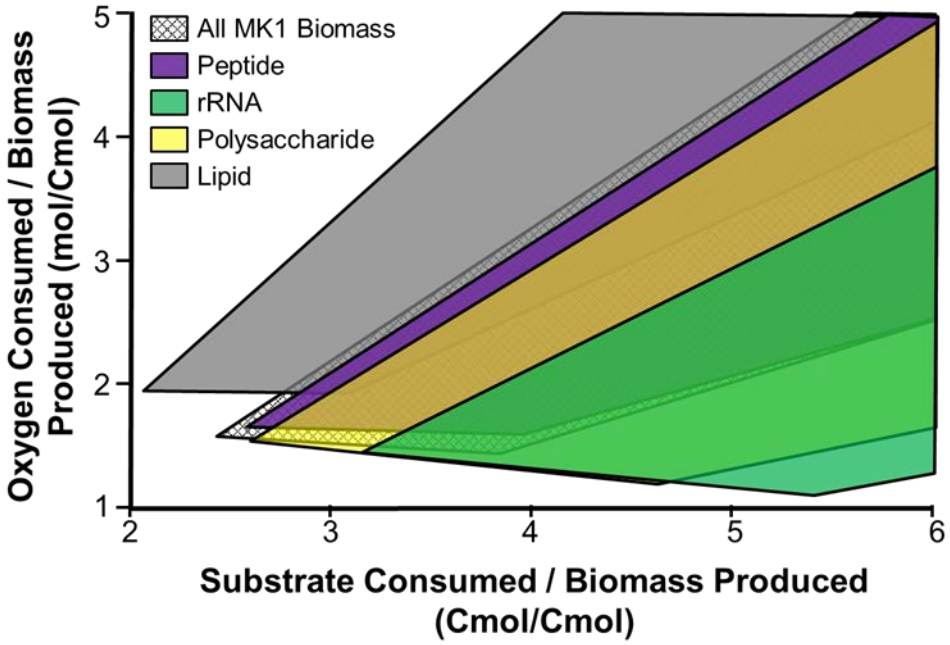


Figure 4.4. The oxygen and substrate consumption (per Cmol biomass) for all biomass producing *Geoarchaeota* elementary flux modes plotted as response surfaces. Specific substrates include lipids, peptides, polysaccharides, rRNA, and *M. yellowstonensis* biomass.

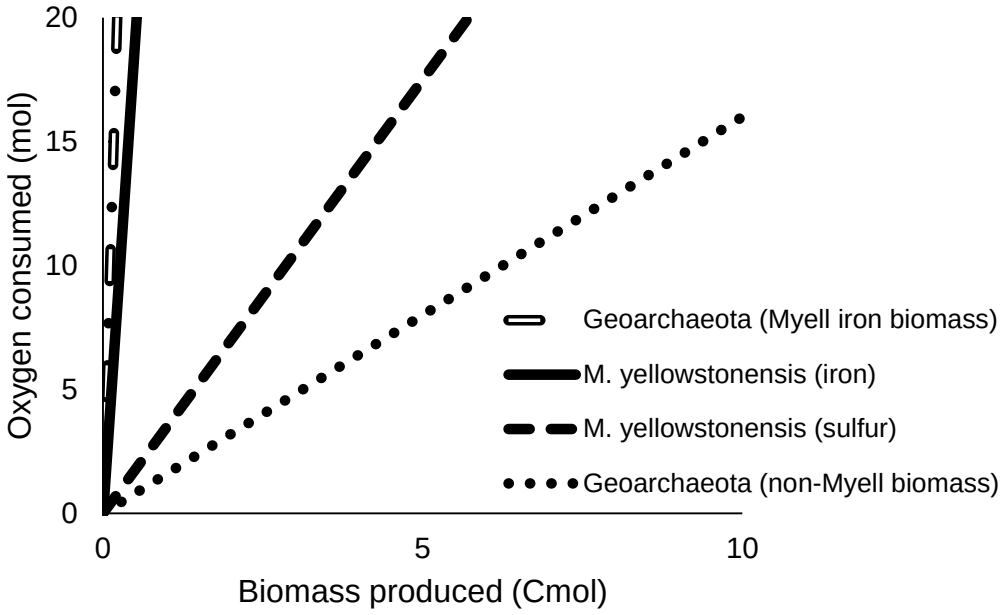


Figure 4.5. Oxygen consumption plotted as a function of biomass production for autotrophic *M. yellowstonensis* utilizing Fe(II) or elemental S, and for heterotrophic Geoarchaeota utilizing *M. yellowstonensis* biomass generated from iron oxidation, or other reduced C sources (i.e., non-*Metallosphaera* biomass).

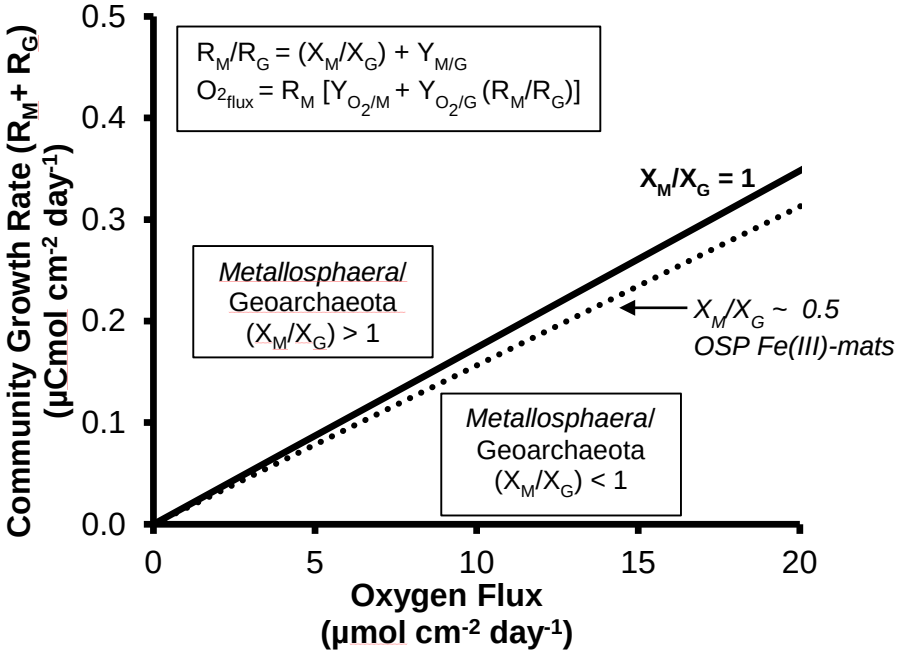


Figure 4.6. Total community growth rate ($R = R_M + R_G$) predicted as a function of oxygen flux ($O_{2_{flux}}$), autotrophic and heterotrophic biomass production yields (Y, Table 4.1), and the relative abundances of *M. yellowstonensis* (X_M) and Geoarchaeota (X_G). The total community growth rate is plotted for the condition $X_M = X_G$ (solid line) and for conditions observed in Fe(III)-oxide mats from One Hundred Spring Plain (OSP) at 75 ^oC ($X_M/X_G \sim 0.5$). R_M and R_G are the total growth rates of *M. yellowstonensis* and Geoarchaeota, respectively.

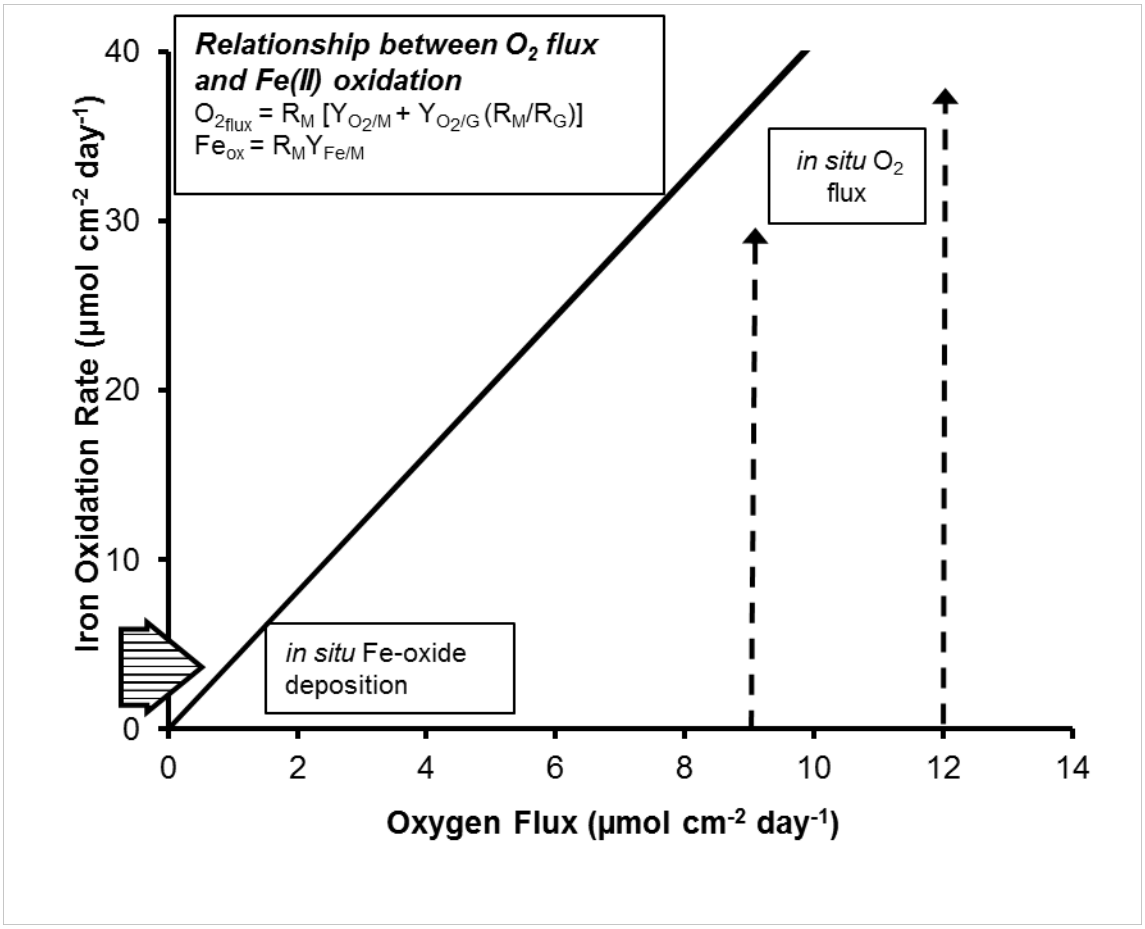


Figure 4.7. Relationship between Fe(II) oxidation (Fe_{ox}) and oxygen consumption ($O_{2_{flux}}$) rates predicted for production of total community biomass (R_M + R_G, *M. yellowstonensis* and Geoarchaeota) from dissolved inorganic C (DIC). Yields were determined by elementary flux mode analysis (Y, Table 4.1). Observed Fe(III)-oxide deposition rates (1-5 µmol cm^{-2} day^{-1}) and oxygen consumption rates (9-12 µmol cm^{-2} day^{-1}) (12, 14) are shown for comparison.

References

1. Falkowski PG, Fenchel T, Delong EF. The microbial engines that drive Earth's biogeochemical cycles. Science. 2008;320(5879):1034-9.

2. Battin TJ, Sloan WT, Kjelleberg S, Daims H, Head IM, Curtis TP, et al. Microbial landscapes: new paths to biofilm research. Nat Rev Microbiol. 2007;5(1):76-81.

3. Inskeep WP, Macur RE, Harrison G, Bostick BC, Fendorf S. Biomineralization of As(V)-hydrous ferric oxyhydroxide in microbial mats of an acid-sulfate-chloride geothermal spring, Yellowstone National Park. Geochim Cosmochim Ac. 2004;68(15):3141-55.

4. Macur RE, Langner HW, Kocar BD, Inskeep WP. Linking geochemical processes with microbial community analysis: successional dynamics in an arsenic-rich, acid-sulphate-chloride geothermal spring. Geobiology. 2004;2(3):163-77.

5. Inskeep W, Macur R, Ackerman G, Kozubal M, Taylor W, Korf S. Linking microbial and geochemical processes in geothermal habitats. Geochim Cosmochim Ac. 2005;69(10):A226-A.

6. Inskeep WP, Rusch DB, Jay ZJ, Herrgard MJ, Kozubal MA, Richardson TH, et al. Metagenomes from high-temperature chemotrophic systems reveal geochemical controls on microbial community structure and function. PLoS One. 2010;5(3):e9773.

7. Kozubal MA, Romine M, Jennings R, Jay ZJ, Tringe SG, Rusch DB, et al. Geoarchaeota: a new candidate phylum in the Archaea from high-temperature acidic iron mats in Yellowstone National Park. ISME J. 2013;7(3):622-34.

8. Kozubal M, Macur RE, Korf S, Taylor WP, Ackerman GG, Nagy A, et al. Isolation and distribution of a novel iron-oxidizing crenarchaeon from acidic geothermal springs in Yellowstone National Park. Appl Environ Microbiol. 2008;74(4):942-9.

9. Kozubal MA, Macur RE, Jay ZJ, Beam JP, Malfatti SA, Tringe SG, et al. Microbial iron cycling in acidic geothermal springs of yellowstone national park: integrating molecular surveys, geochemical processes, and isolation of novel fe-active microorganisms. Front Microbiol. 2012;3:109.

10. Inskeep WP, Jay ZJ, Herrgard MJ, Kozubal MA, Rusch DB, Tringe SG, et al. Phylogenetic and Functional Analysis of Metagenome Sequence from High-Temperature Archaeal Habitats Demonstrate Linkages between Metabolic Potential and Geochemistry. Front Microbiol. 2013;4:95.

11. Beam JP, Jay ZJ, Kozubal MA, Inskeep WP. Niche specialization of novel Thaumarchaeota to oxic and hypoxic acidic geothermal springs of Yellowstone National Park. ISME J. 2014;8(4):938-51.

12. Beam JP, Bernstein HC, Jay ZJ, Kozubal MA, Jennings Rd, Tringe SG, et al. Assembly and Succession of Iron Oxide Microbial Mat Communities in Acidic Geothermal Springs. Geobiology. 2015.

13. Langner HW, Jackson CR, McDermott TR, Inskeep WP. Rapid oxidation of arsenite in a hot spring ecosystem, Yellowstone National Park. Environ Sci Technol. 2001;35(16):3302-9.

14. Bernstein HC, Beam JP, Kozubal MA, Carlson RP, Inskeep WP. In situ analysis of oxygen consumption and diffusive transport in high-temperature acidic iron-oxide microbial mats. Environ Microbiol. 2013;15(8):2360-70.

15. Inskeep WP, Ackerman GG, Taylor WP, Kozubal M, Korf S, Macur RE. On the energetics of chemolithotrophy in nonequilibrium systems: case studies of geothermal springs in Yellowstone National Park. Geobiology. 2005;3(4):297-317.

16. Nordstrom DK, Ball JW, McCleskey RB. Ground water to surface water: chemistry of thermal outflows in Yellowstone National Park. Geothermal biology and geochemistry in Yellowstone National Park. 2005:73-94.

17. Kozubal MA, Dlakic M, Macur RE, Inskeep WP. Terminal oxidase diversity and function in "Metallosphaera yellowstonensis": gene expression and protein modeling suggest mechanisms of Fe(II) oxidation in the sulfolobales. Appl Environ Microbiol. 2011;77(5):1844-53.

18. Jennings RM, Whitmore LM, Moran JJ, Kreuzer HW, Inskeep WP. Carbon dioxide fixation by Metallosphaera yellowstonensis and acidothermophilic iron-oxidizing microbial communities from Yellowstone National Park. Appl Environ Microbiol. 2014;80(9):2665-71.

19. Takacs-Vesbach C, Inskeep WP, Jay ZJ, Herrgard MJ, Rusch DB, Tringe SG, et al. Metagenome sequence analysis of filamentous microbial communities obtained from geochemically distinct geothermal channels reveals specialization of three aquificales lineages. Front Microbiol. 2013;4:84.

20. Jay ZJ, Rusch DB, Tringe SG, Bailey C, Jennings RM, Inskeep WP. Predominant Acidilobus-like populations from geothermal environments in yellowstone national park exhibit similar metabolic potential in different hypoxic microbial communities. Appl Environ Microbiol. 2014;80(1):294-305.

21. Macur RE, Jay ZJ, Taylor WP, Kozubal MA, Kocar BD, Inskeep WP. Microbial community structure and sulfur biogeochemistry in mildly-acidic sulfidic geothermal springs in Yellowstone National Park. Geobiology. 2013;11(1):86-99.

22. Jay ZJ. Linking geochemistry with microbial community structure and function in sulfidic geothermal systems of Yellowstone National Park. 2015.

23. Carlson R, Fell D, Srienc F. Metabolic pathway analysis of a recombinant yeast for rational strain development. Biotechnol Bioeng. 2002;79(2):121-34.

24. Feist AM, Scholten JC, Palsson BO, Brockman FJ, Ideker T. Modeling methanogenesis with a genome-scale metabolic reconstruction of Methanosarcina barkeri. Mol Syst Biol. 2006;2:2006 0004.

25. Taffs R, Aston JE, Brileya K, Jay Z, Klatt CG, McGlynn S, et al. In silico approaches to study mass and energy flows in microbial consortia: a syntrophic case study. BMC Syst Biol. 2009;3:114.

26. Trinh CT, Wlaschin A, Srienc F. Elementary mode analysis: a useful metabolic pathway analysis tool for characterizing cellular metabolism. Appl Microbiol Biotechnol. 2009;81(5):813-26.

27. Schuster S, Hilgetag C. On Elementary Flux Modes in Biochemical Reaction Systems at Steady State. Journal of Biological Systems. 1994;02(02):165-82.

28. herichia coli glucose catabolism under various oxygenation rates. Appl Environ Microbiol. 1993;59(8):2465-73.

29. Carlson RP. Decomposition of complex microbial behaviors into resource-based stress responses. Bioinformatics. 2009;25(1):90-7.

30. Konopka A. What is microbial community ecology? ISME J. 2009;3(11):1223-30.

31. Markowitz VM, Chen IMA, Palaniappan K, Chu K, Szeto E, Grechkin Y, et al. IMG: the integrated microbial genomes database and comparative analysis system. Nucleic acids research. 2012;40(Database issue):D115--22.

32. Caspi R, Altman T, Dale JM, Dreher K, Fulcher CA, Gilham F, et al. The MetaCyc database of metabolic pathways and enzymes and the BioCyc collection of pathway/genome databases. Nucleic acids research. 2010;38(Database issue):D473--9.

33. Caspi R, Altman T, Dreher K, Fulcher CA, Subhraveti P, Keseler IM, et al. The MetaCyc database of metabolic pathways and enzymes and the BioCyc collection of pathway/genome databases. Nucleic acids research. 2012;40(Database issue):D742--53.

34. Kanehisa M, Goto S. KEGG: Kyoto encyclopedia of genes and genomes. Nucleic acids research. 2000;28(1):27--30.

35. Neidhart F, Ingraham J, Schaechter M. Physiology of the bacterial cell. A Molecular Approach, Sinauer, Sunderland, MA. 1990.

36. Shrihari, Kumar R, Gandhi KS. Modeling of Fe-2+ Oxidation by Thiobacillus-Ferrooxidans. Appl Microbiol Biot. 1990;33(5):524-8.

37. Farrand SG, Linton JD, Stephenson RJ, McCarthy WV, Jones CW. The effect of temperature and pH on the growth efficiency of the thermoacidophilic bacterium Bacillus acidocaldarius in continuous culture. Archives of Microbiology. 1983;135(4):276--83.

38. Klamt S, Saez-Rodriguez J, Gilles ED. Structural and functional analysis of cellular networks with CellNetAnalyzer. BMC systems biology. 2007;129(2):329--51.

39. Klamt S, von Kamp A. An application programming interface for CellNetAnalyzer. BioSystems. 2011;105(2):162--8.

40. Jungreuthmayer C, Ruckerbauer DE, Zanghellini Jr. regEfmtool: Speeding up elementary flux mode calculation using transcriptional regulatory rules in the form of three-state logic. Bio Systems. 2013;113(1):37--9.

41. Jungreuthmayer C, Ruckerbauer DE, Zanghellini Jr. Utilizing gene regulatory information to speed up the calculation of elementary flux modes. 2012:7.

42. Amend JP, Shock EL. Energetics of overall metabolic reactions of thermophilic and hyperthermophilic Archaea and bacteria. FEMS Microbiol Rev. 2001;25(2):175-243.

43. Soderberg T. Biosynthesis of ribose-5-phosphate and erythrose-4-phosphate in archaea: a phylogenetic analysis of archaeal genomes. Archaea. 2005;1(5):347-52.

44. Matsumi R, Atomi H, Driessen AJ, van der Oost J. Isoprenoid biosynthesis in Archaea–biochemical and evolutionary implications. Research in microbiology. 2011;162(1):39-52.

45. Macur RE, Jackson CR, Botero LM, McDermott TR, Inskeep WP. Bacterial populations associated with the oxidation and reduction of arsenic in an unsaturated soil. Environ Sci Technol. 2004;38(1):104-11.

46. Hamamura N, Macur RE, Korf S, Ackerman G, Taylor WP, Kozubal M, et al. Linking microbial oxidation of arsenic with detection and phylogenetic analysis of arsenite oxidase genes in diverse geothermal environments. Environ Microbiol. 2009;11(2):421-31.

47. D'Imperio S, Lehr CR, Oduro H, Druschel G, Kühl M, McDermott TR. Relative importance of H2 and H2S as energy sources for primary production in geothermal springs. Applied and environmental microbiology. 2008;74(18):5802-8.

48. Young M, Wiedenheft B, Snyder J, Spuhler J, Roberto F, Douglas T. Archaeal viruses from Yellowstone's high-temperature environments. Geothermal Biology and Geochemistry in YNP Bozeman, MT: Montana State Univ Publications. 2005:289-304.

49. Prangishvili D. The wonderful world of archaeal viruses. Annual review of microbiology. 2013;67:565-85.

50. Kozubal MA. Geomicrobiology of iron oxyhydroxide mats in acidic geothermal springs of Yellowstone National Park, Wyoming, United States of America. 2010.

51. Rohwer F, Prangishvili D, Lindell D. Roles of viruses in the environment. Environ Microbiol. 2009;11(11):2771-4.

52. Suttle CA. Marine viruses—major players in the global ecosystem. Nature Reviews Microbiology. 2007;5(10):801-12.

CHAPTER 5

CONCLUSIONS AND FUTURE DIRECTIONS

Microorganisms capable of inorganic carbon fixation have been identified in numerous geochemically diverse high-temperature environments in Yellowstone National Park (YNP). These organisms include members of the phylum Crenarchaeota (orders Sulfolobales and Thermoproteales) and deeply-rooted bacteria within the Aquificae. Moreover, evaluating the extent of inorganic-origin C in the microbial community demonstrated that chemolithoautotrophy is an important process *in situ*.

Inorganic C fixation was demonstrated in pure culture studies of *Metallospheara yellowstonensis* str. MK1 (order Sulfolobales), which is the predominant Fe(II)-oxidizing organism in acidic Fe(III)-oxide mats of YNP. Protein encoding genes for a complete 3-hydroxypropionate/4-hydroxybutyrate (3-HP/4-HB) pathway were identified in the genome of this YNP isolate. Additionally, the C isotope fractionation factor (ε) was determined for *M. yellowstonensis*, which was used to interpret the ^{13}C content (‰) of Fe(III)-oxide mats, and established a minimum amount of microbial C derived from dissolved inorganic C (DIC). *Hydrogenobaculum* spp. have been identified as early colonizers in Fe(III)-oxide mats and several *Hydrogenobaculum* isolates have been shown to fix inorganic C (i.e., DIC) through the reductive tricarboxylic acid cycle (r-TCA). Thus, *Hydrogenobaculum* was also considered as a possible contributing autotroph for interpreting the ^{13}C isotope content of Fe(III)-oxide mats. Microbial biomass in amorphous Fe(III)-oxide mats of Norris Geyser Basin (YNP) is comprised of

at least ~ 40% DIC, regardless of the absolute contributions made by either *M. yellowstonensis* or *Hydrogenobaculum* (Chapter 2).

Having established the extent of inorganic C fixation in two Fe(III)-oxide mats in Norris Geyser Basin, YNP, a broader study evaluated CO_2 fixation in high-temperature environments across a wide pH range (2.5 – 9) including five iron mats, six sulfur sediments, and four filamentous streamer communities (Chapter 3). Genes encoding enzymes for the 3-HP/4-HB, dicarboxylate/4-hydroxybutyrate (DC/4-HB), or the r-TCA pathway were identified in assembled metagenome sequence of each candidate autotroph found in these different habitats. Carbon isotope (^{13}C) mixing models were constructed based on spring-specific ^{13}C-DIC and ^{13}C-OC values and the relative abundance of candidate autotrophs (and their respective fractionation factors) to evaluate the extent of microbial inorganic C fixation in each microbial system. Results demonstrated CO_2 fixation in all environments. However, the candidate autotrophs may not be obligate CO_2-fixing organisms, thus future work should confirm the specific organisms responsible for CO_2-fixation, while investigating possible regulatory mechanisms governing autotrophic metabolism. Forthcoming meta-transcriptomes and meta-proteomes from these microbial communities should provide additional confirmation of genome predictions for inorganic C fixation to complement the physical isotopic evidence of this important process.

The extent of inorganic C fixation is also a function of the amount of non-microbial C in the sample. Greater amounts of non-microbial C (e.g., exogenous landscape C or adsorbed DOC) in the sample result in higher estimates of the fraction of DIC-derived microbial C. The relative abundance of heterotrophic populations was assessed, and a correlation may exist between environments subject to significant inputs

of landscape C (plant litter, dung, soil erosion, meteoric water inputs) and the establishment of abundant heterotrophic populations. However, this specific environmental context was not tested thoroughly in the current studies. The data collected here illustrate the need to further resolve specific C sources in all microbial systems, in part by determining the composition and biological availability of DOC, as well as identifying specific C compounds consumed by different heterotrophs.

Inorganic C is an important carbon source in high-temperature microbial communities present across geochemically diverse conditions. To further study the role of DIC fixation and potential microbial interactions in a simplified Fe(III)-oxide microbial mat community, genome sequence was used to construct stoichiometric reaction networks representing the metabolism of a primary autotroph (*M. yellowstonensis*) and a primary heterotroph (Geoarchaeota), both of which require oxygen (Chapter 4). To assess potential competition for O_2, which is diffusion-limited in Fe(III)-oxide mats, the cost of oxygen was evaluated as a function of biomass production. Autotrophic growth via Fe(II)-oxidation by *M. yellowstonensis* requires nearly 25 times more oxygen (per Cmol biomass) than is consumed by the organoheterotroph, Geoarchaeota. However, Geoarchaeota is dependent upon organic C, which was modeled as *M. yellowstonensis* biomass. Metabolism of Geoarchaeota requires 2.4 Cmol of *M. yellowstonensis* to produce 1 Cmol of biomass, which establishes a minimum autotroph-heterotroph ratio (2.4:1), based on the most efficient modes of Geoarchaeota biomass production.

The observed *M. yellowstonensis*: Geoarchaeota ratio in mature Fe(III)-oxide mats of One Hundred Spring Plain (OSP) has been determined in complementary

metagenome analysis and ranges from 0.3:1 to 0.5:1, which suggests that there is insufficient autotrophic biomass to support the observed heterotrophic abundance. These comparisons suggest that the two organisms may exhibit different growth (and turnover) rates *in situ*, and/or that Geoarchaeota also utilizes alternate sources of reduced C other than *M. yellowstonensis* biomass. Consequently, future work should focus on the relative growth and turnover rates of key autotrophs and heterotrophs in these communities, evaluate mechanisms of biomass turnover (e.g., viral predation), and clarify specific metabolites involved in the autotroph-heterotroph associations observed in this study.

Elementary flux mode analysis was also used to predict the rate of Fe(II)-oxidation as a function of the total oxygen flux necessary to support an autotroph-heterotroph partnership, and these results were used for comparison to *in situ* observations made in other studies. Genome-enabled stoichiometric models provided a theoretical construct for comparison to measured O_2 flux (microelectrodes) and Fe(III)-oxide deposition rates (longer-term studies using glass slides), which led to an evaluation of other possible O_2-consuming process (i.e., additional electron donors) and assisted in understanding the realized Fe(II)-oxidizing niche of *M. yellowstonensis*. Results from this study provided possible explanations for autotroph-heterotroph interactions, an understanding of carbon and energy flux within the oxic zone of Fe(III)-oxide microbial mats, and predictions (e.g., Fe(II)-oxidation rate) for comparison to *in situ* observations. Future work should investigate carbon and energy flux in the suboxic zone of the Fe-mat as well as the transfer of carbon and energy among all members of the microbial mat community.

Final Statement

Inorganic carbon fixation is a globally important process that, on local scales, provides reduced C constituents to numerous populations of heterotrophs. All known organisms require carbon and energy for growth and the acquisition of these substrates leads to biological interactions, further niche establishment and evolution through natural selection, and subsequent biological diversity. Moreover, genome sequence (if completely known) is a roadmap for the potential metabolism of an individual organism, and the subsequent ability of an organism to survive. Indeed, functioning genes are critical to survival and genes encoding key metabolic pathways must be quantifiably linked with observed processes. This thesis demonstrated microbial inorganic C fixation in geochemically diverse environments and linked genome content with physical evidence of metabolism, such as ^{13}C isotope content, iron oxidation, and oxygen reduction.

REFERENCES CITED

Ali MA, Dzombak DA. Competitive sorption of simple organic acids and sulfate on goethite. Environ Sci Technol. 1996;30(4):1061-71.

Amend JP, Shock EL. Energetics of overall metabolic reactions of thermophilic and hyperthermophilic Archaea and bacteria. FEMS Microbiol Rev. 2001;25(2):175-243.

Auernik KS, Kelly RM. Physiological versatility of the extremely thermoacidophilic archaeon Metallosphaera sedula supported by transcriptomic analysis of heterotrophic, autotrophic, and mixotrophic growth. Appl Environ Microbiol. 2010;76(3):931-5.

Battin TJ, Sloan WT, Kjelleberg S, Daims H, Head IM, Curtis TP, et al. Microbial landscapes: new paths to biofilm research. Nat Rev Microbiol. 2007;5(1):76-81.

Beam J, Jay Z, Kozubal M, Inskeep W, editors. Distribution and ecology of thaumarchaea in geothermal environments. The 11th International Conference on Thermophiles Research; 2011.

Beam JP, Bernstein HC, Jay ZJ, Kozubal MA, Jennings Rd, Tringe SG, et al. Assembly and Succession of Iron Oxide Microbial Mat Communities in Acidic Geothermal Springs. Geobiology. 2015.

Beam JP, Jay ZJ, Kozubal MA, Inskeep WP. Niche specialization of novel Thaumarchaeota to oxic and hypoxic acidic geothermal springs of Yellowstone National Park. ISME J. 2014;8(4):938-51.

Beam JP, Jay ZJ, Schmid MC, Rusch DB, Romine MF, R MJ, et al. Ecophysiology of an uncultivated lineage of Aigarchaeota from an oxic, hot spring filamentous 'streamer' community. ISME J. 2015.

Berg IA, Kockelkorn D, Buckel W, Fuchs G. A 3-hydroxypropionate/4-hydroxybutyrate autotrophic carbon dioxide assimilation pathway in Archaea. Science. 2007;318(5857):1782-6.

Berg IA, Kockelkorn D, Ramos-Vera WH, Say RF, Zarzycki J, Hugler M, et al. Autotrophic carbon fixation in archaea. Nat Rev Microbiol. 2010;8(6):447-60.

Bergfeld D, Lowenstern, J.B., Hunt, A.G., Shanks, W.C.P., III, and Evans, W.C. Gas and isotope chemistry of thermal features in Yellowstone National Park, Wyoming (ver. 1.1, September 2014): U.S. Geological Survey Scientific Investigations Report 2011–5012. 2014.

Bernstein HC, Beam JP, Kozubal MA, Carlson RP, Inskeep WP. In situ analysis of oxygen consumption and diffusive transport in high-temperature acidic iron-oxide microbial mats. Environ Microbiol. 2013;15(8):2360-70.

Blankenship RE. Early evolution of photosynthesis. Plant Physiol. 2010;154(2):434-8.

Boschker HT, Middelburg JJ. Stable isotopes and biomarkers in microbial ecology. FEMS Microbiol Ecol. 2002;40(2):85-95.

Boyd ES, Jackson RA, Encarnacion G, Zahn JA, Beard T, Leavitt WD, et al. Isolation, characterization, and ecology of sulfur-respiring crenarchaea inhabiting acid-sulfate-chloride-containing geothermal springs in Yellowstone National Park. Appl Environ Microbiol. 2007;73(20):6669-77.

Boyd ES, Leavitt WD, Geesey GG. CO2 Uptake and Fixation by a Thermoacidophilic Microbial Community Attached to Precipitated Sulfur in a Geothermal Spring. Applied and Environmental Microbiology. 2009;75(13):4289-96.

Breznak JA, Kane MD. Microbial H2/CO2 acetogenesis in animal guts: nature and nutritional significance1990 1990-12-01 00:00:00. 309-13 p.

Bryant DA, Frigaard NU. Prokaryotic photosynthesis and phototrophy illuminated. Trends Microbiol. 2006;14(11):488-96.

Carlson R, Fell D, Srienc F. Metabolic pathway analysis of a recombinant yeast for rational strain development. Biotechnol Bioeng. 2002;79(2):121-34.

Carlson RP. Decomposition of complex microbial behaviors into resource-based stress responses. Bioinformatics. 2009;25(1):90-7.

Caspi R, Altman T, Dale JM, Dreher K, Fulcher CA, Gilham F, et al. The MetaCyc database of metabolic pathways and enzymes and the BioCyc collection of pathway/genome databases. Nucleic acids research. 2010;38(Database issue):D473--9.

Caspi R, Altman T, Dreher K, Fulcher CA, Subhraveti P, Keseler IM, et al. The MetaCyc database of metabolic pathways and enzymes and the BioCyc collection of pathway/genome databases. Nucleic acids research. 2012;40(Database issue):D742--53.

Colman DR, Jay ZJ, Inskeep WP, Jennings Rd, Maas KR, Rusch DB, et al. Characterization of Novel, Deep-branching Heterotrophic Bacterial Populations Recovered from Thermal Spring Metagenomes ISME J. 2015.

Coplen TB, Brand WA, Gehre M, Groning M, Meijer HA, Toman B, et al. New guidelines for delta13C measurements. Anal Chem. 2006;78(7):2439-41.

Craig H. Isotopic Geochemistry of Hot Springs. Geol Soc Am Bull. 1953;64(12):1410-.

Craig H. The Geochemistry of the Stable Carbon Isotopes. Geochim Cosmochim Ac. 1953;3(2-3):53-92.

D'Imperio S, Lehr CR, Oduro H, Druschel G, Kühl M, McDermott TR. Relative importance of H2 and H2S as energy sources for primary production in geothermal springs. Applied and environmental microbiology. 2008;74(18):5802-8.

Drake HL, Gossner AS, Daniel SL. Old acetogens, new light. Ann N Y Acad Sci. 2008;1125:100-28.

Ehleringer JR, Monson RK. Evolutionary and ecological aspects of photosynthetic pathway variation. Annu Rev Ecol Syst. 1993:411-39.

Estep MLF. Carbon and Hydrogen Isotopic Compositions of Algae and Bacteria from Hydrothermal Environments, Yellowstone-National-Park. Geochim Cosmochim Ac. 1984;48(3):591-9.

Falkowski PG, Fenchel T, Delong EF. The microbial engines that drive Earth's biogeochemical cycles. Science. 2008;320(5879):1034-9.

Farquhar GD, Ehleringer JR, Hubick KT. Carbon Isotope Discrimination and Photosynthesis. Annu Rev Plant Phys. 1989;40:503-37.

Farrand SG, Linton JD, Stephenson RJ, McCarthy WV, Jones CW. The effect of temperature and pH on the growth efficiency of the thermoacidophilic bacterium Bacillus acidocaldarius in continuous culture. Archives of Microbiology. 1983;135(4):276--83.

Feist AM, Scholten JC, Palsson BO, Brockman FJ, Ideker T. Modeling methanogenesis with a genome-scale metabolic reconstruction of Methanosarcina barkeri. Mol Syst Biol. 2006;2:2006 0004.

Fouke BW. Hot-spring Systems Geobiology: abiotic and biotic influences on travertine formation at Mammoth Hot Springs, Yellowstone National Park, USA. Sedimentology. 2011;58(1):170-219.

Hamamura N, Macur RE, Korf S, Ackerman G, Taylor WP, Kozubal M, et al. Linking microbial oxidation of arsenic with detection and phylogenetic analysis of arsenite oxidase genes in diverse geothermal environments. Environ Microbiol. 2009;11(2):421-31.

Havig JR, Raymond J, Meyer-Dombard DAR, Zolotova N, Shock EL. Merging isotopes and community genomics in a siliceous sinter-depositing hot spring. Journal of Geophysical Research. 2011;116(G1).

Hawkins AS, Han Y, Bennett RK, Adams MW, Kelly RM. Role of 4-hydroxybutyrate-CoA synthetase in the CO2 fixation cycle in thermoacidophilic archaea. J Biol Chem. 2013;288(6):4012-22.

House CH, Schopf JW, Stetter KO. Carbon isotopic fractionation by Archaeans and other thermophilic prokaryotes. Organic Geochemistry. 2003;34(3):345-56.

Huber H, Gallenberger M, Jahn U, Eylert E, Berg IA, Kockelkorn D, et al. A dicarboxylate/4-hydroxybutyrate autotrophic carbon assimilation cycle in the hyperthermophilic Archaeum Ignicoccus hospitalis. Proc Natl Acad Sci U S A. 2008;105(22):7851-6.

Huber H, Huber R, Stetter KO. Thermoproteales. Prokaryotes: A Handbook on the Biology of Bacteria, Vol 3, Third Edition. 2006:10-22.

Huber H, Prangishvili D. Sulfolobales. In: Dworkin M, Falkow S, Rosenberg E, Schleifer K-H, Stackebrandt E, editors. The Prokaryotes: Springer New York; 2006. p. 23-51.

Huber H, Stetter KO. Desulfurococcales. Prokaryotes: A Handbook on the Biology of Bacteria, Vol 3, Third Edition. 2006:52-68.

Huber R, Eder W. Aquificales. In: Dworkin M, Falkow S, Rosenberg E, Schleifer K-H, Stackebrandt E, editors. The Prokaryotes: Springer New York; 2006. p. 925-38.

Hugler M, Huber H, Molyneaux SJ, Vetriani C, Sievert SM. Autotrophic CO2 fixation via the reductive tricarboxylic acid cycle in different lineages within the phylum Aquificae: evidence for two ways of citrate cleavage. Environ Microbiol. 2007;9(1):81-92.

Hugler M, Huber H, Stetter KO, Fuchs G. Autotrophic CO2 fixation pathways in archaea (Crenarchaeota). Arch Microbiol. 2003;179(3):160-73.

Hugler M, Krieger RS, Jahn M, Fuchs G. Characterization of acetyl-CoA/propionyl-CoA carboxylase in Metallosphaera sedula - Carboxylating enzyme in the 3-hydroxypropionate cycle for autotrophic carbon fixation. Eur J Biochem. 2003;270(4):736-44.

Hugler M, Sievert SM. Beyond the Calvin cycle: autotrophic carbon fixation in the ocean. Ann Rev Mar Sci. 2011;3:261-89.

Inskeep W, Macur R, Ackerman G, Kozubal M, Taylor W, Korf S. Linking microbial and geochemical processes in geothermal habitats. Geochim Cosmochim Ac. 2005;69(10):A226-A.

Inskeep WP, Ackerman GG, Taylor WP, Kozubal M, Korf S, Macur RE. On the energetics of chemolithotrophy in nonequilibrium systems: case studies of geothermal springs in Yellowstone National Park. Geobiology. 2005;3(4):297-317.

Inskeep WP, Jay ZJ, Herrgard MJ, Kozubal MA, Rusch DB, Tringe SG, et al. Phylogenetic and Functional Analysis of Metagenome Sequence from High-Temperature Archaeal Habitats Demonstrate Linkages between Metabolic Potential and Geochemistry. Front Microbiol. 2013;4:95.

Inskeep WP, Jay ZJ, Tringe SG, Herrgard MJ, Rusch DB, Committee YNPMPS, et al. The YNP Metagenome Project: Environmental Parameters Responsible for Microbial Distribution in the Yellowstone Geothermal Ecosystem. Front Microbiol. 2013;4:67.

Inskeep WP, Macur RE, Harrison G, Bostick BC, Fendorf S. Biomineralization of As(V)-hydrous ferric oxyhydroxide in microbial mats of an acid-sulfate-chloride geothermal spring, Yellowstone National Park. Geochim Cosmochim Ac. 2004;68(15):3141-55.

Inskeep WP, Rusch DB, Jay ZJ, Herrgard MJ, Kozubal MA, Richardson TH, et al. Metagenomes from high-temperature chemotrophic systems reveal geochemical controls on microbial community structure and function. PLoS One. 2010;5(3):e9773.

Jahnke LL, Eder W, Huber R, Hope JM, Hinrichs KU, Hayes JM, et al. Signature lipids and stable carbon isotope analyses of Octopus Spring hyperthermophilic communities compared with those of Aquificales representatives. Appl Environ Microbiol. 2001;67(11):5179-89.

Jay ZJ, Rusch DB, Tringe SG, Bailey C, Jennings RM, Inskeep WP. Predominant Acidilobus-like populations from geothermal environments in yellowstone national park exhibit similar metabolic potential in different hypoxic microbial communities. Appl Environ Microbiol. 2014;80(1):294-305.

Jay ZJ. Linking geochemistry with microbial community structure and function in sulfidic geothermal systems of Yellowstone National Park. 2015.

Jennings RM, Whitmore LM, Moran JJ, Kreuzer HW, Inskeep WP. Carbon dioxide fixation by Metallosphaera yellowstonensis and acidothermophilic iron-oxidizing microbial communities from Yellowstone National Park. Appl Environ Microbiol. 2014;80(9):2665-71.

Jungreuthmayer C, Ruckerbauer DE, Zanghellini Jr. regEfmtool: Speeding up elementary flux mode calculation using transcriptional regulatory rules in the form of three-state logic. Bio Systems. 2013;113(1):37--9.

Jungreuthmayer C, Ruckerbauer DE, Zanghellini Jr. Utilizing gene regulatory information to speed up the calculation of elementary flux modes. 2012:7.

Kandianis MT, Fouke BW, Johnson RW, Veysey J, Inskeep WP. Microbial biomass: A catalyst for CaCO3 precipitation in advection-dominated transport regimes. Geol Soc Am Bull. 2008;120(3-4):442-50.

Kanehisa M, Goto S. KEGG: Kyoto encyclopedia of genes and genomes. Nucleic acids research. 2000;28(1):27--30.

Karner MB, DeLong EF, Karl DM. Archaeal dominance in the mesopelagic zone of the Pacific Ocean. Nature. 2001;409(6819):507-10.

Klamt S, Saez-Rodriguez J, Gilles ED. Structural and functional analysis of cellular networks with CellNetAnalyzer. BMC systems biology. 2007;129(2):329--51.
Klamt S, von Kamp A. An application programming interface for CellNetAnalyzer. BioSystems. 2011;105(2):162--8.

Konhauser KO. Diversity of bacterial iron mineralization. Earth-Sci Rev. 1998;43(3-4):91-121.

Konneke M, Bernhard AE, de la Torre JR, Walker CB, Waterbury JB, Stahl DA. Isolation of an autotrophic ammonia-oxidizing marine archaeon. Nature. 2005;437(7058):543-6.

Konopka A. What is microbial community ecology? ISME J. 2009;3(11):1223-30.

Kozubal M, Macur RE, Korf S, Taylor WP, Ackerman GG, Nagy A, et al. Isolation and distribution of a novel iron-oxidizing crenarchaeon from acidic geothermal springs in Yellowstone National Park. Appl Environ Microbiol. 2008;74(4):942-9.

Kozubal MA, Dlakic M, Macur RE, Inskeep WP. Terminal oxidase diversity and function in "Metallosphaera yellowstonensis": gene expression and protein modeling suggest mechanisms of Fe(II) oxidation in the sulfolobales. Appl Environ Microbiol. 2011;77(5):1844-53.

Kozubal MA, Macur RE, Jay ZJ, Beam JP, Malfatti SA, Tringe SG, et al. Microbial iron cycling in acidic geothermal springs of yellowstone national park: integrating molecular surveys, geochemical processes, and isolation of novel fe-active microorganisms. Front Microbiol. 2012;3:109.

Kozubal MA, Romine M, Jennings R, Jay ZJ, Tringe SG, Rusch DB, et al. Geoarchaeota: a new candidate phylum in the Archaea from high-temperature acidic iron mats in Yellowstone National Park. ISME J. 2013;7(3):622-34.

Kozubal MA. Geomicrobiology of iron oxyhydroxide mats in acidic geothermal springs of Yellowstone National Park, Wyoming, United States of America. 2010.

Langner HW, Jackson CR, McDermott TR, Inskeep WP. Rapid oxidation of arsenite in a hot spring ecosystem, Yellowstone National Park. Environ Sci Technol. 2001;35(16):3302-9.

Macur RE, Jackson CR, Botero LM, McDermott TR, Inskeep WP. Bacterial populations associated with the oxidation and reduction of arsenic in an unsaturated soil. Environ Sci Technol. 2004;38(1):104-11.

Macur RE, Jay ZJ, Taylor WP, Kozubal MA, Kocar BD, Inskeep WP. Microbial community structure and sulfur biogeochemistry in mildly-acidic sulfidic geothermal springs in Yellowstone National Park. Geobiology. 2013;11(1):86-99.

Macur RE, Langner HW, Kocar BD, Inskeep WP. Linking geochemical processes with microbial community analysis: successional dynamics in an arsenic-rich, acid-sulphate-chloride geothermal spring. Geobiology. 2004;2(3):163-77.

Markowitz VM, Chen IM, Palaniappan K, Chu K, Szeto E, Grechkin Y, et al. IMG: the Integrated Microbial Genomes database and comparative analysis system. Nucleic Acids Res. 2012;40(Database issue):D115-22.

Matsumi R, Atomi H, Driessen AJ, van der Oost J. Isoprenoid biosynthesis in Archaea–biochemical and evolutionary implications. Research in microbiology. 2011;162(1):39-52.

Neidhart F, Ingraham J, Schaechter M. Physiology of the bacterial cell. A Molecular Approach, Sinauer, Sunderland, MA. 1990.

Nisbet EG, Sleep NH. The habitat and nature of early life. Nature. 2001;409(6823):1083-91.

Nordstrom DK, Ball JW, McCleskey RB. Ground water to surface water: chemistry of thermal outflows in Yellowstone National Park. Geothermal biology and geochemistry in Yellowstone National Park. 2005:73-94.

Nordstrom DK, Southam G. Geomicrobiology of sulfide mineral oxidation. Rev Mineral. 1997;35:361-90.

Pearson A, McNichol AP, Benitez-Nelson BC, Hayes JM, Eglinton TI. Origins of lipid biomarkers in Santa Monica Basin surface sediment: A case study using compound-specific Delta C-14 analysis. Geochim Cosmochim Ac. 2001;65(18):3123-37.

Pearson A, Pi Y, Zhao W, Li W, Li Y, Inskeep W, et al. Factors controlling the distribution of archaeal tetraethers in terrestrial hot springs. Appl Environ Microbiol. 2008;74(11):3523-32.

Peterson BJ, Fry B. Stable Isotopes in Ecosystem Studies. Annu Rev Ecol Syst. 1987;18:293-320.

Prangishvili D. The wonderful world of archaeal viruses. Annual review of microbiology. 2013;67:565-85.

Prentice IC, G.D. Farquhar, M.J.R. Fasham, M.L. Goulden, M. Heimann, V.J. Jaramillo, et al. The Carbon Cycle and Atmospheric Carbon Dioxide. Climate Change 2001: The Scientific Basis Contribution of Working Group I to the Third Assessment Report of the Intergovernmental Panel on Climate Change. 2001.

Preuß A, Schauder R, Fuchs G, Stichler W. Carbon Isotope Fractionation by Autotrophic Bacteria with Three Different CO2 Fixation Pathways. Zeitschrift für Naturforschung C. 1989;44(5-6):397-402.

Quayle JR, Ferenci T. Evolutionary aspects of autotrophy. Microbiol Rev. 1978;42(2):251-73.

Ramos-Vera WH, Berg IA, Fuchs G. Autotrophic carbon dioxide assimilation in Thermoproteales revisited. J Bacteriol. 2009;191(13):4286-97.

Reinthaler T, van Aken HM, Herndl GJ. Major contribution of autotrophy to microbial carbon cycling in the deep North Atlantic's interior. Deep-Sea Res Pt Ii. 2010;57(16):1572-80.

Reysenbach A-L, Banta AB, Boone DR, Cary SC, Luther GW. Biogeochemistry: microbial essentials at hydrothermal vents. Nature. 2000;404(6780):835-.

Reysenbach AL, Ehringer M, Hershberger K. Microbial diversity at 83 degrees C in Calcite Springs, Yellowstone National Park: another environment where the Aquificales and "Korarchaeota" coexist. Extremophiles. 2000;4(1):61-7.

Reysenbach A-L, Gotz D, Banta A, Jeanthon C, Fouquet Y. Expanding the distribution of the Aquificales to the deep-sea vents on Mid-Atlantic Ridge and Central Indian Ridge. CBM-Cahiers de Biologie Marine. 2002;43(3-4):425-8.

Rohwer F, Prangishvili D, Lindell D. Roles of viruses in the environment. Environ Microbiol. 2009;11(11):2771-4.

Rosman K, Taylor P. Isotopic compositions of the elements 1997 (Technical Report). Pure and Applied Chemistry. 1998;70(1):217-35.

Rothschild L, DesMarais D, Tharpe A. Ultraviolet Radiation Effects on Carbon Isotope Fractionation. 1998.

Rusch DB, Halpern AL, Sutton G, Heidelberg KB, Williamson S, Yooseph S, et al. The Sorcerer II Global Ocean Sampling expedition: northwest Atlantic through eastern tropical Pacific. PLoS Biol. 2007;5(3):e77.

Schäfer S, Barkowski C, Fuchs G. Carbon assimilation by the autotrophic thermophilic archaebacterium Thermoproteus neutrophilus. Arch Microbiol. 1986;146(3):301-8.

Schuster S, Hilgetag C. On Elementary Flux Modes in Biochemical Reaction Systems at Steady State. Journal of Biological Systems. 1994;02(02):165-82.

Shively JM, English RS, Baker SH, Cannon GC. Carbon cycling: the prokaryotic contribution. Curr Opin Microbiol. 2001;4(3):301-6.

Shrihari, Kumar R, Gandhi KS. Modeling of Fe-2+ Oxidation by Thiobacillus-Ferrooxidans. Appl Microbiol Biot. 1990;33(5):524-8.

Soderberg T. Biosynthesis of ribose-5-phosphate and erythrose-4-phosphate in archaea: a phylogenetic analysis of archaeal genomes. Archaea. 2005;1(5):347-52.

Stowe LG, Teeri JA. The geographic distribution of C4 species of the Dicotyledonae in relation to climate. American Naturalist. 1978:609-23.

Suttle CA. Marine viruses—major players in the global ecosystem. Nature Reviews Microbiology. 2007;5(10):801-12.

Taffs R, Aston JE, Brileya K, Jay Z, Klatt CG, McGlynn S, et al. In silico approaches to study mass and energy flows in microbial consortia: a syntrophic case study. BMC Syst Biol. 2009;3:114.

Takacs-Vesbach C, Inskeep WP, Jay ZJ, Herrgard MJ, Rusch DB, Tringe SG, et al. Metagenome sequence analysis of filamentous microbial communities obtained from geochemically distinct geothermal channels reveals specialization of three aquificales lineages. Front Microbiol. 2013;4:84.

Tamura K, Peterson D, Peterson N, Stecher G, Nei M, Kumar S. MEGA5: molecular evolutionary genetics analysis using maximum likelihood, evolutionary distance, and maximum parsimony methods. Mol Biol Evol. 2011;28(10):2731-9.

Trinh CT, Wlaschin A, Srienc F. Elementary mode analysis: a useful metabolic pathway analysis tool for characterizing cellular metabolism. Appl Microbiol Biotechnol. 2009;81(5):813-26.

Tully BJ, Nelson WC, Heidelberg JF. Metagenomic analysis of a complex marine planktonic thaumarchaeal community from the Gulf of Maine. Environ Microbiol. 2012;14(1):254-67.

Varma A, Boesch BW, Palsson BO. Stoichiometric interpretation of Escherichia coli glucose catabolism under various oxygenation rates. Appl Environ Microbiol. 1993;59(8):2465-73.

Walker CB, de la Torre JR, Klotz MG, Urakawa H, Pinel N, Arp DJ, et al. Nitrosopumilus maritimus genome reveals unique mechanisms for nitrification and autotrophy in globally distributed marine crenarchaea. Proc Natl Acad Sci U S A. 2010;107(19):8818-23.

Whitman W, Bowen T, Boone D. The Methanogenic Bacteria. In: Dworkin M, Falkow S, Rosenberg E, Schleifer K-H, Stackebrandt E, editors. The Prokaryotes: Springer New York; 2006. p. 165-207.

Whitman WB, Coleman DC, Wiebe WJ. Prokaryotes: the unseen majority. Proc Natl Acad Sci U S A. 1998;95(12):6578-83.

Young M, Wiedenheft B, Snyder J, Spuhler J, Roberto F, Douglas T. Archaeal viruses from Yellowstone's high-temperature environments. Geothermal Biology and Geochemistry in YNP Bozeman, MT: Montana State Univ Publications. 2005:289-304.

Zhang LM, Offre PR, He JZ, Verhamme DT, Nicol GW, Prosser JI. Autotrophic ammonia oxidation by soil thaumarchaea. Proc Natl Acad Sci U S A. 2010;107(40):17240-5.

APPENDICES

APPENDIX A

STABLE CARBON ISOTOPE ANALYSIS IN BIOLOGICAL SYSTEMS

STABLE CARBON ISOTOPE ANALYSIS IN BIOLOGICAL SYSTEMS

Carbon is the elemental basis for all known life forms in Earth systems and constitutes a significant portion (by dry weight) of the mass of all living organisms (1). Three naturally occurring carbon isotopes (^{12}C, ^{13}C, and ^{14}C) exist. Both ^{12}C and ^{13}C are stable isotopes, while ^{14}C is radioactive (half-life ~ 5700 years), and is used to estimate the age of biological materials (radiocarbon dating). The majority (98.93%) of C on Earth is ^{12}C, while the heavier ^{13}C constitutes 1.07% (2). The relative quantities of the stable isotopes (^{12}C and ^{13}C) in a sample can be measured by mass spectroscopy as a ratio, R ($^{13}C/^{12}C$), then compared to the international standard (PeeDee belemnite, PDB), and reported as a delta (δ) value, where δ equals $(R_{sample}/R_{standard} - 1) \times 1{,}000$.

The stable C isotope content (e.g., $\delta^{13}C$, ‰) of different carbon sources and organisms provides a powerful method for evaluating trophic webs and C cycling. The ^{13}C isotope content of biomass C is a function of the ^{13}C content of C sources consumed, and any fractionation (i.e., differential reaction of specific isotopes) that occurs during biological uptake and metabolism. Organisms that reduce inorganic carbon (i.e., carbon dioxide) into biomass (autotrophs) fractionate C based on the preference of carboxylase enzymes for ^{12}C versus ^{13}C, resulting in marked differences in the $\delta^{13}C$ value of the product (biomass) compared to the substrate (CO_2). For small fractionation factors (ε), $\varepsilon \approx \delta^{13}C_{substrate} - \delta^{13}C_{biomass}$. As an example, the $\delta^{13}C$ of atmospheric CO_2 is ~ -8 ‰ and the $\delta^{13}C$ of plants that use the C_3 photosynthetic pathway is ~ -28 ‰, thus ε for C_3 plants is ~ -20 ‰ (3). Fractionation factors for known autotrophic pathways of carbon dioxide fixation are routinely reported in the literature (e.g., (4, 5)). Heterotrophic metabolism

(i.e., the oxidation of organic carbon) does not discriminate between ^{12}C and ^{13}C, and fractionation factors are close to 0‰ (6). Thus, the isotope signature of heterotrophic biomass is similar to the carbon source.

The isotope content ($\delta^{13}C$) of numerous different sample types from Yellowstone National Park (YNP) was determined in collaboration with Dr. James Moran and Dr. Helen Kreuzer at Pacific Northwest National Laboratories (Richland, WA). The suite of samples focused on (i) possible carbon sources for microorganisms growing in geothermal habitats, which include dissolved inorganic C, dissolved organic C, and/or landscape organic C, and (ii) microbial samples from pure cultures (Chapter 2), and Fe-oxide mats, S sediments and filamentous streamer communities collected from field sites in YNP (Chapter 3). The fractionation factor (ε) for *Metallosphaera yellowstonensis* grown with CO_2 as the sole carbon source was estimated (Chapter 2) and this, along with ε values for other microorganisms capable of inorganic carbon fixation, was used to evaluate carbon sources in natural communities (Chapter 3). Isotope mixing models were constructed that predicted the relative extent to which microbial autotrophy supplied C to the community as a function of the amount of exogenous (landscape) C in the sample.

1. Neidhart F, Ingraham J, Schaechter M. Physiology of the bacterial cell. A Molecular Approach, Sinauer, Sunderland, MA. 1990.
2. Rosman K, Taylor P. Isotopic compositions of the elements 1997 (Technical Report). Pure and Applied Chemistry. 1998;70(1):217-35.
3. Farquhar GD, Ehleringer JR, Hubick KT. Carbon Isotope Discrimination and Photosynthesis. Annu Rev Plant Phys. 1989;40:503-37.
4. Ehleringer JR, Monson RK. Evolutionary and ecological aspects of photosynthetic pathway variation. Annu Rev Ecol Syst. 1993:411-39.
5. House CH, Schopf JW, Stetter KO. Carbon isotopic fractionation by Archaeans and other thermophilic prokaryotes. Organic Geochemistry. 2003;34(3):345-56.
6. Boschker HT, Middelburg JJ. Stable isotopes and biomarkers in microbial ecology. FEMS Microbiol Ecol. 2002;40(2):85-95.

APPENDIX B

SUPPLEMENTAL MATERIAL TO "CARBON DIOXIDE FIXATION BY METALLOSPHAERA YELLOWSTONENSIS AND ACIDOTHERMOPHILIC IRON-OXIDIZING MICROBIAL COMMUNITIES FROM YELLOWSTONE NATIONAL PARK"

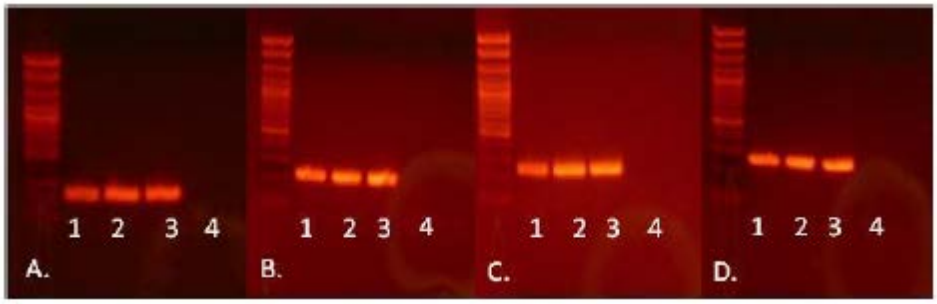


Figure A.1. Amplification of 3-HP/4-HB marker genes: A) *4hcd*; B) *accC*; C) *accB*; D) *pccB*. Lanes 1 & 2 = *M. yellowstonensis;* Lane 3 = Fe(III)-oxide mat environmental sample; Lane 4 = Negative *E. coli* control; Lane 5 = Reagent blank.

Table A.1. Protein coding genes of the 3-hydroxypropionate/4-hydroxybutyrate cycle identified in the *M. yellowstonensis* strain MK1 genome and *M. yellowstonensis*-like *de novo* assemblies from the OSP Fe(III)-oxide mat metagenomes.

Enzymes of the Proposed 3-hydroxypropionate/4-hydroxybutyrate cycle	**Candidate gene in *M. sedula* (9,33)**	**Candidate enzyme in *M.yellowstonensis*, identified through BLASTp homology to *M. sedula*-Accession (expect value, % positives)**	**Candidate enzyme in *M. yellowstonensis*-like HFO metagenome sequences, identified through BLASTp homology to *M. sedula*- IMG Gene ID[a] (expect value, % positives)**
acetyl-CoA carboxylase	msed_0147/msed_0148/ msed_1375	EHP69328.1 (0.0, 93%) / EHP69329.1 (4e-100, 94%) / EHP68101.1 (0.0, 97%)	152750 (0.0, 94%) / 152760 (2e-99, 94%) / 60850 (0.0, 97%)
malonyl-CoA reductase (NADPH)	msed_0709	EHP70731.1 (0.0, 95%)	143020 (1e-138, 97%)
malonate semialdehyde reductase (NADPH)	msed_1993	EHP68707.1 (2e-173, 87%)	79160 (6e-166, 88%)
3-hydroxypropionyl-CoA synthetase (AMP-forming)	msed_1456	EHP68110.1 (0.0, 95%)	60890 (0.0, 96%)
3-hydroxypropionyl-CoA dehydratase	msed_2001	EHP68697.1 (6e-144, 89%)	78860 (1e-121, 89%)
acryloyl-CoA reductase (NADPH)	msed_1426	EHP70486.1 (0.0, 90%)	183700 (4e-180, 90%)
propionyl-CoA carboxylase	msed_0147/msed_0148/ msed_1375	EHP69328.1 (0.0, 93%) / EHP69329.1 (4e-100, 94%) / EHP68101.1 (0.0, 97%)	152750 (0.0, 94%) / 152760 (2e-99, 94%) / 60850 (0.0, 97%)
methylmalonyl-CoA epimerase	msed_0639	EHP70648.1 (7e-80, 91%)	71510 (3e-79, 91%)
methylmalonyl-CoA mutase	msed_0638/msed_2055	EHP70647.1 (0.0, 95%) / EHP68637.1 (5e-80, 94%)	154270 (2e-175, 93%) / 28150 (6e-70, 94%)
succinyl-coA reductase (NADPH)	msed_0709	EHP70731.1 (0.0, 95%)	143020 (1e-138, 97%)
succinate semialdehyde reductase (NADPH)	msed_1424	EHP70477.1 (0.0, 93%)	57730 (0.0, 93%)
4-hydroxybutyryl-CoA ligase (AMP-forming)	msed_0394, msed_0406	EHP71147.1 (0.0, 88%), EHP69042.1 (0.0, 87%)	39960 (0.0, 89%), 155470 (0.0, 88%)
4-hydroxybutryl-CoA dehydratase, Type I	msed_1321	EHP69763.1 (0.0, 97%)	44600 (0.0, 98%)
crotonyl-CoA hydratase	msed_0399	EHP69048.1 (0.0, 81%)	155420 (0.0, 82%)
3-hydroxybutyrl-CoA dehydrogenase	msed_0399	EHP69048.1 (0.0, 81%)	155420 (0.0, 82%)
acetoacetyl-CoA-B-ketothiolase	msed_0656	EHP70668.1 (0.0, 88%)	71440 (0.0, 88%)

"/" separates subunits of enyzme complex, "," separates proposed candidate genes

[a] Actual IMG Gene ID is formatted as "YNPsite14_CeleraDRAFT_" followed by the ID-number reported

Table A.2. Major ion constituents used in synthetic media for growth experiments using *M. yellowstonensis* strain MK1.

Cations	**uM**	**Anions**	**uM**
Na	15800	NO_3	400
K	1547	SO_4	1212
Al	114	Cl	10642
Mg	12	PO_4	100
NH_4	600	F	147
Ca	250	B	717
		CO_3	5000

C:N:P 50:10:01

APPENDIX C

SUPPLEMENTAL MATERIAL TO "THE EXTENT AND MECHANISMS OF CARBON DIOXIDE FIXATION ACROSS GEOCHEMICALLY DIVERSE HIGH-TEMPERATURE MICROBIAL COMMUNITIES"

Table S1. Geochemical summary and isotope content of fifteen high temperature microbial habitats in Yellowstone National Park (YNP), Wyoming, USA. Samples were collected from October 2010 through November 2013, site abbreviations and specific transects are indicated; replicate field samples are indicated and reported below sampling date.

		Geochemical Summary							Stable Isotope Content									
Site Name[1]	Sampling Date (M/D/Y)	pH	T (°C)	Cl^- (mM)	SO_4^{2-} (mM)	DIC^2 (mM)	DOC^2 (mM)	δ^2H (‰)	$\delta^{18}O$ (‰)	$\delta^{13}C$-DIC^2 (‰)	$\delta^{13}C$-DOC^2 (‰)	$\delta^{13}C$ Microbial Habitat[3] (‰)	σ (‰)	n	$\delta^{13}C$ Landscape[4] (‰)	σ (‰)	n
S-Sediments																	
Crater Hills																	
S floc	5/17/2012											-20.7	0.4	5	-26.0	0.2	3
	Rep-2											-20.4	0.8	4	-24.8	0.2	3
Source 1	5/17/2012	2	76	0.02	10.29	0.17	0.22	-128.2	-12.88	5.3	-23.5	-19.7	0.6	4	-24.2	0.3	5
Source 2	5/17/2012					0.08	0.20	-128.4	-12.69	5.6	-23.8	-20.0	0.3	4	-18.2	0.1	3
sediment from tributary	5/17/2012					0.07	0.32	-144.0	-18.77	0.1	-24.0						
Joseph's Coat 2																	
JC2_E	8/6/2012	2.2	79	0.01	4.86	3.36	0.06	-139.2	-15.55	-5.4	-24.9	-16.1	0.5	7	-23.4	0.5	3
JC2_F	8/6/2012	2.2	55			0.36	0.11			-4.4	-23.8						
Monarch Geyser																	
MG	11/16/2011	4.3	82	8.51	0.98	1.61	0.06			-3.2	-17.0	-7.2	0.3	5	-26.2	0.2	5
	Rep-2											-7.6	1.1	6			
MG	4/13/2012	4.1	84	9.77	0.90	0.93	0.06	-129.5	-11.75	-4.5	-19.9	-5.7	0.2	3			
	Rep-2											-5.2	0.2	3			
MG	4/30/2013	3.4	82	10.82	1.23	1.34	0.04			-3.3	-17.9	-4.9	0.1	3			
	Rep-2											-5.0	0.2	3			
MG	11/14/2013	3.5	84	9.92	1.32	0.72	0.04	-124.7	-10.15	-4.9	-15.5	-5.3	0.7	7			
	Rep-2											-5.4	0.4	7			
Cistern Spring																	
CIS	11/16/2011	4.4	78	10.96	1.14	0.57	0.05			-3.9	-18.0	-12.2	0.2	6	-20.0	0.5	6
	Rep-2											-13.3	0.4	6	-26.7	0.1	3
CIS	4/13/2012	4.6	80	11.15	0.84	0.53	0.04	-120.5	-8.73	-4.4	-17.2	-22.0	0.2	3			
	Rep-2											-21.6	0.2	6			
CIS	4/30/2013	4.2	78	11.13	0.83	0.61	0.05			-3.8	-17.5	-19.6	0.2	3			
	Rep-2											-19.7	0.3	3			
CIS	11/14/2013	4.8	81	14.73	0.65	0.95	0.03	-125.8	-11.50	-5.1	-20.6	-20.7	0.1	3			
	Rep-2											-21.0	0.4	7			
Joseph's Coat 3																	
JC3_A (sediment)	8/6/2012	6.1	83	10.45	3.96							-13.0	0.1	4			
JC3_A (M)	8/6/2012	6.1	90	10.45	3.96	0.38	0.05	-123.3	-7.85	-2.4	-16.9	-14.8	0.1	4			
Washburn Spring																	
WS	10/4/2012	6.2	72	0.01	14.08	3.85	1.01	-110.7	-2.04	0.9	-22.8	-23.3	0.1	3			
	Rep-2											**-22.5**	**0.8**	**3**	Convex Feature		
	Rep-3											-23.2	0.1	3			
	Rep-4											-23.9	0.1	3			
Oxic Fe-Mats																	
Joseph's Coat 2																	
JC2_A	8/6/2012	2.2	91	0.01	5.20	0.07	0.06	-140.6	-16.66	-5.0	-25.0				-15.6	0.1	3
JC2_B	8/6/2012	2.2	80	0.01	5.21	0.04	0.04	-140.9	-16.34	-3.7	-24.1	-8.3	0.5	7			

	JC2_C	8/6/2012	2.2	70	0.01	5.57	0.04	0.04	-140.1	-16.17	-3.3	-23.3	-13.9	0.4	3			
	JC2_D	8/6/2012	2.2	60			0.02	0.06	-139.0	-15.67	-1.6	-22.5						
Beowulf Spring																		
	BE_A	10/13/2010	2.8	82	10.76	1.84	2.96	0.03	-140.2	-15.00	-3.9	-22.3						
	BE_D	10/13/2010	2.8	70	10.93	1.88	0.27	0.03	-138.2	-14.50	-3.4	-22.6	-17.4	0.2	3	-28.0	0.3	3
	BE_A	5/11/2011	2.8	80	10.14	1.71	1.56	0.07	-141.2	-16.60	-2.1	-25.2				-28.6	0.1	4
	BE_B	5/11/2011	2.8	76			2.56	0.04	-141.8	-15.81	-3.0	-24.7				-24.4	0.1	6
	BE_C	5/11/2011	2.9	71			0.86	0.04	-140.4	-15.20	-2.7	-24.5	-20.9	0.5	3	-26.7	0.4	6
		Rep-2											**-21.6**	**0.3**	**5**	-24.1	2.3	8
	BE_D	5/11/2011	2.9	67			0.40	0.04	-140.5	-15.41	-2.5	-24.0				-26.9	1.5	6
	BE_E	5/11/2011	2.9	62			0.12	0.06	-140.0	-15.17	-1.2	-23.2	-17.9	0.1	4	-26.8	0.1	7
		Rep-2											**-14.3**	**0.3**	**3**	**-24.6**	**0.1**	**2**
	BE_A	10/11/2011	2.9	86			2.26	0.07	-140.6	-15.33	-3.5	-23.7				-10.7	0.2	3
	BE_D	10/11/2011	2.9	69	8.82	1.27	0.07	0.06			-8.9	-23.1				-25.0	1.6	6
	BE_D	11/16/2011	2.9	68	10.28	1.53							-16.2	0.1	5	**-18.2**	**0.4**	**2**
	BE_A	5/15/2012	2.6	83	10.11	1.58	0.34	0.16	-141.7	-15.86	4.0	-22.1						
	BE_D	5/15/2012	2.6	68	10.56	1.67	0.03	0.15			1.0	-24.8	-17.4	0.0	3			
		Rep-2											-18.4	0.1	6			
	BE_E	5/15/2012	2.6	62			0.02	0.06			-0.6	-24.9						
	BE_A	10/3/2012		8x			1.45	0.02	-141.2	-15.48	-3.0	-23.8						
	BE_D	10/3/2012		66			0.04	0.03			-7.6	-20.5	-15.3	0.2	5			
		Rep-2											-15.9	0.0	3			
	BE_A	5/3/2013	3.1	81	10.73	1.53	3.66	0.05			-3.2	-21.4						
	BE_D	5/3/2013	3.1	68	11.18	1.63	0.34	0.05			-3.0	-21.3	-15.8	0.2	5			
		Rep-2											-15.7	0.1	5			
	BE_A	6/26/2013	3.2	82			2.17	0.03			-3.9	-26.0						
	BE_C	6/26/2013	3.2	71			0.49	0.03			-4.9	-24.7						
	BE_D	6/26/2013	3.2	66			0.08	0.04			-5.7	-23.3						
	BE_A	8/28/2013	3	86	11.97	1.39	2.16	0.03			-4.3	-24.8						
	BE_D	8/28/2013	3	67	12.20	1.55	0.06	0.02			-4.3	-22.5	-15.1	0.2	3			
		Rep-2											-16.0	0.1	3			
	BE_A	11/15/2013	3.1	83			0.60	0.03	-140.4	-15.28	-4.6	-22.1						
Grendel Spring																		
	GRN_A	5/12/2011	3.3	84	11.44	1.14	0.13	0.05	-139.9	-15.06	2.6	-24.8						
	GRN_B	5/12/2011	3.3	71				0.08	-138.7	-14.73		-24.4	-15.5	0.2	3			
		Rep-2											**-11.2**	**0.1**	**2**			
	GRN_B	10/11/2011	3.4	70			0.13	0.08	-134.8	-13.98	2.6	-24.4	-15.8	0.1	3			
	GRN_B	5/15/2012											-17.1	0.1	3			
	GRN_D	5/15/2012					0.04	0.06			2.0	-25.1	-17.3	0.0	3			
	GRN_A	10/3/2012	3.4	78	12.20	1.34	0.72	0.03	-134.6	-14.09	-3.1	-21.8						
	GRN_D	10/3/2012	3.4	70	12.31	1.36	0.06	0.03			-9.8	-20.6	-15.6	0.3	6			
		Rep-2											-16.5	0.3	6			
	GRN_A	11/15/2013					0.36	0.06	-134.3	-13.94	-5.6	-23.5						
	GRN_B	11/15/2013					0.09	0.06			-5.6	-21.5						
	GRN_C	11/15/2013					0.07	0.05			-5.5	-21.6	-17.3	0.2	3			
		Rep-2											-17.3	0.4	4			
Echinus Geyser																		
	ECH_A	11/16/2011	3.4	73												-25.3	0.1	3
	ECH_B	11/16/2011	3.4	67	3.69	2.83	0.14	0.03			-4.1	-21.2	-12.1	0.1	3	-27.4	0.1	5

	ECH_C	11/16/2011		60									-10.8	0.2	6				
	ECH_A	4/14/2012	3.7	75															
	ECH_B	4/14/2012	3.7	66	4.08	2.89	0.05	0.03	-139.1	-16.32	-4.9	-23.5	-10.1	0.1	3				
		Rep-2											-10.6	0.1	3				
	ECH_A	4/30/2013	3.5	77	4.14	2.94	0.46	0.02			-3.8	-23.1							
	ECH_B	4/30/2013	3.5	69	4.06	2.92							-11.6	0.1	5				
		Rep-2											-11.0	0.2	6				
	ECH_A	11/14/2013	3.7	75			0.60	0.03	-138.6	-16.29	-4.6	-22.1							
	ECH_B	11/14/2013	3.6	68			0.03	0.03			-4.5	-21.8	-13.6	0.2	3				
		Rep-2											-12.7	0.1	3				
		Rep-3											-12.1	0.3	3				
		Rep-4											-11.7	0.5	6				
100 Spring Plain																			
	OSP_A	5/12/2011	3.5	74	12.93	0.96	0.28	0.03	-140.4	-15.11	-0.5	-23.5	-17.7	0.2	3	-20.4	0.1	3	
	OSP_G	5/12/2011	3.5	72	12.90	0.98							-17.2	0.5	4	**-23.1**	**0.0**	**2**	
		Rep-2											**-18.4**	**0.1**	**2**	-16.3	0.1	3	
	OSP_C	5/12/2011											-13.5	0.1	3				
		Rep-2											**-11.5**	**0.0**	**3**				
	OSP_A	10/11/2011	3.4	81.5	12.70	1.02	0.42	0.05	-137.7	-14.21	-4.8	-22.6	-15.6	0.2	3				
	OSP_B	10/11/2011	3.4	77			0.16	0.06			-6.0	-22.6	-17.1	0.1	3				
	OSP_C	10/11/2011	3.4	70									-17.3	0.2	3				
	OSP_A	5/11/2012					0.02	0.11			2.3	-25.9							
	OSP_B	10/3/2012		73									-14.2	0.2	6				
		Rep-2											-14.1	0.5	6				
	OSP_A	10/3/2012			12.87	0.98	0.16	0.03	-138.4	-15.07	-4.8	-19.5							
	OSP_A	5/3/2013	3.6	82	12.70	1.02	0.37	0.06			-4.4	-20.8							
	OSP_B	5/3/2013											-13.5	0.2	5				
		Rep-2											**-13.5**	**0.0**	**2**				
		Rep-3											-13.7	0.5	2				
	OSP_A	6/26/2013	3.7	85			0.22	0.05			-5.8	-26.4							
	OSP_A	11/15/2013	3.7	83			0.20	0.06	-138.0	-14.70	-5.5	-22.3							
	OSP_B	11/15/2013	3.7	72									-18.3	0.1	3				
Streamer Communities																			
Dragon & Beowulf Spring																			
	BE_B	10/13/2010	2.8	78			1.62	0.03	-140.0	-14.96	-3.4	-23.2							
	BW_B	10/13/2010											-10.1	0.4	3				
	BW_A	5/12/2011	3	80	10.23	1.72		0.07	-141.6	-15.95		-24.5				See same sites under Fe-oxide samples			
	BW_B	10/3/2012											-9.4	0.5	6				
	DS_B	11/14/2013	3	75									-7.9	0.1	3				
		Rep-2											-9.1	0.2	3				
		Rep-3											**-8.2**	**0.2**	**3**				
		Rep-4											**-9.7**	**0.2**	**4**				
Narrow Gauge - Mammoth Hot Springs																			
	NG_A	5/16/2012	6.2	74	4.34	5.36	13.14	0.02	-148.0	-18.2	1.2	-15.8							
	NG_B	5/16/2012	6.2	72			13.88	0.09			1.1	-23.2	1.9	0.1	3				
		Rep-2											**-12.4**	**0.3**	**8**				
		Rep-3											2.2	0.2	3				
		Rep-4											**-11.3**	**0.1**	**3**				
		Rep-5											2.1	0.0	3				

	NG_C	5/16/2012	6.4	71			12.46	0.08	-148.3	-18.1	1.4	-23.1	2.5	0.0	3			
	NG_C	5/16/2012											**-11.6**	**0.1**	**3**	Convex Feature		
		Rep-2											2.3	0.2	3			
		Rep-3											**-12.3**	**0.1**	**2**			
		Rep-4											2.2	0.3	3			
		Rep-5											**-12.3**	**0.3**	**5**			
	NG_A	11/15/2013	6.4	72			18.28	0.02	-148.7	-18.46	-1.2	-21.1	-1.4	0.3	3			
		Rep-2											**-10.2**	**0.1**	**3**			
		Rep-3											**-9.7**	**0.2**	**4**			
Octopus Spring																		
	OCT_B	10/13/2011	7.7	84	6.59	0.16	4.95	0.02	-142.1	-16.57	-2.2	-22.6	-15.2	0.4	5	-25.3	0.2	6
		Rep-2											-18.7	0.6	6	-26.5	0.3	6
		Rep-3											-16.8	0.1	5	-24.6	0.1	5
	OCT_C	10/13/2011	7.8	82									-15.3	0.6	6	-27.9	0.1	3
		Rep-2											-16.9	0.2	4			
		Rep-3											-15.9	0.2	3			
	OCT_A	10/5/2012	8.2	90	6.62	0.16	5.19	0.02	-143.6	-16.95	-1.9	-21.9						
	OCT_B	10/5/2012	8.6	84			5.31	< 0.008			-1.9	-22.3	-15.8	0.0	3			
	OCT_C	10/5/2012	8.6	82	6.70	0.17	5.35	< 0.008			-1.8	-22.1	-15.7	0.4	6			
		Rep-2											-16.1	0.1	3			
	OCT_D	10/5/2012	8.6	78			5.26	< 0.008			-1.8	-21.8	-16.3	0.2	6			
		Rep-2											-16.3	0.3	8			
	OCT_A	8/28/2013	7.9	90			5.20	0.02			-1.9	-26.3						
	OCT_B	8/28/2013	8	85									-15.8	0.2	3			
		Rep-2											-16.5	0.1	3			
	OCT_C	8/28/2013	8.2	82			5.08	0.01			-1.7	-24.1	-16.9	0.3	10			
		Rep-2											-17.4	0.1	3			
Conch Spring																		
	CON_B	10/13/2011	8.3	84	8.34	0.24	2.71	0.04	-141.5	-16.51	-2.9	-19.0	-0.1	0.1	3			
		Rep-2											0.3	0.6	9			
	CON_A	10/5/2012		93	8.39	0.22	3.17	0.02	-141.2	-16.6	-2.6	-16.7						
	CON_B	10/5/2012	9.9	85			3.18	0.01			-2.7	-21.5	0.5	0.4	6			
		Rep-2											-0.3	0.2	6			
		Rep-3											**-3.6**	**0.6**	**2**			
		Rep-4											**-4.2**	**1.5**	**5**			
	CON_C	10/5/2012	9.8	82	8.62	0.26	3.22	< 0.008			-2.7	-21.3	-0.9	0.4	6			
		Rep-2											-0.1	0.2	6			
	CON_D	10/5/2012	9.8	79			3.60	0.01			-2.3	-20.0	-0.2	1.0	8			
		Rep-2											**-6.4**	**1.1**	**3**			
		Rep-3											0.3	0.2	3			
	CON_E	10/5/2012	9.8	70			3.55	0.01			-2.4	-20.2						
		Rep-2											0.0	0.3	6			
	CON_A	8/28/2013	9	93	8.56	0.21	3.58	0.02			-2.5	-26.4						
	CON_B	8/28/2013	9	85			3.75	0.02			-2.5	-26.4						
	CON_C	8/28/2013	9	82									1.9	0.5	7			
	CON_D	8/28/2013	9	75	8.87	0.23	4.08	0.01			-2.3	-24.8	0.5	0.1	4			
		Rep-2											0.2	0.1	4			

[1] Site latitude/longitude coordinates (standard UTM zone 12, easting/northing): Crater Hills = 540854/4944565, Joseph's Coat 2 = 553378/4954163, Monarch Geyser = 523313/4952366, Cistern Spring = 523439/4952232, Joseph's Coat 3 = 553481/4954197, Washburn Spring = 545079/4956997, Beowulf Spring = 522859/4953159, Grendel Spring = 523000/4952230, Echinus Geyser = 523592/4952118, One Hundred Springs Plain = 523042/4953337, Dragon = 522877/4953208, Narrow Gauge - Mammoth Hot Springs = 522882/4979594, Octopus Spring = 516058/4931215, Conch Spring = 513330/4933689.

[2] DOC = Dissolved Organic Carbon, DIC = Dissolved Inorganic Carbon

[3] Microbial habitats include elemental sulfur sediments, iron oxide mats, and filamentous streamers; samples pretreated with HCl are indicated in bold

[4] Landscape samples included animal dung, leaves, algae, and soils; samples pretreated with HCl are indicated in bold

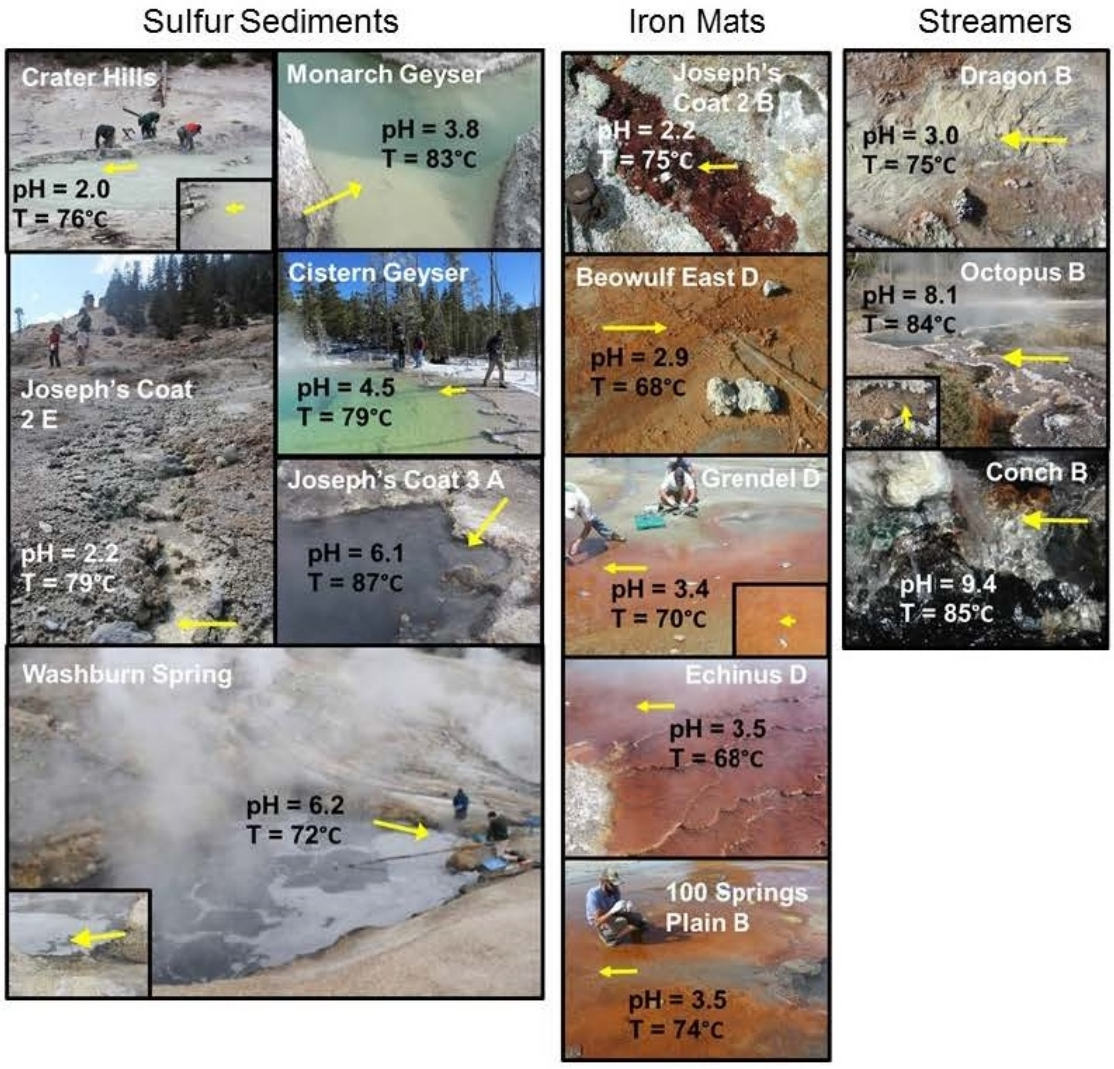
Table S2. Candidate enzymes for CO_2 fixation pathways found in *de novo* phylotype genome sequences, identified through BLASTp homology or IMG/ER pipeline annotation (expect value, % positives).

Enzymes of the proposed Dicarboxylate/4-Hydroxybutyrate Pathway	Candidate Gene in *T. neutrophilus* (Ramos-Vera *et al.*, 2009)	Pyrobaculum yellowstonensis str-WP30	Pyrobaculum T1 r02 (Octopus 11)	Thermoproteales-Type-1-TT1-r01 (from MG_3)	Thermoproteales-Type-2-TT2-r01 (from JCHS_4)
pyruvate synthase (reduced methyldiologen)	Tneu_0130/Tneu_0131, Tneu_0176/Tneu_0177/Tneu_0178/Tneu_0179, Tneu_1526/Tneu_1527/Tneu_1528/Tneu_1529, Tneu_1795/Tneu_1796/Tneu_1796/Tneu_1797	2523066983 (0.0, 91%)/2523066984 (0.0, 85%), 2523066044 (3e-107, 94%)/2523066045 (2e-64, 94%)/2523066046 (0.0, 91%)/2523066047 (0.0, 96%), 2523067547 (0.0, 94%)/2523067546 (0.0, 88%)/2523067545 (1e-46, 93%)/2523067544 (1e-81, 92%), 2523067783 (0.0, 97%)/2523067784 (0.0, 93%)/2523067784 (0.0, 93%)/2523067785 (0.0, 95%)	2554136154 (4e-102, 92%)/2554136155 (0.0, 85%), 2554136489 (3e-28, 54%)/2554136489 (9e-22, 64%)/2554135983 (1e-57, 56%)/2554135985 (8e-60, 72%), 2554135985 (4e-91, 94%)/2554135983 (0.0, 88%)/2554136489 (2e-18, 61%)/2554136489 (2e-20, 52%), 2554135985 (4e-39, 63%)/2554135983 (2e-50, 54%)/2554135983 (2e-50, 54%)/2554136489 (0.0, 94%)	2522193529 (8e-114, 72%)/2522193530 (7e-100, 55%), 2522191273 (9e-46, 65%)/2522191272 (8e-38, 72%)/2522191271 (2e-148, 78%)/2522191270 (2e-152, 81%), 2522193647 (2e-125, 77%)/252219364, (5e-120, 70%)/2522193649 (2e-34, 74%)/2522193650 (1e-36, 66%), 2522191270 (5e-98, 66%)/2522191271 (3e-102, 65%)/2522191271 (3e-102, 65%)/2522191273 (5e-36, 62%)	2522208160 (4e-131, 85%)/2522208162 (1e-107, 76%), 2522207481 (1e-83, 87%)/2522207482 (3e-52, 85%)/2522207483 (3e-171, 84%)/2522207484 (4e-169, 86%), 2522209481 (8e-161, 93%)/2522209482 (0.0, 89%)/2522209483 (2e-46, 93%)/2522209484 (1e-81, 92%), 2522207484 (8e-94, 65%)/2522210211 (0.0, 92%)/2522210211 (0.0, 92%)/2522209894 (9e-45, 96%)
pyruvate:water dikinase	Tneu_1204	2523067106 (0.0, 93%)	2554136757 (2e-114, 94%)	2522191675 (0.0, 77%)	2522207697 (0.0, 88%)
PEP carboxylase	Tneu_0418	2523066289 (0.0, 82%)	2554135880 (2e-160, 69%)	2522194306 (1e-39, 47%)	2522207865 (0.0, 82%)
dehydrogenase (NADH);	Tneu_1509	2523067458 (0.0, 94%)	* No hits found *	2522192201 (7e-147, 82%)	2522206372 (1e-173, 90%)
fumarate hydratase	Tneu_1334, Tneu_1335	2523067269 (4e-113, 94%), 2523067270 (4e-154, 94%)	2554136177 (2e-50, 93%), 2554136179 (2e-156, 95%)	2522193059 (3e-86, 85%), 2522191537 (6e-115, 84%)	2522208170 (5e-94, 89%), 2522208171 (2e-128, 87%)
fumarate reductase (reduced methyl viologen)	Tneu_0423, Tneu_0424	2523066285 (0.0, 83%), 2523066286 (6e-48, 82%)	2554136350 (3e-20, 78%), * No hits found *	2522192969 (4e-111, 66%), 2522192061 (5e-29, 60%)	2522208839 (0.0, 77%), 2522207863 (1e-32, 73%)
succinyl-CoA synthetase (ADP forming)	Tneu_1463, Tneu_1464	2523067415 (0.0, 95%), 2523067416 (4e-151, 96%)	* No hits found *, * No hits found *	2522193736 (1e-116, 71%), 2522193735 (7e-97, 79%)	2522207706 (0.0, 89%), 2522207707 (2e-128, 88%)
succinyl-CoA reductase (NADPH or reduced methyl viologen)	Tneu_0421	2523066283 (0.0, 86%)	2554136616 (2e-56, 61%)	2522193515 (9e-99, 64%)	2522208836 (0.0, 85%)
succinic semialdehyde reductase (NADPH)	Tneu_0419	2523066288 (7e-166, 88%)	2554136861 (2e-35, 55%)	2522194273 (4e-36, 51%)	2522207864 (1e-155, 87%)
4-hydroxybutyrate-CoA ligase (AMP forming)	Tneu_0420	2523066282 (0.0, 91%)	2554136618 (0.0, 69%)	2522191349 (3e-176, 63%)	2522208835 (0.0, 90%)
4-hydroxybutyryl-CoA dehydratase	Tneu_0422	2523066284 (0.0, 91%)	2554136349 (2e-23, 43%)	* No hits found *	2522210138 (0.0, 90%)
crotonyl-CoA hydratase	Tneu_0541	2523066375 (0.0, 92%)	2554136611 (0.0, 91%)	2522192659 (0.0, 71%)	2522208384 (0.0, 92%)
(S)-3-hydroxybutyryl-CoA dehydrogenase (NAD)	Tneu_0541	2523066375 (0.0, 92%)	2554136611 (0.0, 91%)	2522192659 (0.0, 71%)	2522208384 (0.0, 92%)
acetoacetyl-CoA beta-ketothiolase	Tneu_0249	2523066169 (0.0, 93%)	2554137003 (3e-111, 92%)	2522194753 (0.0, 86%)	2522209972 (0.0, 93%)

Enzymes of the Proposed 3-hydroxypropionate/4-hydroxybutyrate cycle	Candidate gene in *M. sedula* (Berg et al. 2007, Hawkins et al. 2013)	*Metallosphaera yellowstonensis* r02
acetyl-CoA carboxylase	msed_0147/msed_0148/msed_1375	2522182268 (0.0, 94%)/2522182269 (3e-100, 94%)/2522181552 (0.0, 97%)
malonyl-CoA reductase (NADPH)	msed_0709	2522181698 (2e-139, 97%)
malonate semialdehyde reductase (NADPH)	msed_1993	2522181468 (9e-167, 88%)
3-hydroxypropionyl-CoA synthetase (AMP-forming)	msed_1456	2522181559 (0.0, 96%)
3-hydroxypropionyl-CoA dehydratase	msed_2001	2522181476 (1e-114, 89%)
acryloyl-CoA reductase (NADPH)	msed_1426	2522182467 (0.0, 90%)
propionyl-CoA carboxylase	msed_0147/msed_0148/msed_1375	2522182268 (0.0, 94%)/2522182269 (3e-100, 94%)/2522181552 (0.0, 97%)
methylmalonyl-CoA epimerase	msed_0639	2522182410 (5e-80, 91%)
methylmalonyl-CoA mutase	msed_0638/msed_2055	2522182409 (9e-134, 93%)/2522181116 (1e-70, 94%)
succinyl-coA reductase (NADPH)	msed_0709	2522181698 (2e-139, 97%)
succinate semialdehyde reductase (NADPH)	msed_1424	2522182513 (0.0, 93%)
4-hydroxybutyryl-CoA ligase (AMP-forming)	msed_0394, msed_0406	2522181891 (0.0, 89%)
4-hydroxybutryl-CoA dehydratase, Type I	msed_1321	2522182761 (0.0, 98%)
crotonyl-CoA hydratase	msed_0399	2522181075 (0.0, 82%)
3-hydroxybutyrl-CoA dehydrogenase	msed_0399	2522181075 (0.0, 82%)
acetoacetyl-CoA-B-ketothiolase	msed_0656	2522182430 (0.0, 88%)

Enzymes of the r-TCA cycle		Candidate gene in *Sulfurihydrogenibium* r01, identified through IMG pipeline annotation	
aconitase		2554146539 (0.0, 68%)	
isocitrate dehydrogenase		2554146492 (0.0, 58%)	
2-oxoglutarate ferredoxin oxidoreductase		2554147741 (3e-65, 35%)/2554147742 (3e-65, 33%)	
succinyl-CoA synthetase		2554147743 (2e-117, 70%)/2554147744 (0.0, 60%)	
succinate dehydrogenase		2554146754 (3e-64, 43%)/2554147562 (0.0, 56%)	
fumarase		2554147747 (5e-100, 52%)/2554147746 (1e-56, 53%)	
malate dehydrogenase		2554147748 (6e-91, 45%)	
ATP-citrate lyase		2554147107 (0.0, 97% to *Sulfurihydrogenibium* sp. YO3AOP1)/2554147109 (0.0, 98% to Sulfurihydrogenibium sp. YO3AOP1)	
Enzymes of the r-TCA cycle (with citrate cleavage via two enzymes)	**Query sequence**		
		***Hydrogenobaculum* r01, identified through IMG pipeline annotation**	***Thermocrinis* r01, identified through IMG pipeline annotation**
aconitase		2522214166 (0.0, 30%)	2548771353 (0.0, 31%)
isocitrate dehydrogenase		2522213994 (9e-127, 47%)	2548772285 (0.0, 52%)
2-oxoglutarate ferredoxin oxidoreductase		2522213999 (3e-67, 32%)/2522214000 (9e-75, 38%), 2522214053 (1e-63, 31%)/2522213357 (6e-58, 39%)	*No hits found*
succinyl-CoA synthetase		*No hits found*	2548771788 (5e-77, 40%)
succinate dehydrogenase		2522214897 (0.0, 51%)/2522213674 (1e-48, 33%) or 2522214922 (3e-51, 37%)	2548772157 (0.0, 56%)/2548772344 (1e-57, 40%) or 2548772797 (3e-51, 41%)
fumarase		2522213301 (0.0, 67%)	2548772724 (2e-102, 54%)
malate dehydrogenase		2522214167 (1e-92, 47%)	2548771354 (2e-94, 48%)
citryl-CoA synthetase	GI:46849517, citryl-CoA synthetase small subunit *Hydrogenobacter thermophilus* TK-6 (Hydth_0200)	2522213416 (0.0, 87%)	2548771788 (0.0, 94%)
citryl-CoA lyase	GI:46849510, citryl-CoA lyase *Hydrogenobacter thermophilus* TK-6 (Hydth_0309)	2522213760 (8e-152, 90%)	2548772907 (8e-116, 94%)
/ separates enzyme subunits			
, separates candidate genes			

Figure S1. Site photographs of representative sulfur seditment, iron oxide mat, and filamentous streamer chemotrophic geothermal systems in Yellowstone National Park (YNP), WY, USA



APPENDIX D

SUPPLEMENTAL MATERIAL TO “GENOME-ENABLED MULTI-SCALE ANALYSIS OF AUTOTROPH-HETEROTROPH INTERACTIONS IN A HIGH-TEMPERATURE MICROBIAL COMMUNITY”

To request DVD copies contract your local public or university library to place an interlibrary load request to Montana State University. Questions call 406-994-3161.